OLIVOCOCHLEAR EFFERENT PLASTICITY DURING DEVELOPMENT AND REORGANIZATION DURING HEARING LOSS

by

Stephen Paul Zachary

A dissertation submitted to The Johns Hopkins University in conformity with the requirements for the degree of Doctor of Philosophy

Baltimore, MD

November 2016

Abstract

Inner hair cells (IHCs) are the primary sensory receptors of the auditory system. Before the onset of hearing, immature IHCs have numerous cholinergic efferent synapses that are eliminated in the second postnatal week. These efferents, which are functionally inhibitory, exist during an important period of cellular and circuit maturation. Efferent inhibition is brought about via the gating of postsynaptic nicotinic acetylcholine receptors (nAChRs), which flux calcium to activate calcium-dependent potassium (SK) channels. Whole-cell recordings revealed that calcium-induced calcium release from internal stores and voltage-gated calcium channel function also contribute to the calcium signal that shapes SK channel activation. These additional calcium sources underlie a plasticity mechanism that encodes recent IHC depolarization in cholinergic responses. Thus, the activity of the IHC modulates the strength of efferent inhibition.

Recordings from aged animals were also performed to investigate whether efferent neurons re-innervate IHCs during aging. Functional efferent synaptic activity was observed in aged animals, and the degree of efferent innervation increased alongside afferent loss, outer hair cell death, and threshold elevation. Such efferent synapses were inhibitory and utilized the same ionic mechanisms found in early postnatal IHCs. These data are the first recordings from aged hair cells and show that the damaged cochlea assumes features reminiscent of development.

Advisor: Dr. Paul Fuchs, Ph.D.

Readers: Dr. Paul Fuchs, Ph.D. & Dr. Shanthini Sockanathan, Ph.D.

Acknowledgements

I would like to thank my PhD advisor, Dr. Paul Fuchs, for his support over the course of my graduate studies. Paul is a model of the professional and personal qualities that make a successful scientist, and his commitment to mentorship is unparalleled. His reputation in the field of auditory neuroscience and within the Hopkins community is well deserved, and I'm proud to be one of his trainees. I would also like to thank Dr. Elisabeth Glowatzki for her invaluable contributions to my work and all of the members of the Fuchs and Glowatzki labs for making our research environment so positive and productive.

My thesis committee consisted of Dr. Dwight Bergles, Dr. Shan Sockanathan, and Dr. Brad May. Each is a leader in their field, and their expertise and perspectives greatly enhanced the quality of my research. I would like to thank Rita Ragan, Beth Wood-Roig, Faye Mackall, and Carol Reynolds for administrative assistance and for always being generous with their time. I'm grateful to Dr. Charles E. Connor for his mentorship while I worked as a technician in his lab. It has been a pleasure to be a part of the Hopkins community, especially the Neuroscience Department, the Center for Hearing & Balance and the Center for Sensory Biology.

I am especially thankful for the support of Maureen Frances Connolly, Sean Philbin, Patrick Philbin, Nick Sadoski, Brian Smith, Brandon Seale, and Jamie & Patrick Halloran. I would also like to thank the Zachary, McNally, Webbert, and Philbin families.

Finally, I would like to thank my parents, who I love very much.

Table of contents

List of figures

Chapter 1

Introduction

Hearing begins with the transduction of sound waves into electrical signals that can be interpreted and processed by the nervous system, and the peripheral auditory organ – the cochlea – carries out this task. Given the complex nature of hearing, which involves wide frequency and intensity ranges as well as high temporal precision, it is remarkable that the cochlea, which has a simple structure and few cell types, can encode all relevant acoustic features. In fact, a single class of receptors, inner hair cells (IHCs), is responsible for the transduction and the initial processing of acoustic content.

IHCs, like cutaneous receptors of the skin, are mechanoreceptors; and the structure, physical properties, and coupling of the entire cochlear apparatus shape the mechanical stimulus IHCs receive. Numerous feedback processes contribute to and determine functional capacity at every step of acoustic transduction. Such feedback includes top-down modulation of cochlear function, effects prior to IHC signal generation in the form of the "cochlear amplifier," and even activity of single receptor channels in the form of adaptation. Thus, feedback occurs at the systems, cellular, and molecular levels to shape the neural activity that gives rise to auditory perception.

The present work investigates one facet of such feedback: the synaptic mechanisms of efferent inhibition of IHCs. Such inhibition occurs developmentally before the onset of hearing in rodents, and experiments presented in Chapter 4 demonstrate a form of efferent synaptic plasticity and the calcium-dependent mechanisms

that underlie it. This plasticity relies, in part, on calcium signals typically associated with the afferent pathway, and thus represents a form of synaptic crosstalk. It is proposed that the interaction of the afferent and efferent systems at the level of the IHC may be important for the functional maturation of the auditory pathway, and future work may build on the current results to investigate this intriguing possibility.

Though IHCs lose their efferent contacts at the onset of hearing, Chapter 5 shows that efferent neurons re-innervate IHCs during age-related hearing loss. These synapses utilize the same molecular components and ionic mechanisms of efferent synapses present on immature IHCs; and thus efferent transmitter release produces IHC inhibition. Renascent IHC inhibition may contribute to hearing impairment, serve as a form of neuroprotection for sensitive afferent contacts, or perform some other function. The present work suggests that efferent synapses on aged IHCs could be therapeutic targets for positive or negative modulation as hearing loss progresses and shows that the aged cochlea, while displaying many pathological features, also reverts to a developmental state in terms of efferent organization.

The implications of the efferent plasticity described in the present work are best understood in the broader context of sound encoding; and a discussion of the relevant cell types and their functions is also presented below.

1.1 Cochlear mechanics and sound encoding

Sound is energy structured in the form of a vibrating wave that travels through a medium, such as air. Sound is captured, transformed, and focused by the outer ear,

which directs the energy through the ear canal to the middle ear. The middle ear ossicles couple the tympanic membrane (ear drum) to the fluid-filled cochlea.

The cochlea is tonotopically organized with low frequencies represented at the base and high frequencies represented at the apex. Once cochlear fluids are sent in motion, the structure of the cochlear spiral and the stiffness of the basilar membrane shape the mechanical stimulus into a frequency discriminator. Basilar membrane motion in response to sound is said to be a "traveling wave" that produces maximum movement at the appropriate position along the cochlear tonotopic map (Von Békésy, 1960; Olson et al., 2012).

Differential motion of the tectorial membrane in response to basilar membrane vibration bends stereocilia bundles atop hair cells. Stereocilia in different rows are connected by tip-links composed of cadherin 23 and protocadherin 15 (Siemens et al., 2004; Ahmed et al., 2006), and tip-link tension during bundle deflection gates mechanosensitive channels in the shorter rows (Beurg et al., 2009). Though promising candidates have been proposed, the molecular identity of the hair cell mechanotransduction channel remains unknown despite decades of intense investigation (Effertz et al., 2015). Whatever protein or proteins constitute the channel, the transduction current is dominated by potassium influx due to the high potassium concentration of endolymph bathing the apical surfaces of hair cells (Hudspeth, 1997).

The opening of transduction channels depolarizes the hair cells and shapes their graded receptor potentials, leading to glutamate release onto spiral ganglia afferents (Glowatzki & Fuchs, 2002). The perilymph bathing hair cell bodies and

afferent processes has appropriate calcium and sodium concentrations for hair cell transmitter release and afferent spiking (Fettiplace & Kim, 2014). Hair cell and afferent function are discussed in more detail below.

Spiral ganglion afferents comprise the auditory nerve and send their central processes to the cochlear nucleus. From the cochlear nucleus, processes extend ipsi- and contralaterally; and acoustic information is transformed at various brainstem relays before reaching the inferior colliculus, medial geniculate nucleus of the thalamus, and primary auditory cortex. Central activity allows for higher order function, such the binaural processing that underlies sound localization (Avan et al., 2015) and the complex integration that produces "auditory objects" (Bizley & Cohen, 2013). Though activity throughout the ascending central auditory pathway is not directly relevant to the present work, such activity produces top-down signals that inform efferent spiking behavior.

1.2 Cochlear cell types, synaptic connections, and functions

1.2.1 Inner hair cells and type I afferents

As stated above, IHCs are the primary receptors of the auditory system, and they are organized in a single row along the cochlear spiral. Though IHCs exhibit broad calcium spikes during the first postnatal week, they lose this spiking behavior as larger potassium conductances develop (Marcotti et al., 2003a; Marcotti et al., 2003b). Graded receptor potentials endow IHCs with analog responses that cover large dynamic ranges of sound intensities.

Receptor potentials, shaped by transduction currents, gate L-type voltage-gated calcium channels (CaV1.3) during depolarization (Brandt et al., 2003). IHC active zones contain an electron dense "ribbon" with tethered vesicles that fuse to the membrane in a calcium-dependent fashion (Safieddine et al., 2012). The presynaptic machinery utilized by IHCs includes some noteworthy proteins, such as RIBEYE, which is abundant in ribbons, as well a Otoferlin, which may serve as the calcium sensor at IHC active zones (reviewed in Wichmann, and Moser, 2015). Vesicular glutamate transporter 3 packages glutamate into IHC synaptic vesicles, and released glutamate binds AMPA type receptors in postsynaptic afferent neurons (Glowatzki & Fuchs, 2002; Seal et al., 2008).

Type I afferents, which constitute 90-95% of the auditory nerve, contact IHCs; and each IHC is presynaptic to many type I afferents, ranging from ~10 in the apex to ~30 in the base (Spoendlin & Schrott, 1989; Figure 1.1). Each IHC active zone contains a single ribbon that communicates to a postsynaptic afferent. These large diameter, myelinated type I afferents are known to provide the totality of acoustic information to the brain, including frequency content, timing, and intensity (Young, 2008). Type I afferents vary in terms of their spontaneous rates, acoustic thresholds, and dynamic range. Thus, as a populaiton, they can cover wide acoustic ranges, with "low spont" fibers covering louder sounds for which "high spont" fibers are saturated. The mechanisms giving rise to type I afferent diversity are poorly understood; but, as the IHC is isopotential, presynaptic factors must involve differences at individual ribbons. The density of voltage-gated calcium channels at individual active zones may vary in a fashion that drives heterogeneity in afferent spiking (Frank et al., 2009;

Meyer et al., 2009). Postsynaptic variability likely exists as well, and "low spont" fibers tend to localize to the modiolar side of the IHCs while "high spont" fibers tend to localize on the pillar side (Liberman, 1982).

1.2.2 Outer hair cells and type II afferents

Outer hair cells (OHCs), orgnaized in three rows, serve as the "cochlear amplifier" via the electromotile signal amplification function they perform (Dallos, 2008). The motor protein prestin, which undergoes voltage-dependent conformational changes, endows OHCs with electromotility; and OHC movement amplifies the sound-driven motion of the basilar membrane (Zheng et al., 2000; Robles & Ruggero, 2001). This motion results in increased IHC sensivity and type I afferent responses.

Type II afferents contact OHCs and comprise only about 5-10% of the auditory nerve. The 2-3 ribbons found in each OHC are far less than those found in IHCs; and, correspondingly, OHCs have only 2-3 type II afferent synaptic contacts. These afferents are unmyelinated; and, upon reaching the OHC area, they turn basally and extend their dendritic process for hundreds of microns (Figure 1.1). Though each type II neuron forms synaptic contacts with many OHCs, they are unresponsive to sound when recorded from *in vivo* (Brown, 1994; Robertson, 1984; Robertson et al., 1999). It is known, however, that OHCs can release glutamate onto type II afferents, which use AMPA-type receptors (Martinez-Monedero et al., 2016; Weisz et al., 2009; Weisz et al., 2012).

Cochlear Afferent Organization

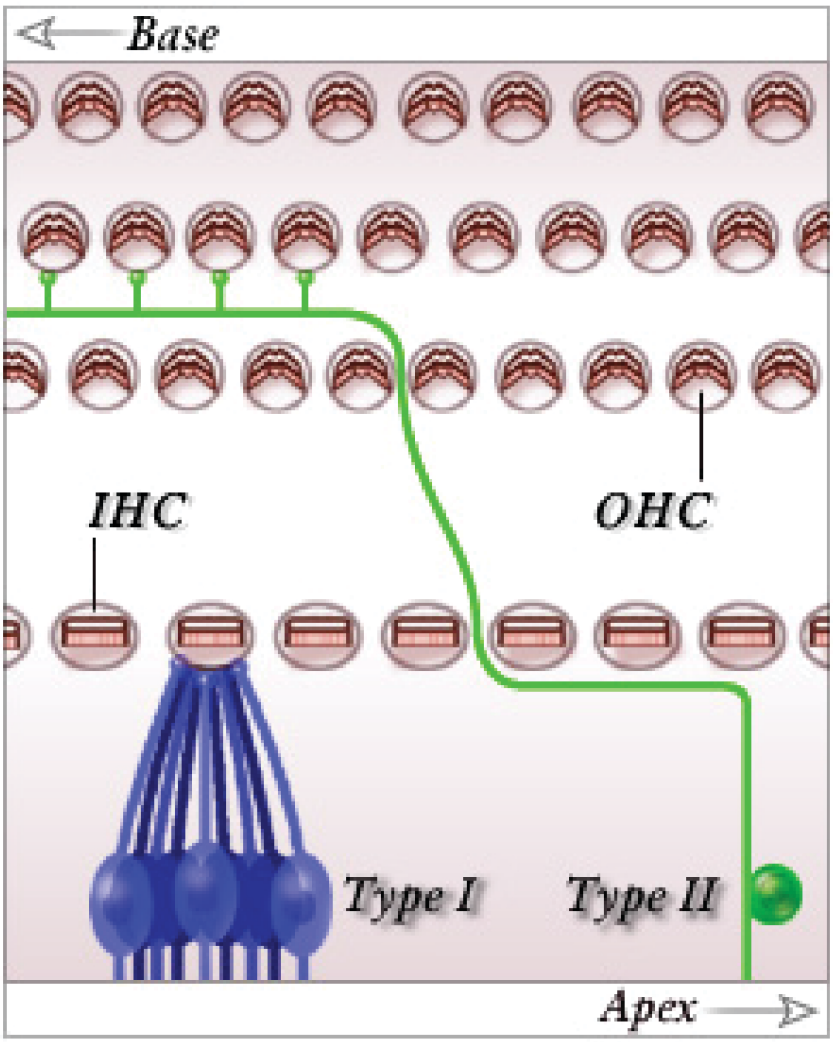

Figure 1.1: Type I and type II cochlear afferents. Each type I afferent contacts a single IHC, and each IHC is presynaptic to many type I afferents. In contrast, type II afferents turn basally to contact many OHCs. Each OHC is presynaptic to 2-3 type II afferent dendrites. From *Promenade 'Round the Cochlea.*

Though type II fibers are only weakly excited by sound and OHC glutamate release, they respond strongly to ATP released upon the rupture of OHC membranes (Liu et al., 2015), and traumatizing sound increases C-FOS expression in the granule cell region of the cochlear nuclei, where type II neurons are known to make synaptic connections (Benson & Brown, 2004). These findings support the hypothesis that OHCs are nociceptors specialized for sensing tissue damage accompanying traumatic sound.

1.2.3 MOC efferents

Medial olivocochlear (MOC) efferents are one of two efferent populations that innervate the cochlea. MOC efferents have cell bodies in the medial superior olivary complex of the brainstem, and their large diameter myelinated axons form cholinergic synapses on OHCs in the adult animal (Guinan, 1996, Figure 1.2). These efferents are driven by sound, and their response properties are akin to those of type I afferent neurons (Robertson & Gummer, 1985).

Acetylcholine (ACh) release from MOC terminals inhibits OHCs. OHCs express ionotropic α9/α10 nicotinic acetylcholine receptors (nAChRs), which are calcium permeant (Elgoyhen et al., 1994; Elgoyhen et al., 2001). Calcium influx through nAChRs gates functionally coupled calcium-dependent potassium channels, which results in membrane hyperpolarization (Ballestero et al., 2011; Oliver et al., 2000; Rohmann et al., 2015). Near membrane synaptic cisterns are ubiquitous postsynaptic features of efferent synapses on hair cells, and these cisterns are thought

to be involved in synaptic calcium regulation (Lioudyno et al., 2004; Fuchs et al., 2014).

The opening of potassium channels shunts and hyperpolarizes OHC membranes. This results in diminished type I afferent sensitivity due to a decrease in OHC motility and subsequent basilar membrane motion (Dallos et al., 1997; Guinan, 2010). Thus, MOC feedback dampens the "cochlear amplifier;" and, because MOCs project tonotopically, they are thought to play a role in cochlear frequency tuning. Additionally, the activity of MOC efferents is thought to protect against noise-induced hearing loss, and the evidence for this hypothesis is discussed in Chapter 5.

Prior to the onset of hearing and MOC synapse formation on OHCs, MOC efferents transiently form synapses with IHCs (Glowatzki & Fuchs, 2000; Roux et al., 2011; Figure 1.2). These efferent contacts inhibit IHCs via a similar two-channel mechanism as that described above for OHCs, and thus shape IHC function during a developmentally important period. While the functional role of efferent contacts on early postnatal IHCs is poorly understood, it has been proposed that IHC inhibition helps establish central tonotopy (Clause et al., 2014).

1.2.4 LOC efferents

Lateral olivococochlear (LOC) efferents are smaller diameter, and they form synapses on the dendrites of type 1 afferents (Figure 1.2). Though ACh is the dominant neurotransmitter used by LOC efferents, other transmitters, such as GABA and dopamine, have been implicated in the LOC system as well (Puel, 1995; Reijntjes

Cochlear Efferent Organization

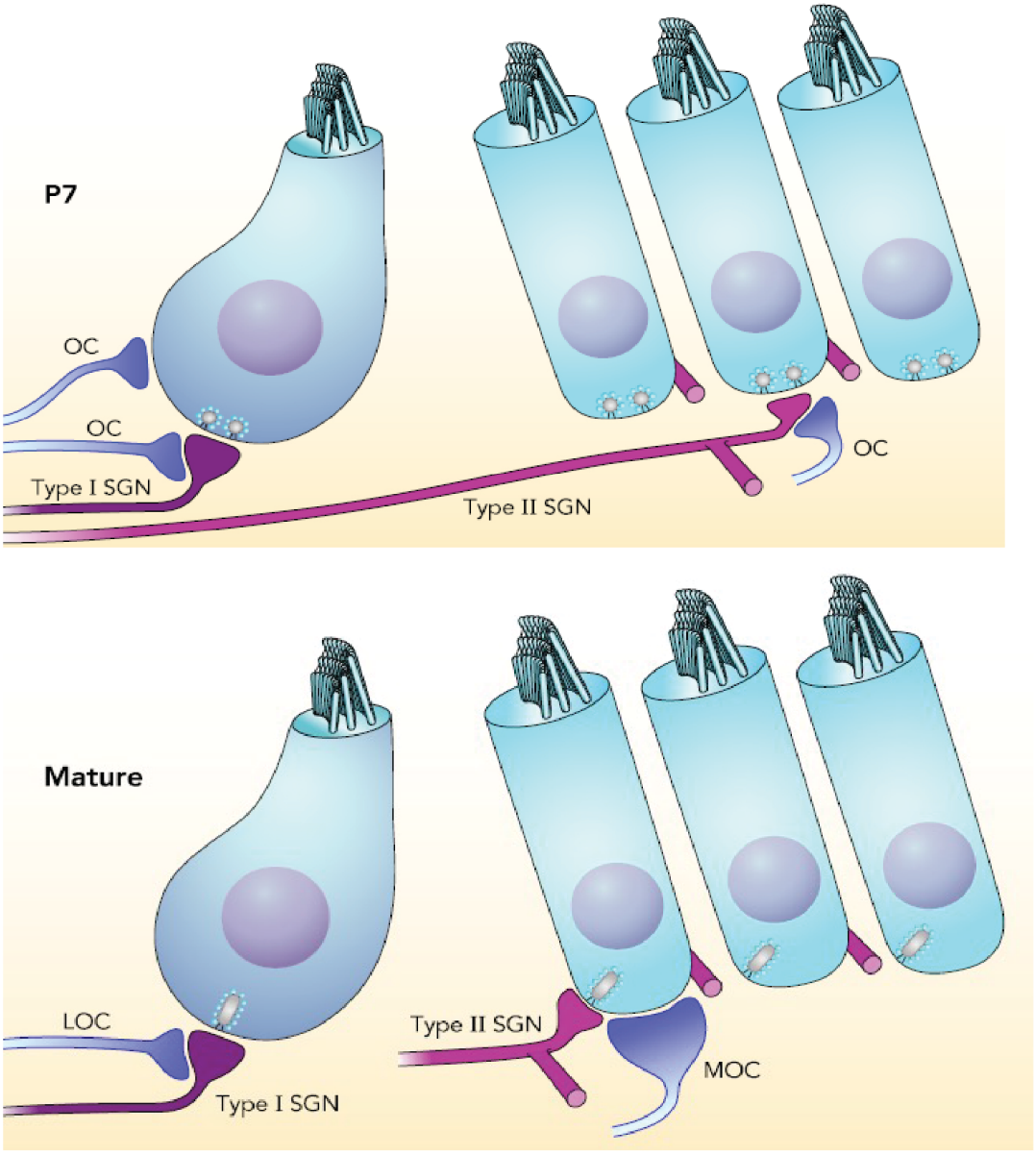

Figure 1.2: During the first two postnatal weeks, IHCs are contacted by olivocochlear efferent neurons (top). Around the onset of hearing, efferent synapses on IHCs are eliminated and OHCs receive MOC efferent innervation (bottom). LOC efferents form synapses with the dendrites of type I afferents. From Bulankina & Moser, 2012.

& Pyott, 2016). ACh perfusion into the cochlea increased afferent firing rates, while GABA perfusion had the opposite effect (Felix & Ehrenberger, 1992). Whole-cell recordings from cultured spiral ganglion neurons revealed reduced sodium currents during dopamine agonist application (Valdes-Baizabal et al., 2015).

Our understanding of LOC efferent function relies on cochlear microperfusion data, lesion studies, and postsynaptic recordings from afferent cell bodies or dendrites. The use of both excitatory and inhibitory neurotransmitters by LOCs suggest that these efferents dynamically modulate afferent activity, perhaps in a manner that gives rise to the afferent diversity described above (i.e. "high spont" and "low spont" fibers). Nevertheless, direct experimental evidence supporting this hypothesis is lacking.

1.3 Conclusion

The efferent synapses studied in the present work exist on IHCs at the extremes of the lifespan: during the first two postnatal weeks and during advanced stages of aged-related hearing loss. They are therefore found during periods of functional consolidation as well as functional decline. In both of these epochs, efferent synapses on IHCs operate within the complex system of mechanics, circuit interactions, and cellular functions that determine cochlear output.

The experimental results described in Chapter 4 are relevant in the context of prehearing cochlear function. As such, consideration is given to the role of efferent synapses in the maturation of the auditory pathway. In Chapter 5, efferent synaptic

function is described during age-related hearing loss, and a discussion of cochlear pathology underlying hearing loss is provided for context.

Chapter 2

Aims of the study

2.1 Specific aims

Sensory hair cells of the cochlea are subject to feedback and modulation by olivocochlear efferent neurons. Acetylcholine (ACh) released from efferent terminals activates nicotinic acetylcholine receptors (nAChRs) composed of α9 and α10 nAChR subunits. Calcium influx through these nAChRs activates small conductance calcium-dependent potassium (SK) channels to render these synapses functionally inhibitory. Such efferent synapses exist on early postnatal inner hair cells (IHCs) but disappear around the developmental onset of hearing in rodents. In the adult animal, efferent synapses are found on outer hair cells and the dendrites of type I afferents contacting IHCs.

Thee specific aims of this thesis are:

1. Determine if calcium sources other than nAChRs contribute to SK channel gating in early postnatal IHCs.

2. Determine if efferent neurons re-innervate IHCs during hearing loss and characterize the molecular components of those synapses.

2.1.1 Determine if calcium sources other than nAChRs contribute to SK channel gating in early postnatal IHCs.

Though nAChRs flux calcium and trigger postsynaptic events, other calcium sources and handling mechanisms may shape the extent of SK channel activation. Specifically, a near membrane postsynaptic cistern exists at all efferent synapses on hair cells, and this structure may modulate synaptic calcium signals. Additionally, young IHCs possess voltage-gated calcium channels that trigger glutamate release onto type I afferents, and calcium fluxed through these channels may participate in efferent inhibition.

Experimental results addressing this aim are presented in Chapter 4.

2.1.2 Determine if efferent neurons re-innervate IHCs during hearing loss and characterize the molecular components of those synapses.

Ultrastructural studies in both the mouse and guinea pig suggest that efferent innervation may return to IHCs during hearing loss, but no physiology has been carried out to confirm these observations. Therefore, it is unknown if such synaptic contacts are functional. Additionally, because numerous transmitters are implicated in the olivocochlear system, the effect of efferent transmitter release on IHCs during hearing loss is unclear.

Experimental results addressing this aim are presented in Chapter 5.

Chapter 3

Materials and methods

3.1 Experimental animals

The birthday of all experimental animals is counted as postnatal day 0 (P0). For all experimental procedures, animals were placed in a chamber and deeply anesthetized with isoflurane prior to sacrifice. All animal protocols and all procedures involving the use of animals were approved by the Johns Hopkins University Animal Care and Use Committee.

3.1.1 CD rats

All experiments performed for Chapter 4 used CD rats from Charles River Laboratories (Wilmington, MA). Pups were sacrificed between the ages of P7 and P9 via decapitation.

3.1.2 C57BL/6J mice

All experiments performed for Chapter 5 used female C57BL/6J mice (C57) from the Jackson Laboratories (Bar Harbor, ME). Mice over the age of 6 months were retried breeders with well-documented dates of birth. Mice were sacrificed via decapitation.

3.2 Electrophysiology

3.2.1 Tissue preparation

Each recorded cell was from an individual animal. Mice were deeply anesthetized with isoflurane, decapitated and the temporal bone removed. An apical region of the cochlear sensory epithelium was excised and pinned to a coverslip, then placed in a recording chamber on the microscope stage where it was continuously perfused with saline at room temperature.

This work includes the first recordings obtained from hair cells during age-related hearing loss. The vast majority of hair cell recordings published to date are from early postnatal animals, when the bone surrounding the cochlear epithelium is soft and the tissue is relatively easy to access. After becoming proficient in the early postnatal dissection, the dissection was practiced on continually older animals until successful dissections and recordings were commonplace in mice over a year old. The oldest recording obtained came from an 18 month-old mouse.

While numerous parameters were explored to promote tissue survival, the quality of the dissection technique appears to be the most important factor in obtaining healthy and usable tissue.

3.2.2 Solutions

The standard internal (pipette) solution was (in mM): 135 KCl, 3.5 $MgCl_2$, 0.1 $CaCl_2$, 5 EGTA, 5 HEPES, and 2.5 Na-ATP (pH: 7.2). The standard extracellular solution was (in mM): 5.8 KCl, 144 NaCl, 1.3 $CaCl_2$, 0.9 $MgCl_2$, 0.7 NaH_2PO, 5.6 D-

Glucose, and 10 HEPES. For experiments where elevated extracellular potassium (40 mM or 80 mM) was used to drive transmitter release, there was a corresponding decrease in the concentration of NaCl. Similarly, for experiments performed in low extracellular potassium (2.5 mM, Chapter 4), there was a corresponding increase in the concentration of NaCl. Extracellular solution was perfused into the bath continuously at a rate of 2 mL/minute.

Some experiments in Chapter 5 used solutions to manipulate the reversal potential of chloride. To set E_{Cl} at -132mV, the following internal solution was used: 140 Cs-methanesulfonate, 0.7 $MgCl_2$, 0.1 $CaCl_2$, 5 HEPES, 5 EGTA, and 2.5 Na-ATP (pH: 7.2). To set E_{Cl} at -80 mV, the following internal solution was used: 140 Cs-methanesulfonate, 2.6 KCl, 3.5 $MgCl_2$, 0.1 $CaCl_2$, 5 HEPES, 5 EGTA, and 2.5 Na-ATP (pH: 7.2). Cs-based internals had a corrected junction potential of -10 mV.

Solution changes were made by bath application or by a gravity-fed multichannel glass pipette with an opening of ~150 μM. Acetylcholine application was made via a pipette connected to a Picospritzer II (General Valve Corporation), allowing for controlled application.

3.2.3 Data collection

Whole-cell, tight seal voltage-clamp recordings were made on an Axioskop2 microscope (Zeiss) with differential interference contrast and a 40x water-immersion objective. A Multiclamp 700B (Axon), pClamp 10 (Axon), and a Digidata 1440A (Axon) were used for data collection. Recording pipettes had resistances of 3-6 MΩ

and were advanced through the tissue with positive pressure to maintain tip cleanliness. Series resistance was less than 15 MΩ and not compensated.

3.2.4 Electrical stimulation recordings

Electrical stimulation was used to evoke efferent transmitter release while recording from P7-9 rat IHCs. Electrical stimulation of efferent axons was delivered via silver wire inserted into a glass micropipette with a diameter of 20-30 μM and a return wire was inserted in the bath. This pipette was positioned about 20 μM modiolar to the base of an IHC subjected to tight seal voltage-clam recording. The pipette position was adjusted until current flow through it evoked postsynaptic currents in the IHC under study. An electrically-isolated constant current source (Digitimer Limited, model DS3) was triggered manually while scanning for axons and digitally via the data acquisition computer thereafter. Efferent axons were stimulated via pulses of ~50 – 100 μA, 30 – 300 μs long. With practice, stimulation pipette movement in the tissue could be achieved without disrupting the integrity of IHC recordings. As expected, during high-quality recordings with proper stimulation pipette placement, postsynaptic currents could be recorded from all P7-9 rat IHCs.

3.2.5 Auditory brainstem response recordings

Acoustic thresholds were determined for C57 mice at three ages – 1 month, 8.5 – 9.5 months, and 11- 12 months – via auditory brainstem response (ABR) recordings. ABR's provide an electrophysiological readout of the synchronous

activity of various neuronal populations along the ascending auditory pathway. Mice were first anesthetized by intraperitoneal injection of 100mg/kg ketamine and 20mg/kg xylazine dissolved in 14% EtOH, then placed inside a small sound-attenuating chamber 30 cm from two speakers. Mice were maintained at 37°C using a heating pad. ABR recordings utilize differential electrodes placed over the left bulla and vertex of the skull. A ground electrode was inserted into the leg muscle and taped to the paw to maintain stability. Stimulus presentation and ABR measures were controlled and collected using custom Matlab (Mathworks) software. The stimuli were: broadband "clicks" as well as tones at 4 kHz, 8 kHz, 16 kHz, and 32 kHz. Stimuli were played through a pair of SuperTweeter speakers (Radio Shack). ABRs were averaged over 300-500 stimulus presentations and bandpass filtered between 300 to 3000 Hz. Stimuli were initially presented at high intensities and then gradually diminished until the software determined acoustic threshold. Threshold was defined as the sound level at which the ABR magnitude was 2 standard deviations above the average background noise level.

Great effort was taken to maintain consistent electrode placement as well as animal-to-speaker distance across all experiments. The number of animals tested per age group were: 1 month (4), 8.5 – 9.5 months (4), 11 -12 months (5).

3.3 Immunohistochemistry and confocal microscopy

3.3.1 Immunohistochemistry

Immunohistochemical techniques were used to assess age-related cochlear pathology in C57 mice. Mice were euthanized at 1 month, 8.9 - 9.5 months, and 11 - 12 months and cochlear whole mounts were prepard.

After euthanasia, cochleae were dissected out of the temporal bone and perfused through the round window with 4% paraformaldehyde in cold phosphate-buffered saline (PBS). Cochleae were fixed for 30 minutes on a shaking platform at room temperature, then rinsed with PBS 3 times for 15 minutes each rinse. Well-fixed cochleae were then dissected. The apical portion of the sensory epithelium was excised and placed in a small eppendorf tube, and all reactions occurred within this tube via solution exchange with pipettes. Cochlear epithelia were permeabilized with 0.5% Triton for 30 minutes at room temperature on a shaking platform and rinsed 3 times for 15 minutes with PBS. Blocking occurred for 1.5 hours in 4% bovine serum albumin (BSA), followed by another round of PBS rinsing. Incubation with primary antibodies (1:200) in 2.5% BSA occurred overnight at 4°C on a shaking platform. After thorough washing, incubation with secondary antibodies (1:1,500) in 3% BSA occurred for 1 hour at room temperature. After further washing in PBS, the tissue was mounted on slides using FluorSave mounting medium.

Numerous other protocols were performed in an attempt to identify a suitable protocol for aged cochlear tissue, but they either failed to label strongly or produced

unacceptably high background signal. The protocol described above labeled well with minimal background and was use for all three ages.

3.3.2 Confocal microscopy

Cochlear whole mounts were visualized on a Zeiss LSM-700 microscope. Confocal micrographs were taken using 40x and 63x water immersion objectives. Care was taken to document the anatomical region within the preparation where confocal micrographs were acquired. Z-stacks were taken through the entirety of the hair cell population of interest. Data acquisition was controlled by Zen software (Zeiss).

3.4 Reagents

3.4.1 Antibodies

Afferent synaptic contacts on IHCs were determined by immunolabeling the presynaptic dense body ribbon. These structures were labeled with antibodies against C-Terminal Binding Protein 2 (CTBP2) acquired from Santa Cruz Biotechnology (Santa Cruz, CA).

Outer hair cell (OHC) quantification across the lifespan was determined by immunolabeling the OHCs with antibodies against Myosin 7A acquired from Developmental Studies Hybridoma Bank (Iowa City, IA).

3.4.2 Pharmacological agents

Curare, strychnine, ACV1, apamin, bicuculline, picrotoxin, ryanodine, acetylcholine, and Bay K 8644 were all acquired from Tocris Biosciences (Bristol, United Kingdom). The use and concentration of each agent is described in the text.

3.5 Data analysis

Synaptic currents were analyzed in MiniAnalysis (Synaptosoft). For both inward events evoked by elevated external potassium and outward events evoked by electrical stimulation, identification was performed manually with a threshold of 5 pA. Decay time constants were analyzed only in those events that were not compromised by other events in their falling phase.

For the electrophysiological experiments presented in Chapter 4, data were pooled across multiple cells in the same condition, and the means and standard deviations of the pooled data are presented. For that chapter's key measures during pharmacological manipulation (half width and time constant of decay), figures found in the Appendix reproduce the data for each recorded cell.

Additional analysis was performed in Origin 7.5 (OriginLab Corp), Excel (Microsoft Corp), and GraphPad Prism 5 (GraphPad Software). Fisher's exact test (two-sided) was used to compare proportions of innervated IHCs across the lifespan. A value of $p < 0.05$ was considered statistically significant. Mean values are presented along with standard error (SE) or standard deviation (SD). For experiments testing whether or not IHCs have efferent innervation, an IHC was considered lacking

innervation if no postsynaptic currents were observed after 5 minutes of continuous exposure to high potassium solution.

Confocal images and z-stack files were analyzed in Imaris (Bitplane). Ribbon counts were carried out in the 5-6 kHz region of the cochlear apex. Tonotopic position was estimated by converting distance from apex into an approximation of % length along the cochlear extent and applying that percentage to previously published mouse frequency maps (Ding et al., 2001; Viberg & Canlon, 2004). Ribbon analysis was performed on 31 cells from 3 animals at 1 month, 40 cells from 4 animals at 8.5-9.5 months, and 30 cells from 3 animals at 11-12 months.

OHC counts were performed in the same tissues and regions, and OHC survival was determined by counting the total number of cells across a 200 μm distance.

Chapter 4

Calcium handling at the efferent-IHC synapse

4.1 Background and significance

Cholinergic olivocochlear efferent neurons transiently innervate inner hair cells (IHCs) during the first two postnatal weeks. These efferents activate an unusual nicotinic acetylcholine receptor (nAChR) with distinctive pharmacological properties. nAChR activation leads to IHC inhibition via the subsequent gating of calcium-dependent potassium channels. Such inhibition, mediated by ionic flux as opposed to metabotropic signaling, has been referred to as the "two-channel mechanism of cholinergic inhibition."

Though calcium entering the IHC through nAChRs triggers inhibitory postsynaptic currents (IPSCs), other calcium sources and calcium handling mechanisms may contribute to potassium channel activation. Postsynaptic cisterns are ubiquitous features of efferent synapses on hair cells and may release calcium to increase or prolong inhibition. Calcium entry through voltage-gated channels may contribute to inhibition as well.

The experiments presented here investigate these possibilities and demonstrate that cholinergic responses are determined, in part, by the prior activity of IHCs. This mode of plasticity encodes recent depolarization, and thus may be important in the context of auditory circuit maturation during development.

4.1.1 Efferent synapses

Acetylcholine (ACh) is the dominant neurotransmitter of the olivocochlear efferent system, and efferent innervation of hair cells is thought to be as phylogenetically ancient as hair cells themselves (Fuchs, 1996; Manley & Koppl, 1998). Cholinergic inhibition is common among vertebrate efferents, having been shown in frog (Ashmore & Russell, 1983), reptile (Art et al., 1984), bird (Shigemeoto & Ohmori, 1991; Fuchs & Murrow, 1992a), and mammalian (Glowatzki & Fuchs, 2000) hair cells. At most potentials, cholinergic responses consist of a brief inward current consisting of cation influx through nAChRs followed by a larger and longer outward current consisting of potassium efflux.

Based on the strange pharmacological profile of cholinergic responses recorded from hair cells, it was proposed that an uncharacterized nAChR is used by hair cells (Fuchs & Murrow, 1992b). The hair cell nAChR is not activated by muscarine and is blocked by high concentrations of nicotine. Moreover, nicotinic antagonists (curare and α-bungarotoxin) as well as muscarinic antagonists (atropine) block this nAChR. Blockade by α-bungarotoxin, which is irreversible at motor terminals, is reversible at efferent synapses on hair cells. Additionally, glycinergic (strychnine) and GABAergic (bicuculline) antagonists can also block the hair cell nAChR. This pharmacology is reviewed in Elgoyhen & Katz, 2011.

The cloning of the α9 nAChR subunit and the demonstration of its expression in cochlear hair cells provided molecular verification that a novel receptor operates at efferent synapses (Elgoyhen et al., 1994). Analysis of the primary structure of this

protein shows that it belongs to the "Cys-loop" superfamily of receptors, which includes nAChRs, glycine, $GABA_A$, $5HT_3$, and histamine receptors (Karlin, 2002). The α9 subunit diverged early from the nAChR family, which may explain the pharmacological traits it shares with glycine and GABA receptors (Le Novere & Changeux, 1995; Le Novere et al., 2002; Rothlin et al, 1999). The cloning of the α10 nAChR subunit allowed for co-expression of heterologous α9/α10 in *Xenopus laevis* oocytes; and recordings demonstrated that hair cell cholinergic responses are recapitulated in this expression system (Elgoyhen et al., 2001). It has been proposed that hair cells use a pentameric receptor composed of $(\alpha9)_2(\alpha10)_3$ (Plazas et al., 2005). These receptors have a high degree of calcium permeability in expression systems as well as in native hair cells (Weisstaub et al., 2002; Gomez-Casati et al., 2005).

Calcium imaging as well as calcium buffering experiments have demonstrated that the potassium current that follows nAChR activation relies on calcium influx (Shigemoto & Ohmori, 1991; Fuchs & Murrow, 1992a; Oliver et al., 2000). For IHCs, the calcium-dependent potassium channels carrying this outward current are of the SK2 subtype (Glowatzki & Fuchs, 2000; Katz et al., 2004). For outer hair cells (OHCs), waveform analysis, pharmacology, and recordings from BK alpha subunit null mice demonstrate that BK channels support inhibition in high frequency (basal) regions and SK channels support inhibition in low frequency (apical) regions (Rohmann et al., 2015). That basal OHCs utilize large conductance BK channels with rapid kinetics makes sense given the rapidly fluctuating receptor potential expected in high frequency OHCs.

Efferent release mechanisms have been studied using electrical stimulation of axons terminating on early postnatal IHCs. With low frequency stimulation, efferents have low release probabilities, but postsynaptic events facilitate and sum during high frequency stimulation (Goutman et al., 2005). Efferent terminals have P/Q as well as N-type voltage-gated calcium channels that support vesicle release (Zorrilla de San Martin et al., 2010). Pharmacology and immunohistochemistry also suggests that L-type calcium channels can activate BK channels to speed repolarization of efferent terminals in the wake of action potentials (Zorrilla de San Martin et al., 2010).

Knockout mice lacking the α9 subunit have disorganized efferent terminals below OHCs and suppression of cochlear responses fails to occur during efferent stimulation (Vetter et al., 1999). Mice lacking the α10 subunit also have reduced efferent function and only a subpopulation of OHCs displays cholinergic responses (Vetter et al., 2007), presumably mediated by homomeric α9 nAChRs. SK2 channels are necessary for the assembly of efferent synapses, as SK2 knockout hair cells tend to lack efferent innervation (Kong et al., 2008). Thus, both nAChR subunits and SK channels are required for normal efferent function and synaptic assembly.

Knockin mice with a gain of function point mutation in the α9 subunit, which leads to greater calcium influx, have also been generated; and these mice display prolonged IPSCs and less susceptibility to noise-induced hearing loss (Taranda et al., 2009). This finding is consistent with the hypothesis that the efferent system is protective against sound damage (discussed in greater detail in Chapter 5).

4.1.2 Postsynaptic cisterns

Electron micrographs taken through cochlear tissues reveal the postsynaptic cisterns associated with efferent contacts (Smith & Sjostrand, 1961; Saito, 1980). While cisterns exist at efferent synapses on IHCs, only recently has analysis of these cisterns been undertaken. OHC cisterns, on the other hand, have been more extensively studied.

Fuchs and colleagues (2014) reconstructed OHC cisterns from adult mice and performed a detailed analysis of their ultrastructure. These cisterns are co-extensive with the presynaptic efferent terminal (0.93 ratio of cisternal coverage across presynaptic area). Cisterns are consistently spaced from the postsynaptic membrane (~14 nM) and are tethered postsynaptically by unknown molecules visible in many EM sections. Their luminal spacing also tends to be tightly regulated across the synaptic zone.

In the same study, Fuchs and colleagues reconstructed cisterns from mutant mice with altered or absent efferent function. Cisterns from α9 knockin mice (discussed above) differ only in that they have larger luminal gaps, and thus larger volumes than wild-type cisterns. Surprisingly, α9 knockout cisterns, which lack efferent function, have no significant differences from wild-type cisterns. Mouse models lacking potassium channels have more pronounced cisternal phenotypes. Though SK2 knockout OHCs typically lack efferent terminals, Fuchs and colleagues were able to reconstruct a few efferent contacts from the basal turn. Cisterns from these animals had very thin luminal gaps that appeared to fuse occasionally, and thus

they showed the most disorganization of the mouse lines under study. BK channels participate in cholinergic inhibition of basal OHCs, and mice lacking the BK pore-forming subunit have cisterns that are less co-extensive with the presynaptic terminal (Rohmann et al., 2015).

Unfortunately, the phenotypes displayed by these mice do not provide clear clues to the function or functions these structures serve at efferent synapses. Given that wild-type cisterns span the length of presynaptic terminals and that they lie in close proximity to the membrane, they likely serve as diffusion barriers that sequester calcium in the synaptic area. Postsynaptic recordings have provided other insights into cisternal function. Lioudyno and colleagues (2004) recorded from OHCs and found that inhibition of SERCA pumps, which load calcium into stores, reduced the amplitude of currents induced by exogenous ACh application. In the same study, these authors showed that inward synaptic events, evoked by application of high potassium solution, had reduced amplitudes when store-operated calcium release was blocked pharmacologically. These results support the hypothesis that OHC cisterns release calcium to increase inhibition. Nevertheless, ACh application occurred continuously for many seconds, a stimulus that is very distinct from the milliseconds long ACh signal that occurs synaptically. Additionally, because the synaptic events analyzed were evoked by solution exchange, these authors had no control over presynaptic release, making detailed waveform analysis difficult. Perhaps this explains why the time constant decay of these synaptic events, which reflects the total

amount of calcium available to gate potassium channels, showed no apparent change with pharmacological manipulation of cisternal function.

Im and colleagues (2014) investigated cisternal function in chicken hair cells of the basilar papilla, and their recordings showed that the initiation of SK currents depended on calcium entry through nAChRs. Next, these authors took advantage of the fact that neither α9/α10 nAChRs nor SK channels desensitize during long applications of ACh. In the middle of cholinergic responses, the hair cell's membrane potential was stepped to positive voltages, which reduces calcium influx through nAChRs. Instead of recording declining SK currents during steps to -20 mV, they often recorded prolonged currents. Blockade of voltage-gated calcium channels reduced this effect while potentiation of voltage-gated calcium channels prolonged the effect, suggesting that calcium entry through such channels can sustain responses to extended ACh application. Similar voltage step experiments using pharmacology manipulating calcium store operation suggested that calcium release from stores prolongs inhibition as well. When synaptic activity was evoked with high potassium solution, pharmacological potentiation of store-operated calcium release *reduced* the time constant of decay, a curious finding given the results obtained from voltage step recordings. Caveats to these results are similar to those described above. Long ACh application produces a very large calcium signal through the nAChRs, and calcium stores may go through numerous cycles of release and reloading. Additionally, presynaptic effects and effects on the activity of nAChRs during pharmacological manipulation were not investigated.

Electrical stimulation of efferent axons allows the experimenter to control efferent release rates. When evoked with high potassium, efferent release tends to accelerate as calcium builds up in the presynaptic terminal. This often leads to high frequency transmission, where calcium entering through nAChRs may accumulate postsynaptically and obscure the effects of other calcium sources. Additionally, high potassium stimulation only induces inward waveforms that must be recorded at negative holding potentials; and electrical stimulation is superior in that it allows for interrogation of the outward SK currents at different membrane potentials. Unfortunately, due to the geometry of the cochlear epithelium, electrical stimulation of efferent axons contacting OHCs has proved challenging for many investigators, and future studies may benefit from optogenetic control of efferent release.

Experiments presented below investigate the role of cisternal calcium release in shaping efferent inhibition of young IHCs. Cisternal calcium release has been implicated in both the "fast effect" and the "slow effect" of auditory nerve compound action potential (CAP) suppression during high frequency stimulation of the olivocochlear bundle (OCB; Sridhar et al., 1995; Sridhar et al., 1997). Sridhar and colleagues propose that OHC synaptic cisterns can release calcium to increase the fast CAP suppression that occurs within 100 ms of OCB stimulation. Slow CAP suppression can occur over tens of seconds, and calcium release from "sub-surface cisterns" (which are not synaptically localized) may allow for the extended gating of calcium-dependent potassium channels during slow effects. The data presented below may provide a better understanding of how fast effects are regulated. Slow

effects are seen under high frequency stimulation conditions (~300 Hz for 300 ms) and the low frequency protocols used in the present study (1 Hz stimulation) will not produce the large calcium signals thought to underlie slow effects generated by OHCs.

4.1.3 CaV1.3 and voltage-gated calcium currents

IHCs express CaV1.3 L-type voltage-gated calcium channels, and recordings from IHCs of CaV1.3 null mice reveal dramatically reduced calcium currents and exocytosis (Brandt et al., 2003). Calcium spikes, which IHCs exhibit prior to the onset of hearing (Marcotti et al., 2003a), are also absent in CaV1.3 knockout mice (Brandt et al., 2003). IHC calcium spikes produce glutamate release onto afferent neurons that shape ascending auditory activity during development (Tritsch et al., 2010). CaV1.3 function is crucial to IHC maturation as CaV1.3 null animals fail to develop mature potassium conductances and retain efferent synaptic contacts characteristic of immature IHCs (Brandt et al., 2003).

The arrangement of CaV1.3 channels changes during development in a manner that promotes maturation of IHC afferent synapses. While IHCs are capable of firing calcium spikes, many extrasynaptic CaV1.3 channels are present (Zampini et al., 2010; Wong et al., 2014). During this period, the calcium dependence of transmitter release is less efficient than for mature IHCs (Johnson et al., 2005; Wichmann & Moser, 2015). Around the onset of hearing, extrasynaptic CaV1.3 channels disappear, ribbon refinement and enlargement occurs, CaV1.3 channel

clusters achieve their mature stripe-like arrangement around ribbons, and the calcium efficiency of exocytosis increases (Johnson et al., 2005; Wong et al., 2014; Wichmann & Moser, 2015). Thus, ribbons and their associated vesicles are more tightly associated with voltage-gated calcium channels, and this refinement underlies better functional performance at IHC afferent synapses.

It is intriguing that global calcium signals, mediated by extrasynaptic CaV1.3 channels and calcium spiking behavior, exist alongside efferent innervation of IHCs. This situation may be permissive to interactions between the afferent and efferent pathways at the level of the IHC. Indeed, some evidence exists that this may be the case. As stated above, CaV1.3 knockout mice retain their efferent synapses, suggesting that voltage-gated calcium influx and spiking behavior may regulate efferent innervation of IHCs. SK2 channels that confer inhibition to efferent synapses also shape IHC action potentials (Marcotti et al., 2004), and SK2 knockout mice display an increase in the calcium dependence of exocytosis (Johnson et al., 2007). Though this defect has been attributed to disturbed action potential patterning, the absence of efferent function may also contribute to the exocytosis phenotype. Mice lacking the α9 subunit or synaptotagmin in efferent terminals also have abnormal maturation of exocystosis, providing confirmation that efferent synapses on IHCs contribute to afferent maturation (Johnson et al., 2013).

4.2 Experimental results

The discussion above motivated the experiments presented in this chapter. Specifically, experiments were designed to test the hypothesis that postsynaptic cisterns and voltage-gated calcium contribute to SK channel gating at efferent synapses on early postnatal IHCs. Whole-cell voltage-clamp recordings from P7-9 rat IHCs were carried out, and electrical stimulation was used to evoke efferent transmitter release. Stimulation was carried out at 1 Hz, a low frequency that minimized IHC calcium loading via nAChR influx. Analysis was performed on evoked and "spontaneous" events. It should be noted that low (2.5 mM) external potassium was used in the external solution, which sets E_K at -100 mV; and that these conditions are not conducive to true spontaneous release. Rather, events that are not time-locked to the electrical stimulus may be considered delayed release in that they likely depend on the ongoing excitatory stimulus. See Chapter 3, Methods, for a complete description of the experimental procedures.

Analysis was performed on outward SK waveforms at holding potentials that produce varying degrees of voltage-gated calcium influx. Pharmacological manipulations were performed to test whether or not cisternal calcium and voltage-gated calcium contribute to efferent inhibition. Finally, the hypothesis that IHC cholinergic responses encode prior depolarization was tested.

For synaptic responses, data is present for event amplitude, half width, and time constant of decay. While amplitude changes during pharmacological manipulations may be relevant, more emphasis should be placed on how event

duration (half width) and decay kinetics (time constant of decay) are altered. These measures reflect the calcium signal that gives rise to SK channel activation; and, thus, larger calcium signals can be read out via longer event half width and prolonged time constants of decay. Therefore, pharmacological manipulations that alter cisternal function and voltage-gated calcium channel activity are expected to have large effects on event half width and time constant of decay, if these elements are indeed involved in efferent inhibition.

4.2.1 Voltage dependence of IPSC waveforms

Recordings revealed that IPSC waveforms display voltage dependence. Figure 4.1 A shows representative traces of outward IPSCs recorded at -60 mV (n = 4 cells), -40 mV (n = 3 cells), and -20 mV (n = 4 cells). As described above, these outward currents are potassium currents carried by SK2 calcium-dependent potassium channels. Thus, as expected, the amplitude of IPSCs increased as the membrane potential was stepped to depolarized potentials further away from E_K (Figure 4.1 B). Mean (SD) amplitudes were: 15.31 pA (7.9) at -60 mV, 21.95 pA (10.9) at -40 mV, and 37.61 pA (13.33) at -20 mV.

Less expected is the effect voltage had on IPSC time course. At depolarized potentials, the inward driving force of calcium ions through nAChRs is reduced, though it should be noted that the reduction is fairly minor given the very positive reversal potential of calcium (see Martin & Fuchs, 1992 for quantitation). With less

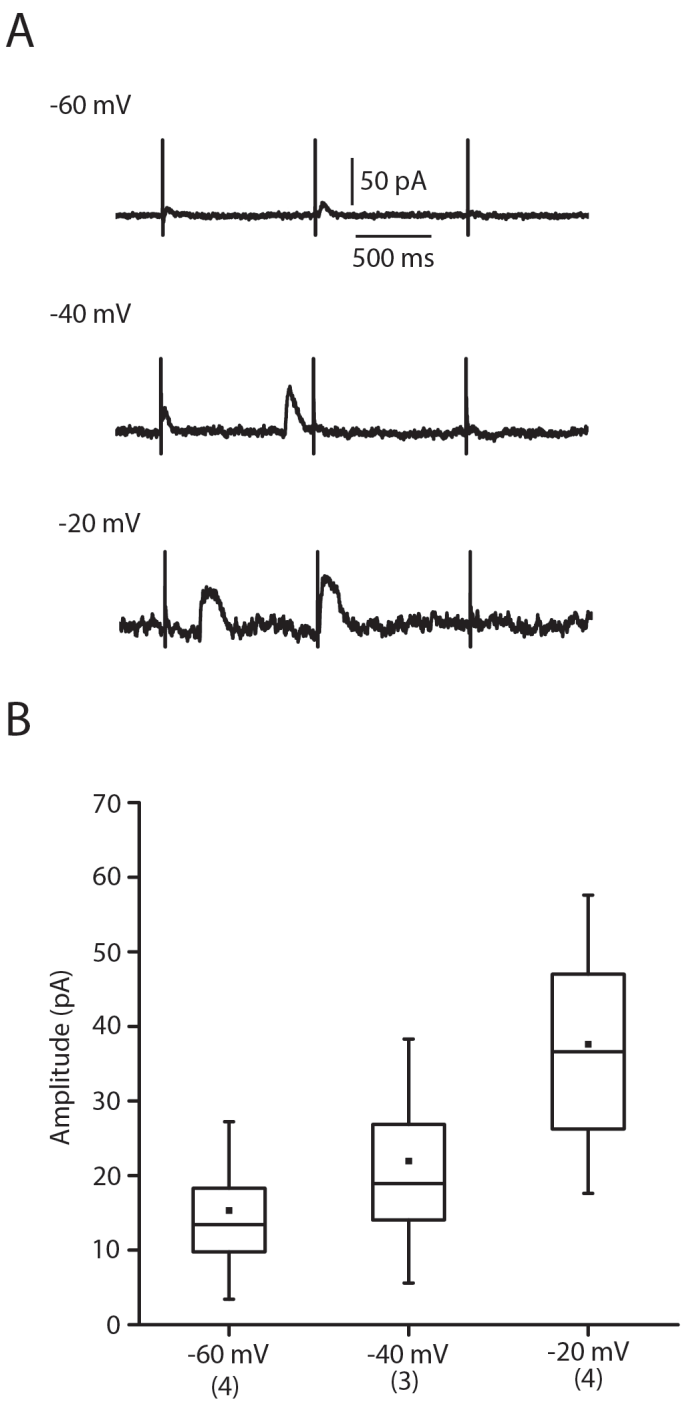

Figure 4.1: IPSC waveforms and membrane potential. A, Exemplar IPSCs evoked by electrical stimulation at -60 mV, -40 mV, and -20 mV. B, Events recorded at depolarized potentials have larger amplitudes, reflecting the larger outward driving force on potassium ions. Box (upper and lower quartiles) and whisker (standard deviation) plots of data; center line: median; black box: mean.

calcium entering the IHC through nAChRs, one would expect a briefer calcium signal and shorter SK currents. The data, however, reveal the opposite effect.

The half width duration of IPSCs was longer at depolarized potentials (Figure 4.2 A). Mean (SD) half widths were: 49.16 ms (22.2) at -60 mV, 54.35 ms (29.8) at -40 mV, and 82.93 ms (44.6) at -20 mV. The time constant of decay of IPSCs was analyzed and also revealed prolonged events at depolarized potentials (Figure 4.2 B). The mean (SD) time constants of decay were: 41.79 ms (17.1) at -60 mV, 47.63 ms (24.9) at -40 mV, and 74.85 ms (39.3) at -20 mV. Consistent with this analysis, the cumulative probabilities of decay time constants show a rightward shift (towards longer time constants) at depolarized voltages.

These data indicate that with depolarization, and presumably reduced calcium influx through nAChRs, IPSC waveforms are unexpectedly prolonged. One explanation for this finding is that other calcium sources contribute to SK channel activation. However, presynaptic effects on efferent transmitter release can be induced upon IHC depolarization (see Discussion). Therefore, pharmacological manipulations were performed at a single voltage (-40 mV) to investigate the role of postsynaptic cisterns and voltage-gated calcium in shaping efferent IPSCs.

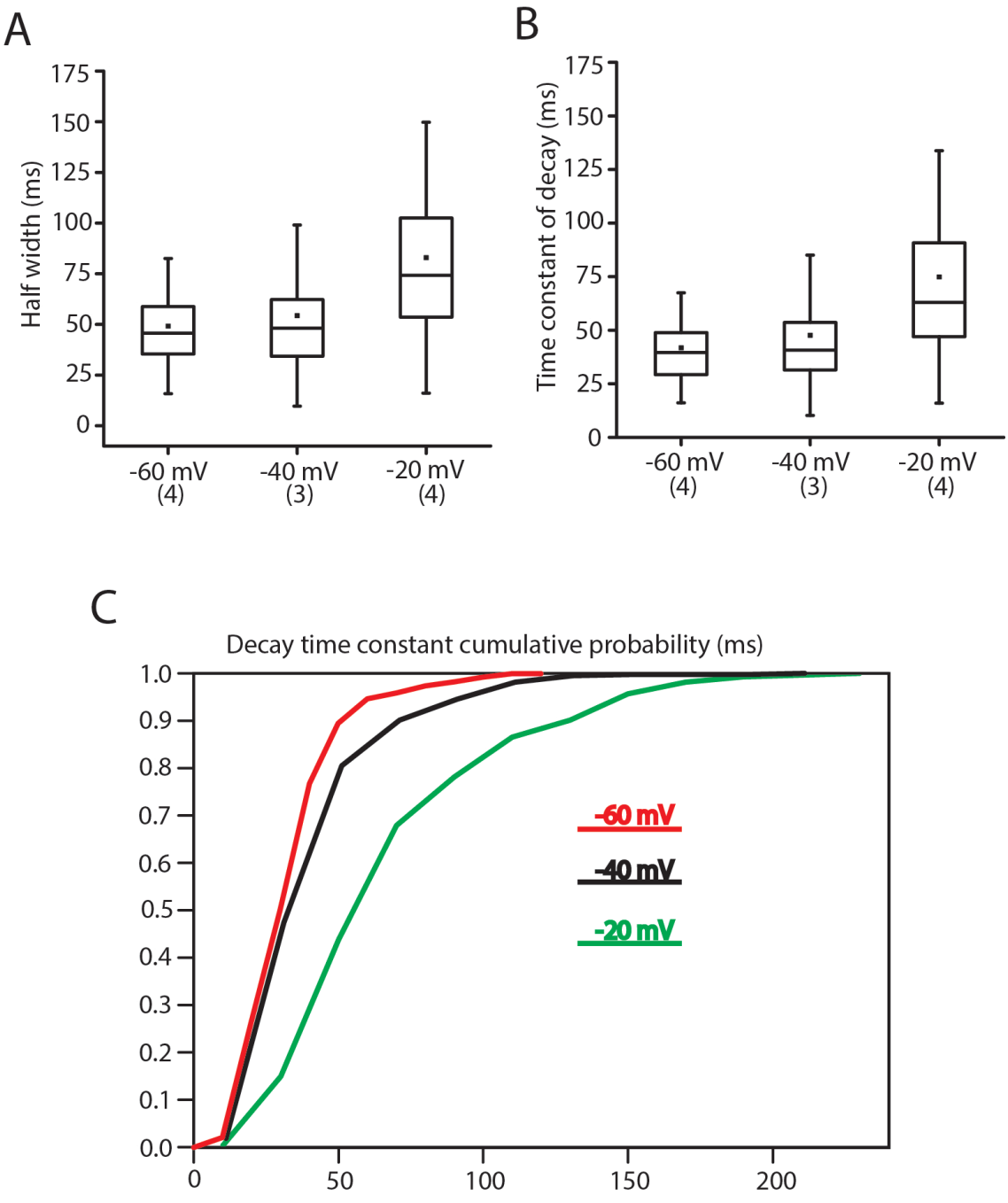

Figure 4.2: IPSC duration and membrane potential. A, B Box (upper and lower quartiles) and whisker (standard deviation) plots of IPSC half width and time constant of decay at -20 mV, -40 mV, and -60 mV (center line: median; black box: mean). C, Cumulative probability plots of IPSC time constant of decay at -20 mV, -40 mV, and -60 mV.

4.2.2 Calcium-induced calcium release contributes to IPSC waveforms

It is thought that postsynaptic cisterns in hair cells release their stores in a calcium-induced calcium release (CICR) fashion (Lioudyno et al., 2004). Ryanodine modulates CICR by inhibiting CICR at high concentrations and potentiating CICR at low concentrations (McPherson et al., 1991; Shmigol et al., 1994; Verkhratsky & Shmigol, 1996). We recorded IPSCs at -40 mV in control conditions (n = 3 cells) as well as in the presence of inhibiting (150 μM, n = 3 cells) and potentiating (1 μM n = 3 cells) concentrations of ryanodine to test whether CICR prolongs efferent synaptic waveforms, and representative traces are reproduced in Figure 4.3 A. The mean (SD) IPSC amplitudes were: 21.95 pA (10.9) for control recordings, 17.11 pA (7.3) for recordings in 150 μM ryanodine, and 22.81 pA (13.2) for recordings in 1 μM ryanodine (Figure 4.3 B).

Interestingly, ryanodine had dramatic effects on IPSC time course. IPSC half width means (SD) were: 54.35 ms (29.8) for control recordings, 30.37 ms (10) for recordings in 150 μM ryanodine, and 73.91 ms (47.7) for recordings in 1 μM ryanodine (Figure 4.4 A). Similar effects were found for IPSC time constants of decay in these recordings. Mean (SD) time constants of decay were: 47.63 ms (24.9) for control recordings, 27.42 ms (8.3) for recordings in 150 μM ryanodine, and 64.21 ms (43.7) for recordings in 1 μM ryanodine (Figure 4.4 B). Cumulative probability plots of the decay time constants reveal a leftward shift (shorter time constants) in 150 μM ryanodine and a rightward shift (longer time constants) in 1 μM ryanodine (Figure 4.4 C). As discussed in Chapter 3 (Methods), data from multiple cells were

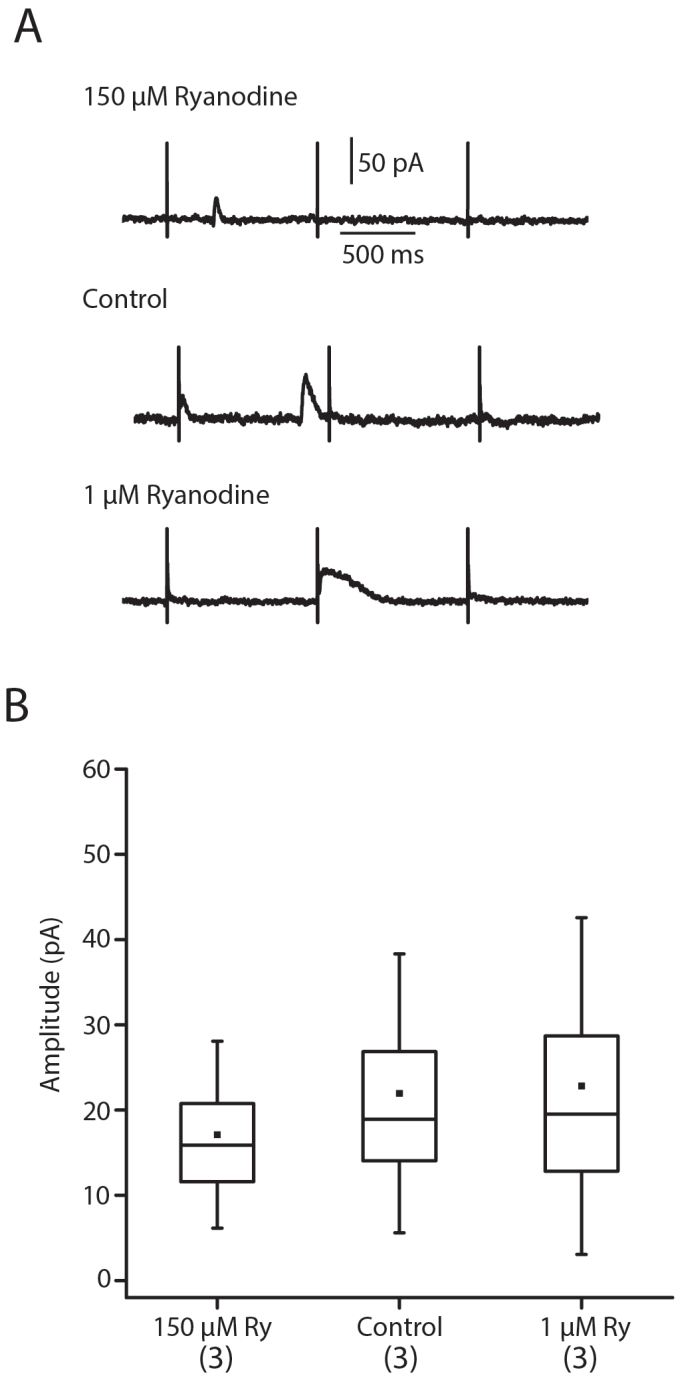

Figure 4.3: IPSC waveforms and CICR. A, Exemplar IPSCs evoked by electrical stimulation at -40 mV for recordings in 150 µM ryanodine, control recordings, and recordings in 1 µM ryanodine. B, Event amplitudes. Box (upper and lower quartiles) and whisker (standard deviation) plots of data; center line: median; black box: mean.

pooled in each of these conditions. Box and whisker plots of half width and time constant of decay are plotted individually for each cell in Appendix Figure A1.

To complement recordings of outward SK currents, recordings of isolated receptor currents were made by voltage clamping cells at E_K in the presence of the SK channel blocker apamin (400 nM). In control conditions, nAChR currents had amplitudes of 8.7 pA (SD: 3.4) and decay time constants of 15.56 ms (SD: 7.4). Interestingly, receptor currents recorded in 150 μM ryanodine decayed with slower kinetics (tau: 19.04 ms, SD: 9.6 ms) and had no change in amplitude (8.6 pA, SD: 2.8). Thus, even though outward currents were briefer in 150 μM ryanodine, isolated currents through nAChRs were ~3.5 ms longer on average. Previous work demonstrated that high concentration of ryanodine enlarges α9/ α10 receptor currents in response to exogenous ACh application (Zorrilla de San Martin et al., 2007), and the present work extends those findings to synaptic responses. Receptor currents in 1 μM ryanodine had larger amplitudes than control currents (10.37 pA, SD: 4.2) but slightly shorter decay time constants (14.15 ms, SD: 6.8), similar to results obtained for chicken hair cells (Im et al., 2014).

Taken together, these results indicate that CICR contributes to the calcium signals giving rise to SK currents. Removing CICR reduces SK current durations and decay time constants even though nAChR currents are longer lasting; and potentiating CICR dramatically prolongs SK currents. These findings are in keeping with the ustrastructure of efferent synapses on IHCs, which always feature postsynaptic cisterns that are the likely source of the CICR described here.

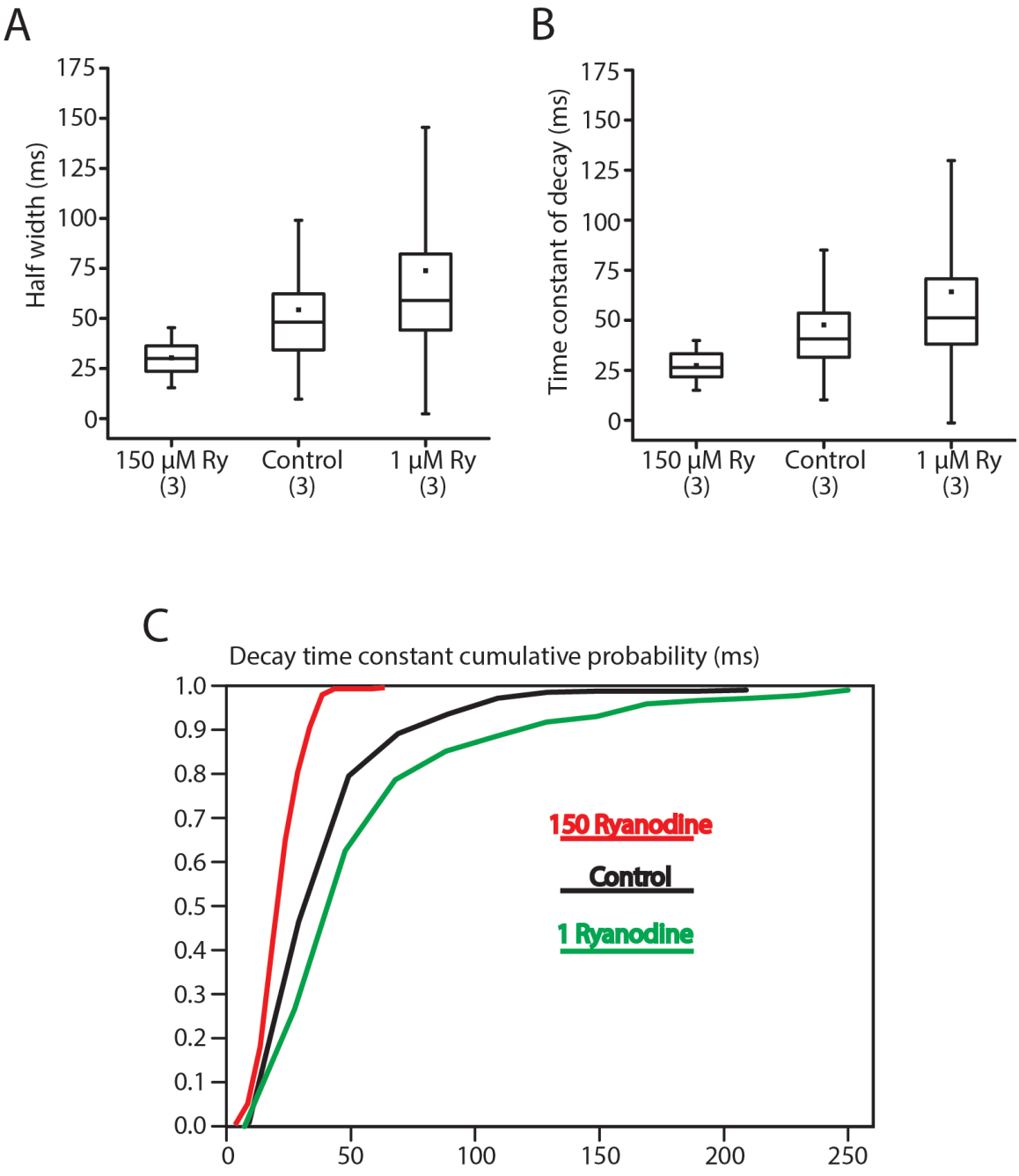

Figure 4.4: IPSC duration and CICR. A, B Box (upper and lower quartiles) and whisker (standard deviation) plots of IPSC half width and time constant of decay for recordings in 150 µM ryanodine, control recordings, and recordings in 1 µM ryanodine. (center line: median; black box: mean). C, Cumulative probability plots of IPSC time constant of decay.

4.2.3 Voltage-gated calcium contributes to IPSC waveforms

Though postsynaptic cisterns may uptake calcium that is fluxed through nAChRs to reload their stores, this possibility seems more likely to occur under high frequency stimulation conditions. Under the 1 Hz stimulation conditions used in present experiments, cisterns are far more likely to be loaded with calcium that enters the IHC through voltage-gated calcium channels. Indeed, when IHCs are voltage clamped at -20 mV, IPSCs are prolonged (Figures 4.1 & 4.2); and -20 mV is near the potential at which IHC whole cell calcium currents are the largest (Brandt et al., 2003) and CaV1.3 channels have the greatest open probability (Zampini et al., 2010).

To test for the involvement of voltage-gated calcium during efferent inhibition of IHCs, we recorded IPSCs at -40 mV in control conditions (n = 3 cells) and while modulating Cav1.3 channel function. Nimodipine, an L-type calcium channel blocker, was used at 10 μM to block CaV1.3 currents (n = 5 cells); and Bay K 8644 (Bay K), a L-type calcium channel activator, was used at 10 μM to potentiate CaV1.3 currents (n = 3 cells). Representative traces are reproduced in Figure 4.5 A.

The mean (SD) IPSC amplitudes were: 21.95 pA (10.9) for control recordings, 20.42 pA (13.4) for recordings in 10 μM nimodipine, and 26.11 pA (11.1) for recordings in 10 μM Bay K (Figure 4.5 B). These amplitude changes are slight; and, as discussed above, measurements of event duration better reflect the calcium signals that shape SK channel activity.

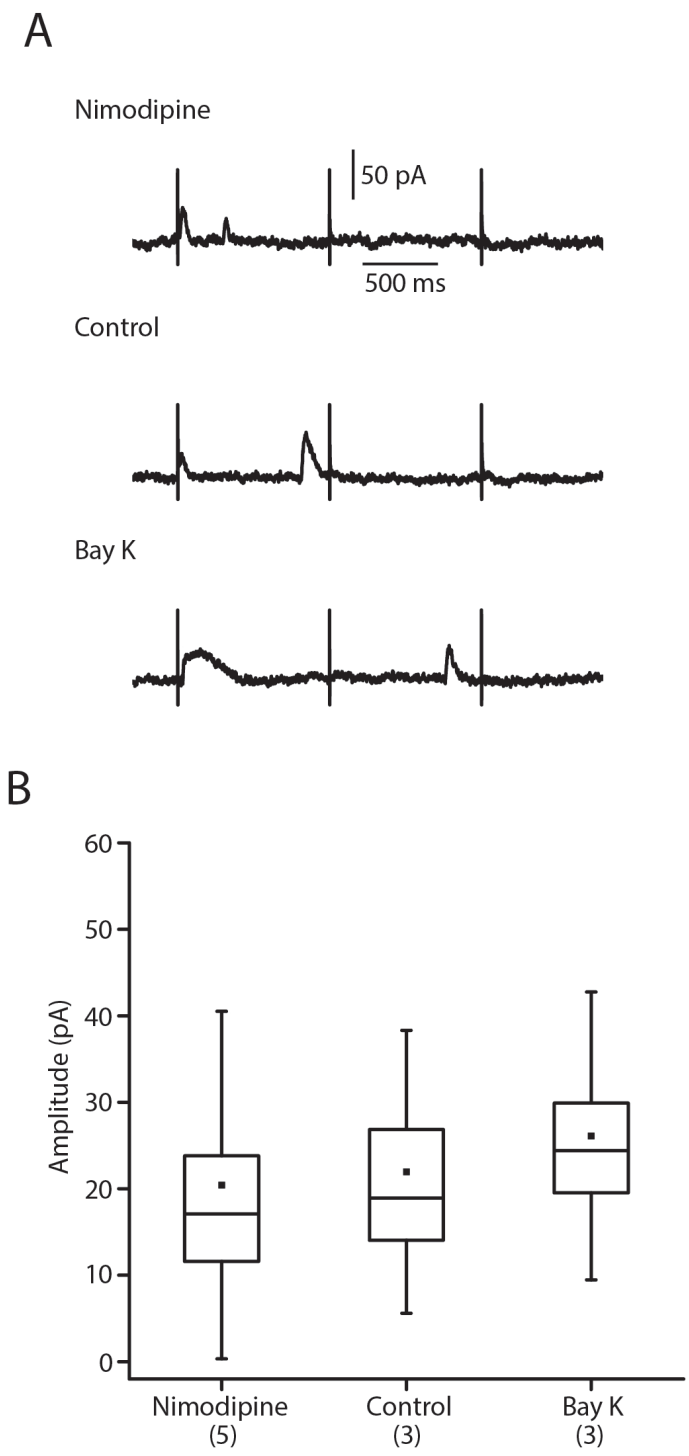

Figure 4.5: IPSC waveforms and voltage-gated caclium. A, Exemplar IPSCs evoked by electrical stimulation at -40 mV for recordings in 10 µM nimodipine, control recordings, and recordings in 10 µM Bay K. B, Event amplitudes. Box (upper and lower quartiles) and whisker (standard deviation) plots of data; center line: median; black box: mean.

Consistent with the notion that voltage-gated calcium prolongs the calcium signal that gives rise to SK channel activation, the time course of IPSCs was altered dramatically in these drug conditions. IPSC half width means (SD) were: 54.35 ms (29.8) for control recordings, 39.01 ms (13.9) for recordings in 10 μM nimodipine, and 87.38 ms (62.5) for recordings in 10 μM Bay K (Figure 4.6 A). Similar effects were found for IPSC time constant of decay in these recordings. Mean (SD) time constants of decay were: 47.63 ms (24.9) for control recordings, 33.32 ms (10.57) for recordings in 10 μM nimodipine, and 74.96 ms (52.8) for recordings in 10 μM Bay K (Figure 4.6 B). Cumulative probability plots of the decay time constants reveal a leftward shift in 10 μM nimodipine and a rightward shift in 10 μM Bay K (Figure 4.6 C). As discussed in Chapter 3 (Methods), data from multiple cells were pooled in each of these conditions. Box and whisker plots of half width and time constant of decay are plotted individually for each cell in the Appendix, Figure A2.

These results indicate that CaV1.3 channel activity can be positively and negatively modulated to alter IPSC waveform. Reducing CaV1.3 function shortens IPSC time course and decay kinetics, while potentiating CaV1.3 function has the opposite effect. Importantly, the voltage-gated calcium that shapes IPSCs does so in response efferent transmitter release (as opposed to generating a standing SK current), suggesting that it is stored until it is deployed. This supports the notion that voltage-gated calcium is stored in postsynaptic cisterns and released in a CICR fashion after nAChR activation.

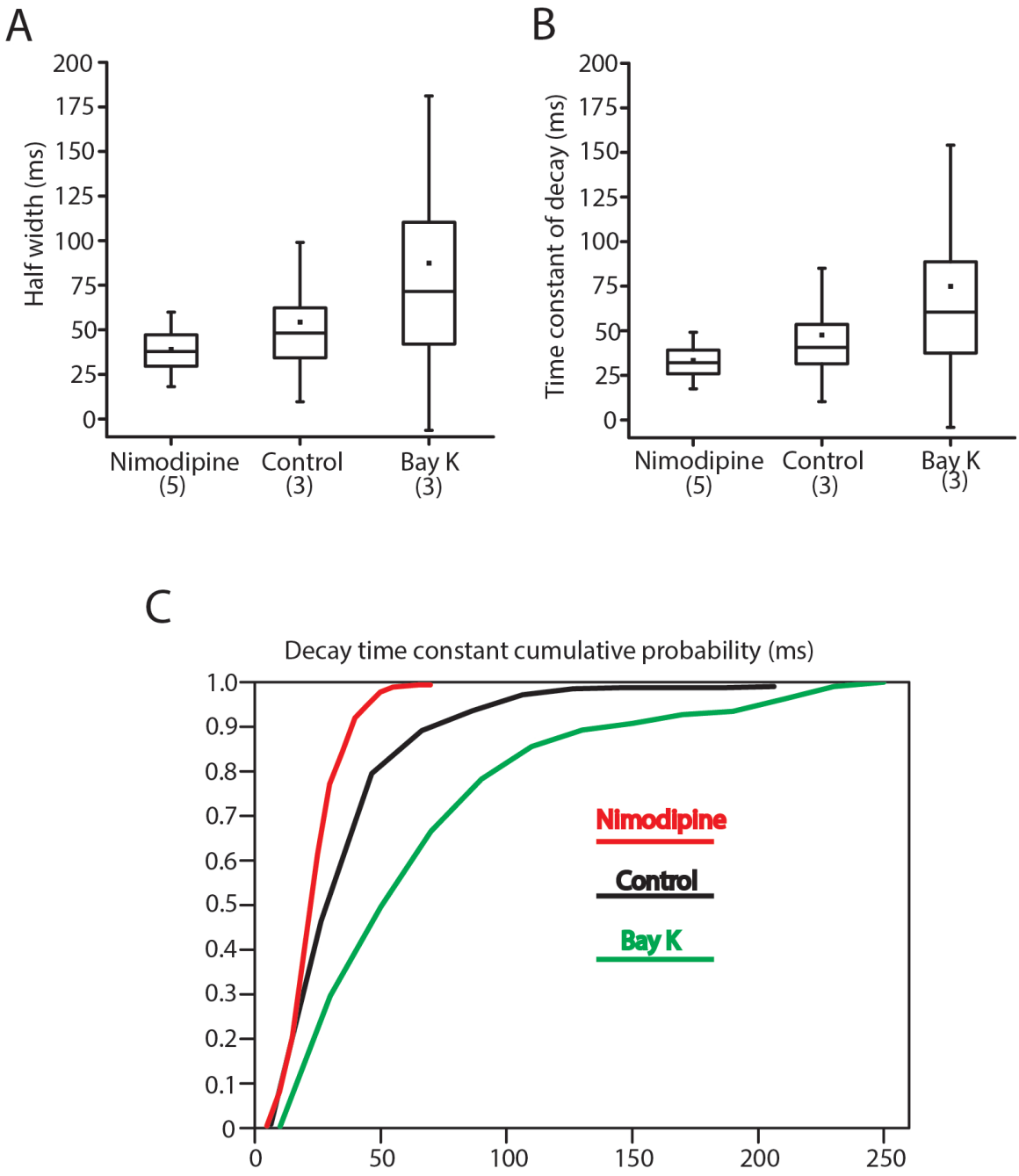

Figure 4.6: IPSC duration and voltage-gated calcium. A, B Box (upper and lower quartiles) and whisker (standard deviation) plots of IPSC half width and time constant of decay for recordings in 10 µM nimodipine, control recordings, and recordings in 10 µM Bay K. (center line: median; black box: mean). C, Cumulative probability plots of IPSC time constant of decay.

4.2.4 Cholinergic responses encode recent IHC depolarization

The experiments above suggest cholinergic responses may be modulated by depolarization via calcium influx through CaV1.3 channels, storage in synaptic cisterns, and subsequent release. This hypothesis was tested by exogenously applying ACh with a picospritzer, which allows for controlled ACh delivery. Micropipettes filled with external solution containing 100 μM ACh were lowered toward IHCs after attaining the whole-cell configuration with a recording pipette. It was important to position the solution delivery pipette such that very brief ACh puffs produced consistent responses, and the puffer pipette was regularly embedded in the tissue near the IHC to achieve this effect. The duration of ACh application was as brief as possible to avoid saturation (5 – 50 ms).

Once stable recordings were achieved and ACh application parameters were fine tuned, the following protocol was applied: IHCs were voltage clamped at -60 mV and ACh was briefly applied (1st response) and IHCs remained at -60 mV for another 2 s to record the entire response and allow the membrane current to return to rest, then membrane voltage was stepped to -20 mV for 5 s and returned to -60 mV for 2 s to allow the membrane current to return to rest, then ACh was applied once more (2nd response). A membrane current response to this protocol is shown at the top of Figure 4.7 A. Every other protocol provided the same ACh application without a depolarizing step, and the membrane current response to such a protocol is shown at the bottom of Figure 4.7 A.

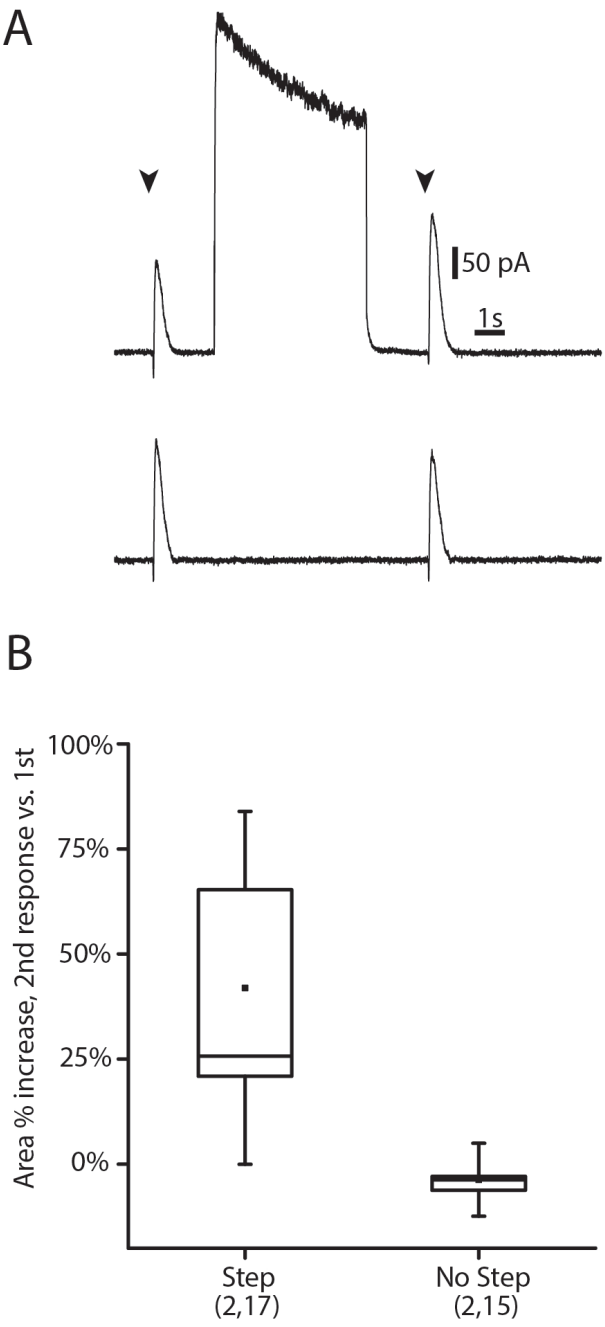

Figure 4.7: Cholinergic responses encode recent IHC depolarization. A, IHC responses to brief ACh puffs are larger after depolarizing steps to -20 mV (top). For interleaved trials without depolarization steps, cholinergic responses were unaltered (bottom). Arrow heads: ACh application. B, Quantification of the percent change in area (second response vs first) for trials with depolarizing step and trials without depolarizing step. Box (upper and lower quartiles) and whisker (standard deviation) plots of data; center line: median; black box: mean.

For every trial, the area of both the 1st and 2nd responses were determined and compared. It was crucial to compare responses within trial, as opposed to lumping all 1st responses and 2nd responses together, because responses change over time as the IHC deteriorates. Additionally, slight changes in the distance between the IHC and the puffer pipette occur over the course of the recording, which may result in altered waveforms. For trials in which a depolarizing step separated the 1st and 2nd responses, the 2nd response was 41.9% larger than the 1st response (SD: 27%). However, for interleaved trials in which there was no voltage step, there was effectively no difference between the 2nd and 1st responses (2nd responses were 3.7% smaller than the 1st, SD: 5.8%). These data are presented in Figure 4.7 B. Thus, cholinergic responses are modulated by recent IHC depolarization.

To test the hypothesis that voltage-gated calcium influx during depolarization is necessary for the potentiation of cholinergic responses, similar recordings were performed in the presence of the L-type calcium channel blocker nimodipine (10 μM). Traces of membrane current responses with and without depolarizing voltage steps are presented in Figure 4.8 A. With depolarizing steps, the 2nd response was 2.6% larger than the 1st response (SD: 11%); and without depolarizing steps, the 2nd response was 0.7% larger than the 1st response (SD: 7.9%). These date are quantified in Figure 4.8 B. Thus, there was no change in cholinergic responses in nimodipine even when depolarizing voltage steps were applied, and cholinergic potentiation required the influx of voltage-gated calcium.

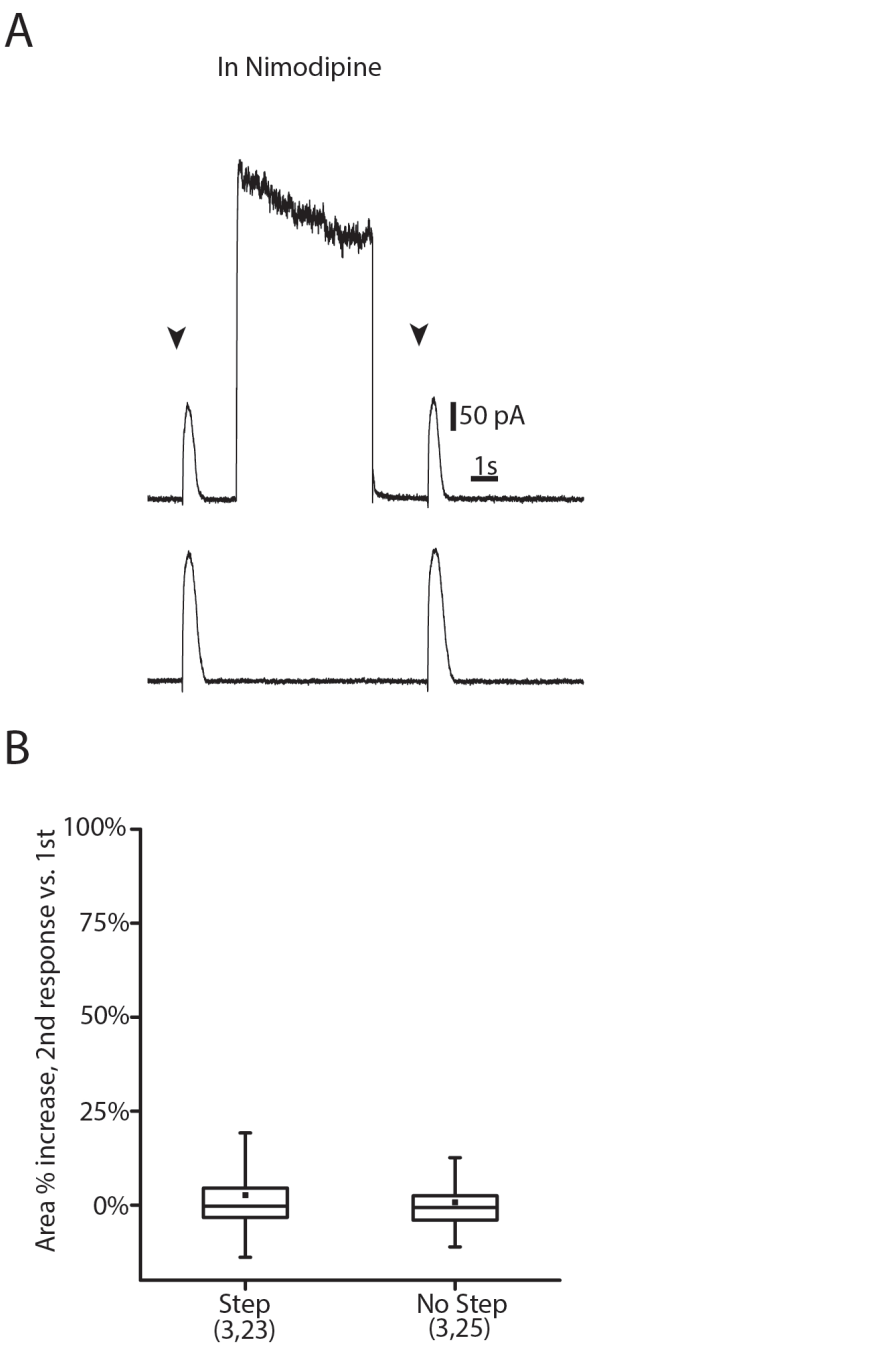

Figure 4.8: Cholinergic potentiation after depolarization requires voltage-gated calcium influx. A, IHC responses to brief ACh puffs are unchanged after depolarizing steps to -20 mV (top) in 10 μM nimodipine. For interleaved trials without depolarization steps, cholinergic responses were unaltered as well (bottom). Arrow heads: ACh application. B, Quantification of the percent change in area (second response vs first) for trials with depolarizing step and trials without depolarizing step (all in nimodipine) Box (upper and lower quartiles) and whisker (standard deviation) plots of data; center line: median; black box: mean.

4.3 Discussion

While collecting the data presented here, care was taken to avoid sample biases. Nevertheless, some cells were excluded from analysis if the recording ended prematurely. No cells were excluded based on the profile or characteristics of their IPSC waveforms. Traces were analyzed manually using MiniAnalysis software and the experimenter was not blinded to the drug condition of the recordings, which may introduce bias into event selection.

The present work provides strong evidence that calcium signals from non-synaptic (i.e. not via nAChRs) sources contribute significantly to efferent inhibition of early postnatal IHCs. These recordings were carried out exclusively in apical cochlear tissue, and the role of cisternal calcium and voltage-gated calcium in efferent inhibition of basal IHCs is unknown. Given that many features of the cochlea display gradients across the tonotopic axis, it is possible that CICR and voltage-gated calcium differentially shape SK channel activation in basal IHCs.

The half width and time constant of decay of IPSCs are proxies for the calcium signal that activates SK channels, with longer events and longer time constants of decay suggesting that more calcium is available to gate these channels. A simple comparison of IPSC waveforms across voltages (-60 mV, -40 mV, and -20 mV) produced unexpected results: IPSCs are longer at depolarized potentials even though nAChR calcium flux should not increase. Further experiments showed that IPSC half width and time constant of decay are reduced when cisternal function and voltage-gated calcium channel activity are inhibited; and both measures are prolonged when

cisternal function and voltage-gated calcium channel activity are potentiated. Such bidirectional modulation is strong evidence that both of these elements (cisterns and CaV1.3 channels) contribute to the function of efferent synapses on IHCs.

Additional evidence exists in the variation in half widths and time constants of decay. The apparent variation increased when cisternal and voltage-gated calcium channel function were potentiated and reduced when these calcium sources were inhibited (Figures 4.4, 4.6, Appendix A1 & A2). Thus, when additional calcium sources were removed, IPSC waveforms were more consistent, as one would expect if the dominant calcium signal shaping SK waveforms was quantal-like influx through nAChRs. Increased variation when cisternal and voltage-gated calcium channel function were potentiated is expected given that cisterns must load and release dynamically during these recordings. This dynamic activity could produce "short," "normal," and "long" events as cisterns will at various points in time have depleted, normal, and large calcium loads. It is important to emphasize here that voltage-gated calcium reaches SK channels via the synaptic cisterns (i.e. events in Bay K are triggered by efferent release and do not represent a standing SK current).

These observations provided the foundation for the final set of experiments demonstrating that cholinergic responses encode recent IHC depolarization (Figure 4.7). Because cholinergic potentiation was shown via exogenous ACh application, the mechanism supporting this potentiation must be postsynaptic in origin. This potentiation was blocked in the presence of nimodipine, demonstrating that voltage-gated calcium influx is required. A model of calcium flow and regulation across afferent and efferent synapses is overlaid onto an electron micrograph in Figure 4.9.

The following discussion frames these findings in the context of presynaptic efferent plasticity, the development of the afferent auditory pathway, and the growing appreciation of synaptic crosstalk between the efferent and afferent systems at the level of the IHC.

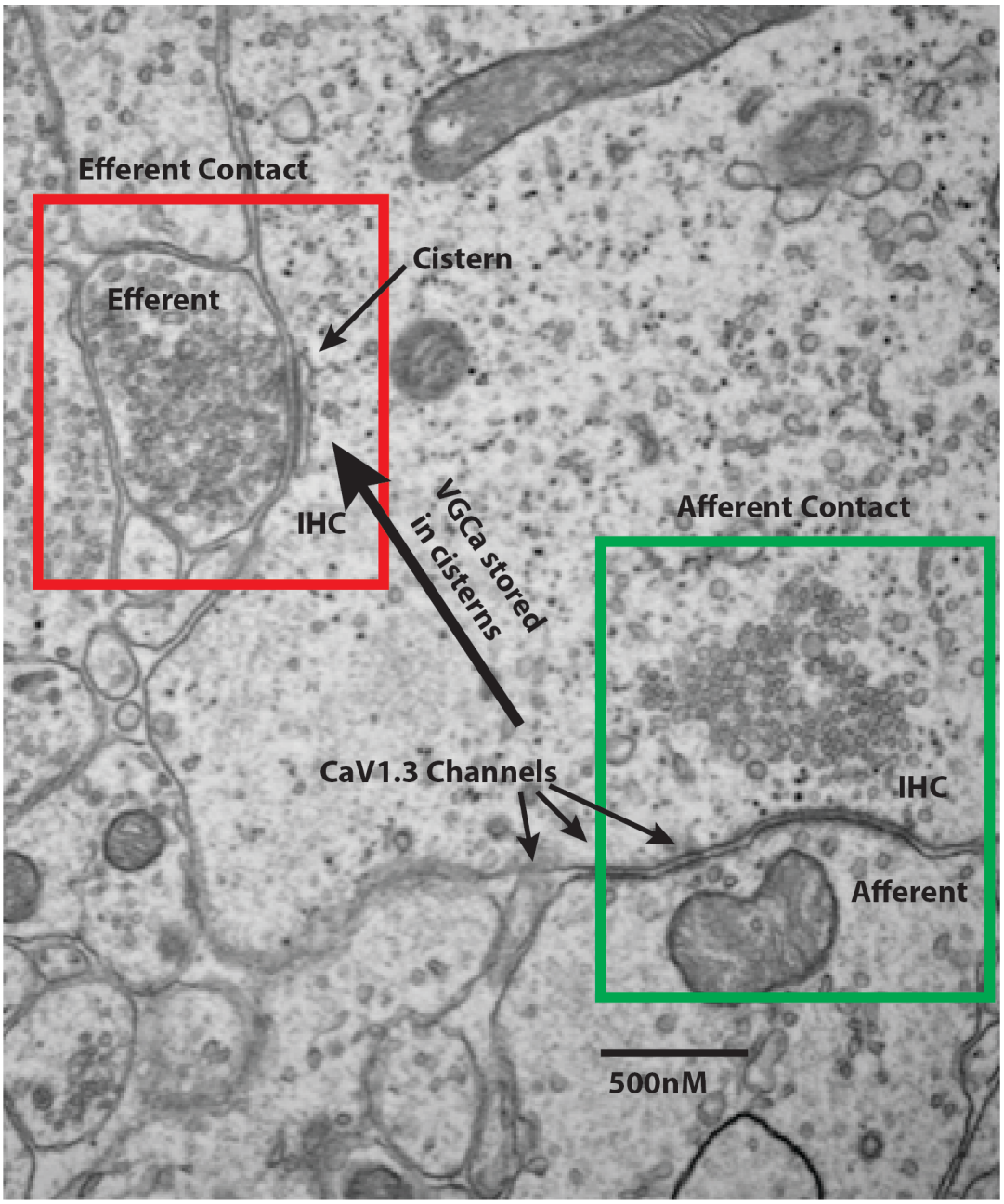

Figure 4.9: Model of synaptic interaction. EM from a P7 rat IHC. Afferent area in green box. The presynaptic ribbon is present in a nearby section, and the cloud of synaptic vesicles is associated with that ribbon. Efferent area in red box, with a vesicle dense presynaptic terminal and a postsynaptic cistern clearly visible. Both synaptic and extrasynaptic CaV1.3 channels are present at this age. Some calcium that enters the IHC through CaV1.3 channels is stored in cisterns present at efferent synaptic contacts. Cisternal calcium is released through CICR to activate SK channels.

4.3.1 IHC regulation of presynaptic efferent function

The experiments here demonstrate that calcium handling within the IHC lead to plasticity of synaptic waveforms and that cholinergic responses are modulated by recent IHC depolarization. Calcium entry into the IHC though voltage-gated channels is a key mechanistic element in this postsynaptic form of plasticity; but calcium entry into IHCs also produces two forms of presynaptic plasticity, which are described below. All of these mechanisms operate synergistically to potentiate inhibition.

Kong and colleagues (2012) found that elevating IHC free calcium increases presynaptic release probability via the generation of nitric oxide, which crosses into the efferent terminal where it has second messenger effects. Kong performed IHC recordings with internal solution containing cADPR, a membrane impermeant compound that releases intracellular calcium stores, and observed increases in release probability that presumably resulted from the generation of a calcium-dependent second messenger. Raising intracellular calcium via brief voltage steps also increased release probability. Nitric oxide was implicated as the second messenger at work because nitric oxide scavengers blocked increases in release probability and nitric oxide donors increased spontaneous release. Importantly, neuronal nitric oxide synthase, which is activated by calcium-calmodulin, is expressed in the cochlea (Fessenden et al., 1994).

In addition to the findings of Kong and colleagues, unpublished data from the Glowatzki lab indicate that efferent release probability can be increased via activation of presynaptic metabotropic glutamate receptors. Such facilitation can occur via IHC

glutamate release and spillover onto efferent terminals. This form of presynaptic plasticity is necessarily calcium-dependent, as IHC vesicle release occurs in a calcium-dependent fashion.

Thus increases in IHC calcium can act in at least three ways to potentiate efferent inhibition: (i) presynaptic facilitation via nitric oxide, (ii) presynaptic facilitation via metabotropic glutamate receptor activation, and (iii) postsynaptic potentiation of SK channel activation via CICR and voltage-gated calcium influx. These synergistic mechanisms may function to instruct the maturation of auditory pathways.

4.3.2 Cholinergic potentiation in the context of maturation

Future experiments must be carried out to determine why the IHC has retrograde effects on efferent release probability and mechanisms for postsynaptic potentiation of efferent inhibition. However, that these efferent synapses exist on IHCs during a crucial period of circuit development suggests that they may be important for auditory system maturation. It may be the case that potentiation of inhibition sharpens boundaries of excitation in a manner that promotes circuit refinement.

The prehearing cochlea contains a layer of supporting cells, known as Kölliker's organ, that sits above IHCs and their associated afferent and efferent contacts (Retzius, 1884; Wada, 1923; Hinojosa, 1977). Tritsch and colleagues (2007) found that these supporting cells coordinate activity of groups of IHCs via ATP

release. Bouts of ATP release from supporting cells induced long depolarizing currents in IHCs; and, when recorded in current clamp, ATP release drove IHCs to fire calcium action potentials. Afferent recordings revealed that these cells too exhibited spiking behavior that was initiated by supporting cell activation. ATP release binds autoreceptors on supporting cells, producing osmotic changes in cell shape and potassium efflux, which depolarizes nearby IHCs (Wang et al., 2015). While the exact role of this spontaneous prehearing activity is unclear, the activity generated in the cochlea propagates to higher auditory centers (Tritsch et al., 2010); thus it may be crucial for circuit establishment and refinement.

Supporting cell driven IHC excitation is spatially restricted, and this feature may be important for functional consolidation of auditory pathways. In this context, the potentiation of efferent inhibition, which is driven presynaptically and postsynaptically by IHC calcium loading, becomes relevant. Supporting cell depolarization of IHCs can last for many seconds, presumably leading to cisternal calcium loading and presynaptic potentiation via nitric oxide and metabotropic glutamate receptor activation. A subsequent action potential invading efferent terminals would be expected to have a higher likelihood of producing transmitter release due to the presynaptic mechanisms described, and the IHC inhibitory effect would be stronger via CICR. These effects could sharpen boundaries of excitation in the wake of supporting cell excitation, and thus increase signal to noise in the afferent pathway. Importantly, because supporting cells release potassium during waves of excitation, potassium's equilibrium potential shifts in a manner that reduces the inhibitory effect of efferent transmitter release. Thus, inhibition may be lessened

during waves of excitation (when IHCs should be active) and increased after (when IHCs should be silent). Future experiments are required to define the role of efferent activity in the context of auditory circuit refinement.

4.3.3 Synaptic crosstalk

Because voltage-gated calcium triggers vesicle release from IHCs to afferent neurons, CaV1.3 channels are most often associated with transmission through the afferent pathway. The experiments above, however, show that voltage-gated calcium is a major contributor to SK channel-mediated inhibition during efferent synaptic activity. Thus, synaptic crosstalk between the afferent and efferent systems occurs at the level of the IHC via calcium handling.

Such crosstalk is facilitated by the synaptology of early postnatal IHCs because numerous efferent and afferent contacts exist in close proximity. An example of closely associated afferent and efferent synapses is shown in Figure 4.9. Moreover, though voltage-gated calcium channels are clustered tightly around ribbons in adult IHCs, these channels are more widely dispersed at the ages studied (Zampini et al., 2010; Wong et al., 2014). The extrasynaptic localization of CaV1.3 channels during the first two postnatal weeks likely facilitates cisternal calcium loading. Additionally IHCs have larger whole-cell calcium currents during development; and thus are subjected to greater calcium loads during periods of depolarization (Johnson et al., 2005).

These immature features of are likely permissive, and potentially necessary, for the synaptic interactions described here. Future studies may utilize similar experimental strategies (i.e. Figure 4.7) to quantify the extent of synaptic crosstalk at ages when afferent function is more consolidated. It would be interesting to see if reduced CaV1.3 currents and increased efficiency of vesicle release at P12 occurs alongside decreased calcium spread to efferent cisterns. Preliminary data collected in the course of the present experiments suggests that crosstalk is reduced near the end of the second postnatal week.

Chapter 5

IHC re-innervation during age-related hearing loss

Hearing loss among the elderly correlates with diminished social, mental and physical health. Age-related cochlear cell death does occur, but growing anatomical evidence suggests that synaptic rearrangements on sensory hair cells also contribute to auditory functional decline. Voltage-clamp recordings from inner hair cells of the C57BL6/J mouse model of age-related hearing loss reveal that cholinergic synaptic inputs re-emerge during aging. These efferents are functionally inhibitory, utilizing the same ionic mechanisms of efferent contacts present transiently before the developmental onset of hearing. The strength of efferent inhibition of inner hair cells increases with hearing threshold elevation and cochlear pathology. These data indicate that the aged cochlea regains features of the developing cochlea, and that efferent inhibition of the auditory system's primary receptors re-emerges with hearing impairment.

5.1 Background and significance

5.1.1 Age-related hearing loss

According to a 2012 World Health Organization (WHO) study, 360 million people worldwide have disabling hearing impairment (Duthey, 2013). Many of these people are suffering from acquired age-related hearing loss, which is also known a "presbycusis." Audiologists assess hearing loss by determining audiometric

thresholds, and "disabling" hearing loss is typically defined as threshold elevation greater than 40 dB (WHO: Deafness & hearing loss 2015). By this definition, the WHO estimates that one-third of individuals 65 and older are suffering from disabling hearing impairment (WHO: Prevention of blindness & deafness 2012).

For individuals suffering from age-related hearing loss, the consequences can extend beyond impaired auditory function. Presbycusis has been associated with poor balance and falls (Lin & Ferrucci, 2012), depression (Davis et al., 2016), increased cognitive decline (Lin et al., 2013), and increased mortality risk (Gopinath et al., 2013). Older adults have increasing difficulty processing complex acoustic stimuli (Humes & Dubno, 2010), which includes speech and speech perception in noisy environments (Brant et al, 1996; Peelle & Wingfield, 2016), often leading to social isolation.

Age-related hearing loss is typically sensorineural in nature. Such hearing loss arises from peripheral damage in the cochlea and can be distinguished from other forms of hearing loss, such as conductive hearing loss, which arises due to middle ear dysfunction. Sensorineural hearing loss involves the damage or death of sensory receptor hair cells and/or their auditory nerve contacts. These cell types have limited capacity for repair after damage, and sensorineural hearing loss lacks curative therapies.

5.1.2 Pathology associated with sensorineural hearing loss

Much of the literature describing peripheral pathology accompanying sensorineural hearing loss involves experimental animals that have been exposed to ototoxic drugs or subjected to traumatic sound, both of which produce threshold elevation and tissue damage. Histological studies of human samples replicate the gross pathology found in damaged cochleae of cats, guinea pigs, mice, and other experimental models (Bahmad et al., 2008).

Hair cell loss is the most conspicuous histological feature of the damaged cochlea, and outer hair cells (OHCs) are more susceptible to death than inner hair cells (IHCs; Liberman & Kiang, 1978). Because OHCs serve as the "cochlear amplifier" (via their electromotile enhancement of sound-induced basilar membrane motion; Dallos, 2008) and IHCs serve as the primary auditory receptors, loss of either cell type leads to functional decline. Hair cell death can be induced via necrotic or apoptotic mechanisms (Furness, 2015). Necrotic death involves the release of cellular materials, which often causes inflammation and damage to other cells (Naganska & Matyja, 2001). Inflammation is a common feature of hearing loss, and pro-inflammatory cytokines (Wakabayashi et al., 2010), leukotrienes (Park et al., 2014), and leukocytes (Hirose et al., 2005) have been found in the damaged inner ear. Programmed cell death via apoptosis can be triggered in hair cells by reactive oxygen and reactive nitrogen species, which are generated after acoustic trauma or ototoxic insults (Shi & Nuttall, 2003; Henderson et al., 2006; Hu et al., 2006).

With some exceptions, the trajectory of hair cell death grossly follows a basal to apical trajectory (Furness, 2015). High frequency hair cells of the base may have metabolic biases that render them more susceptible to cell death (Jensen-Smith et al., 2012), and basal hair cells appear to have a greater intrinsic vulnerability to free radicals (Sha et al., 2001). Such metabolic differences between OHCs and IHCs are also thought to underlie the differential vulnerability these cells display (Tiede, et al., 2009). The tonotopic structure-function relationship of the cochlea is useful for comparing audiometric thresholds with cytocochleograms of hair cell counts along the cochlear length (Liberman, 2016).

Even in the absence of cell death, hair cell function can be impaired in a manner that leads to decreased acoustic sensitivity. Studies have identified damaged hair cell stereocilia after exposure to acoustic trauma (Liberman & Kiang, 1984; Pettigrew et al., 1984). Such damage can take the form of collapsed or fused stereocilia, and the pattern of stereocilia damage can be correlated with changes in acoustic thresholds (Robertson et al., 1980). Additionally, damage to the rootlets that embed the stereocilia to apical surface of hair cells has been observed (Liberman & Dodds, 1987). There may be additional submicroscopic damage to hair cells in the absence of death; and proper hair cell function can be impaired by numerous mechanisms, including altered signaling cascades (Fransen et al, 2015) and calcium homeostasis (Esterberg et al., 2013).

While the studies described above report hair cell loss that can occur shortly after acoustic trauma or other ototoxic insults, early investigations of auditory nerve

survival noted significant delays before the onset of neuronal loss (Johnson, 1974). In some instances, neuronal death could be delayed by weeks or months compared to hair cell death (Liberman & Kaing, 1978; Bohne & Harding, 2000). These studies supported the view that spiral ganglion neuron (SGN) death was "secondary" to the "primary" loss of hair cells. Later studies on the role of neurotrophins in the inner ear suggested that hair cells provide trophic support to SGNs, the removal of which promotes SGN death (Erphors et al., 1995; Fritzsch et al., 1997; Takeno et al., 1998). This hypothesis has been challenged by the observation that genetic ablation of IHCs (in the absence of acoustic trauma or ototoxic insult) does not result in SGN death (Zilberstein et al., 2013), suggesting that other cell types in the cochlea provide SGN trophic support. In the context of aging, it is believed that apoptotic processes govern SGN cell death (Alam et al., 2001; Nevado et al., 2006), and glutamate exitotoxicity has been shown to play an important role in SGN damage (discussed below).

Recordings from labeled single units indicate that type I SGN thresholds elevate and characteristic frequencies can shift after damage (Liberman, 1984). Spontaneous discharge rates tend to be lower and tuning curves constructed for individual units tend to lack sharp peaks (Liberman & Dodds, 1984). These studies indicate a loss of acoustic sensitivity in the SGN population, which is certainly attributable to hair cell death and/or dysfunction. Nevertheless, the extent to which damage induces intrinsic functional changes in SGNs is unclear. Important changes that occur at type I SGN synaptic contacts with IHCs are discussed in the "Synaptopathy" section below.

As discussed in Chapter 1, type I and type II SGNs each have unique features and properties that distinguish them, and differences between the two populations have been described in the context of hearing loss as well. Unlike type I afferents, which typically undergo a delayed death, type II afferents persist in the damaged cochlea, even when OHC loss is near complete (Spoendlin, 1971; Ryan et al., 1980). While synaptic drive from OHCs to type II afferents is weak (Weisz et al., 2009; Weisz et al., 2013), recent work indicates that these neurons are reliably driven to spike in response to OHC lysis; and these spikes are triggered, in part, by ATP-induced excitation (Liu et al., 2015). Noise exposure has been shown to increase cochlear ATP concentration (Munoz et al., 2001) and leads to the upregulation of molecules involved in purinergic signaling (Wang et al., 2003). Moreover, cell damage can initiate ATP-dependent "calcium waves" that propagate through cochlear tissue (Gale et al., 2004), potentially sensitizing type II afferents and driving them to relatively high activity levels. Taken together, these data support the hypothesis that type II afferents serve as nociceptors, suggesting their function is protective in the context of acoustic trauma.

5.1.3 Synaptopathy during sensorineural hearing loss

Cochlear synaptopathy at IHC synapses with type I afferents is increasingly appreciated as an important facet of sensorineural hearing loss. Early examples of synaptopathy were described during experiments designed to identify the neurotransmitter used by IHCs (Puel, 1995). The injection of 200 μM AMPA into the

cochlear fluid of guinea pigs produced afferent swelling and dendritic retraction, as demonstrated by EM (Pujol & Puel, 1999). In addition to glutamate's excitatory effects on the cochlea (Bobbin, 1979), the excitotoxic effects of glutamate agonists strongly suggested that glutamate is indeed the IHC neurotransmitter, a hypothesis confirmed by SGN dendritic recordings (Glowatzki & Fuchs, 2002).

Despite these early results, IHC synaptic loss drew far less research interest than hair cell death, partially because neuropathy of SGNs – measured at the level of their cell bodies – was understood to occur later than hair cell death, as described above. Additionally, synaptopathy in the guinea pig cochlea was considered transient (Pujol & Puel, 1999), and it was suggested that the IHC synaptic complex eventually recovered its characteristic organization. This interpretation is problematic, however, because early studies relied on EM, which is notoriously low throughput and produces relatively few synaptic contacts per sample.

More recent advancements in light microscopy, as well as the development of antibodies against key synaptic proteins, have enabled studies of afferent innervation across the entire cochlear length (Meyer et al., 2009) using relatively simple and efficient tissue processing. Kujawa and Liberman (2009) subjected CBA/CaJ (CBA) mice to "moderate" noise trauma, resulting in a temporary threshold shift, and counted presynaptic and postsynaptic elements of afferent contacts. They reported massive loss of IHC synaptic contacts, as well as delayed SGN death. Though thresholds of these animals recovered, the authors speculated that the synaptopathy

induced might contribute to more complicated auditory deficits, such as difficulty hearing in noisy environments.

It has been long known that acoustic thresholds fail to capture dysfunction of the auditory nerve. In the cat, lesions producing 50% loss of SGNs failed to elevate acoustic thresholds when hair cells were unaffected (Schuknecht & Woellner, 1955). Nevertheless, Wave I of the auditory brainstem response (ABR) captures the synchronous activation of auditory nerve fibers; and it is believed that cochlear synaptopathy can be identified by a characteristic reduction in suprathreshold Wave I amplitude (Furman et al., 2013). Because the ABR is regularly used in the clinical setting, there is hope that patients suffering from this so-called "hidden hearing loss" may have their underlying cochlear synaptopathy identified.

Though most studies of synaptopathy use acoustic trauma to induce cochlear damage, there is strong evidence that IHC synaptic loss occurs during the aging process as well. Stamataki and colleagues (2006) performed EM on IHCs from young (2-3 months) and old (8-12 months) C57BL/6J (C57) mice and reconstructed afferent contacts, finding that older animals had a ~50% reduction in afferent terminals but no significant change in total SGN density. Using immunolabeling in CBA/CaJ mice, Sergeyenko and colleagues (2013) found a progressive loss of IHC synaptic contacts with type I afferents over the lifespan, with early loss beginning long before threshold elevation and hair cell death.

5.1.4 Olivocochlear efferent system and hearing loss

Though olivocochlear efferent function is poorly understood in the contexts of development and normal auditory processing, there is a growing consensus that efferents serve protective roles during acoustic trauma and aging. Efferent neurons residing in the brainstem are driven by acoustic signals (Robertson & Gummer, 1985) as well as top-down activity through the descending auditory pathway (Guinan, 2010). Medial olivoocochlear (MOC) efferent activity serves as negative feedback to the cochlea, reducing basilar membrane motion (Murugasu & Russell, 1996) and afferent firing rates (Winslow & Sachs, 1987). As a result, direct activation of MOC efferents can reduce threshold shifts induced via sound exposure (Rajan, 1988). Moreover, surgical de-efferentation produces more pronounced threshold shifts after sound exposure (Kujawa & Liberman, 1997). Additionally, mice carrying a gain of function point mutation in the *Chrna9* gene (coding for the α9 receptor subunit) have prolonged efferent synaptic events and enhanced protection against noise-induced hearing loss (Taranda et al., 2009).

Despite this evidence, the hypothesis that efferents are involved in acoustic protection has been questioned. The negative feedback effect of MOC efferents on the basilar membrane tends to diminish at high sound intensities, possibly due to OHC transduction current saturation (Zwicker, 1979; Patuzzi et al., 1989). Additionally, natural environments do not typically produce sound levels that lead to widespread cochlear damage, leaving in doubt the adaptive pressures that would give rise to a cochlear protection system (Christopher Kirk & Smith, 2003). The recent

finding that widespread synaptic loss can occur after moderate noise exposure (described above) may reconcile experimental evidence that efferent activity is protective with concerns over the absence of selective pressure in the natural environment. Indeed, in aged mice, unexposed to acoustic trauma, the efferent system appears to slow functional decline and synaptopathy (Liberman et al., 2014).

In contrast to the afferent pathway, which undergoes synaptopathy during hearing loss, aberrant efferent terminals have been observed in the damaged cochlea, suggesting efferent synaptogenesis occurs during hearing loss. Lauer and colleagues (2012) examined IHC synaptic organization in young and old C57 mice via EM. In accordance with previous results (Stamataki et al., 2006), these authors noted a dramatic loss in afferent contacts per hair cell in aged tissue. Interestingly, they also observed presynaptic contacts, presumably of efferent origin, on aged IHCs. In sections taken at favorable angles, postsynaptic cisterns were observed at putative synapses. As discussed in Chapter 4, such cisterns are obligatory features of efferent synapses on hair cells. EM analysis of adult guinea pig cochleae subjected to AMPA perfusion also reveals efferent contacts on IHCs occurring alongside deafferentation (Pujol & Puel, 1999). These synapses are reminiscent of early postnatal development, when IHCs are innervated by many efferent presynaptic contacts (Chapter 4).

These histological observations of efferent re-innervaiton of IHCs during hearing loss motivated the physiological experiments described below.

5.2 Experimental results

5.2.1 Obtaining recordings from aged IHCs

We set out to determine if the presumptive efferent contacts observed on aged C57 IHCs via EM are indeed functional. Additionally, we designed experiments to determine the transmitter system at work, the receptor subtype utilized by IHCs, and whether or not accessory channels are involved in IHC synaptic responses. Whole-cell, tight seal recordings in voltage clamp mode are commonly used to address such questions, but attaining these recordings from aged IHCs posed a significant challenge. As animals age, the bone surrounding the epithelium hardens and the difficulty of the required dissection increases. Moreover, aged tissue is less robust and survives poorly *ex vivo*. Indeed, no such hair cell recordings can be found in the literature.

Based on the work of Lauer et al. (2012), we determined that recordings would be necessary from C57 animals that were approximately 1 year old. After many months of practicing dissections on mice of increasing age and becoming familiar with aged tissue, successful recordings were regularly achieved. Figure 5.1 shows current responses to a series of voltage steps applied to a year-old IHC, demonstrating the feasibility of obtaining high quality recordings from aged tissue.

Due to challenges associated with the dissection, recordings were restricted to the apical, low frequency portion of the cochlea, corresponding to ~4-10 kHz on the mouse tonotopic map. With additional practice and slight alterations to the dissection, recordings can be achieved from more basal sections of the cochlea. The

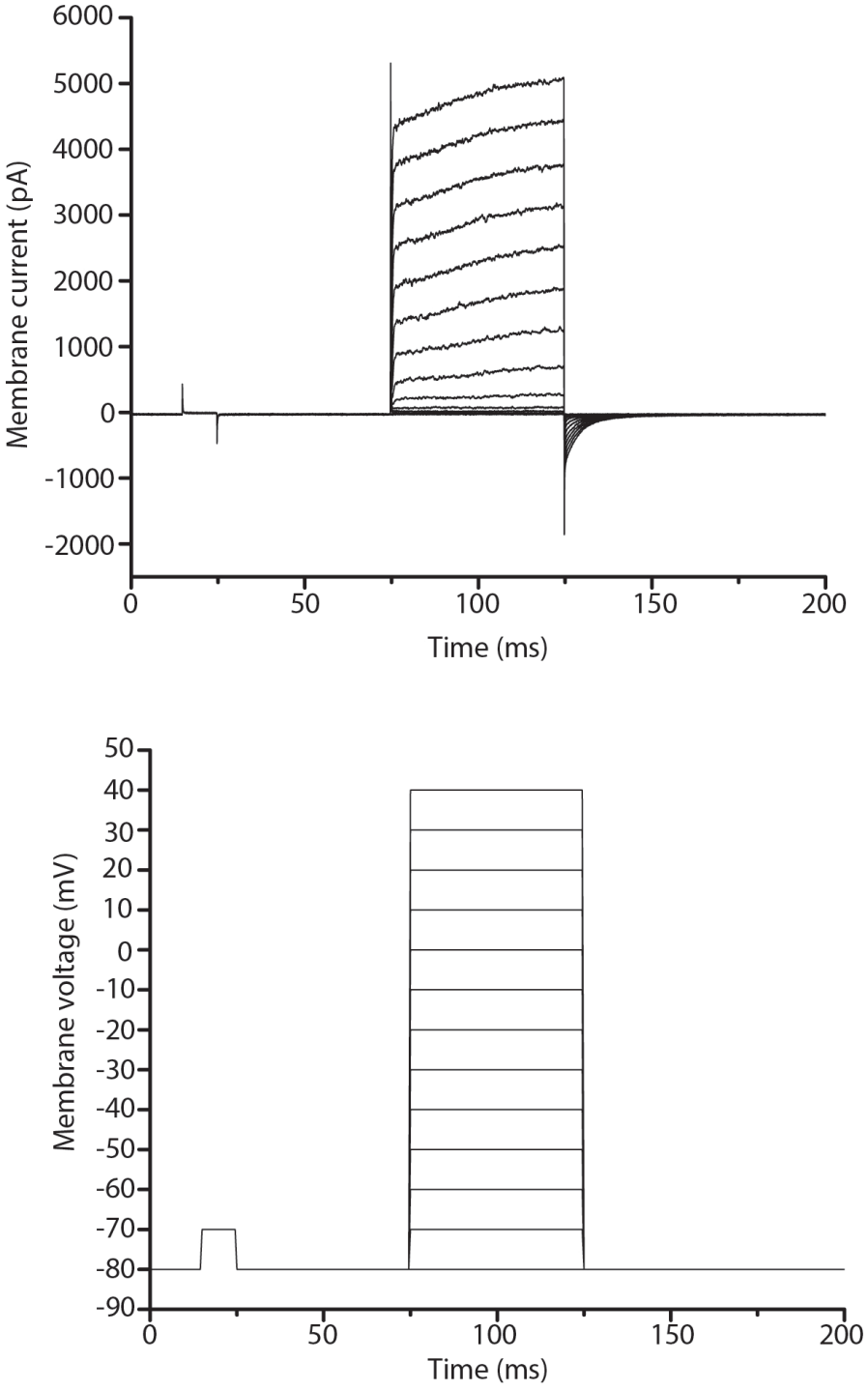

Figure 5.1: Recordings from aged IHCs. Membrane current responses (top) to a series of voltage steps (bottom) applied to a year-old C57 IHC.

oldest hair cell recording obtained from an animal with a verified birth date was 18 months old.

5.2.2 Efferent innervation of IHCs across the lifespan

Due to the close proximity of the IHC basal pole, afferent dendrites, and lateral efferent terminals, confocal microscopy cannot resolve whether or not efferent neurons innervate IHCs in the adult animal. Instead, EM-level resolution of pre- and postsynaptic densities is necessary for histological approaches, as shown in figure 5.2. Therefore, physiology was used to survey the proportion of apical IHCs innervated by efferent neurons across the lifespan.

After obtaining the whole-cell configuration, cells were voltage clamped at -80 mV and a nearby perfusion pipette applied 40 mM potassium external solution. This solution depolarized any synaptically connected efferent neurons, producing transmitter release and inward postsynaptic events. If no postsynaptic currents were observed after 5 minutes of continuous perfusion of 40 mM potassium, a cell was classified as lacking efferent innervation. Recordings were made from animals with verified birthdates at the following ages: P7-10, P30, 8.5-9.5 months, and 11-12 months. Examples of membrane current responses to the application of elevated external potassium solution are presented in Figure 5.3.

As expected, postsynaptic currents were observed in all P7-10 IHCs, and no postsynaptic events were observed in P30 IHCs (Figure 5.3 A). These data reflect the

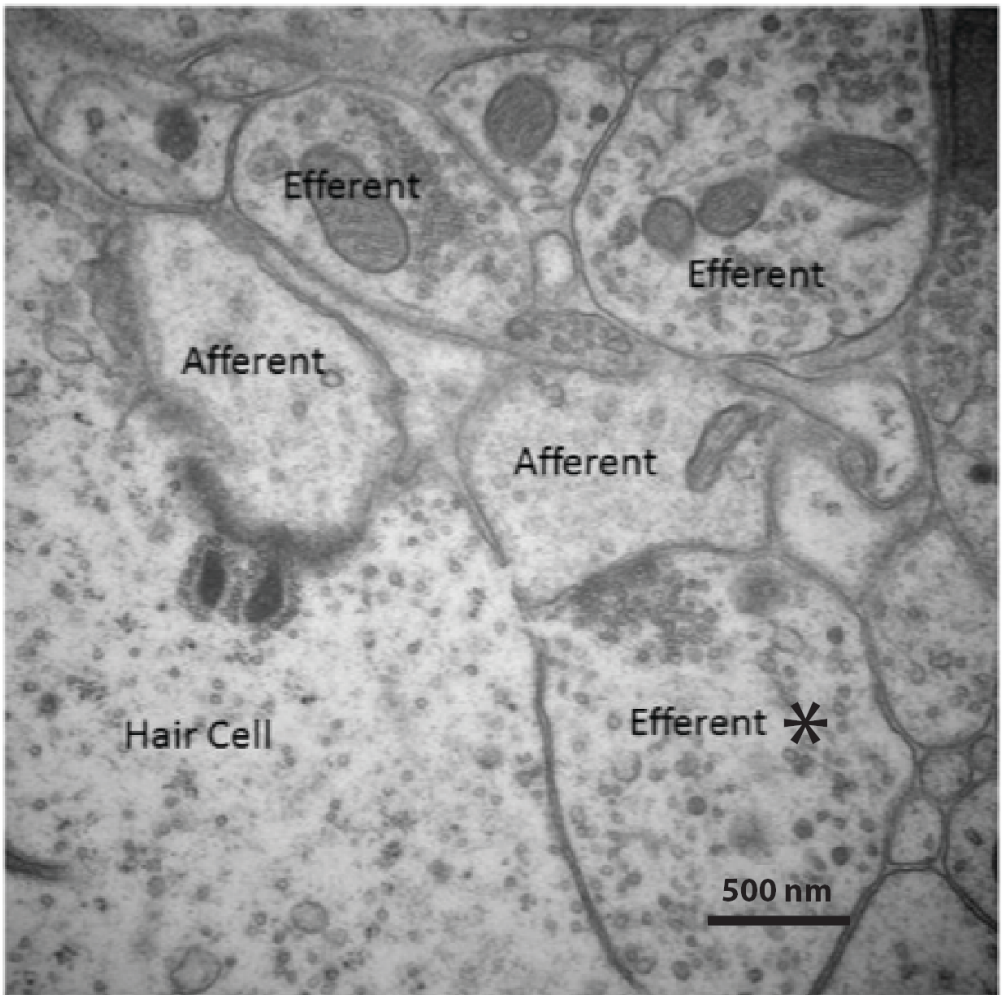

Figure 5.2: Proximity of neuronal contacts on IHCs. An electron micrograph of the synaptic pole of a P21 C57 IHC. Note the vesicle rich efferent contact touching the IHC membrane but forming a synaptic contact on the adjacent afferent terminal (asterisk).

formation and subsequent elimination of efferent innervation of IHCs during development.

However, at 8.5-9.5 months, ~20% of IHCs had postsynaptic currents, and this proportion increased to 50% at 11-12 months (Figure 5.3 A, B). These recordings confirm Lauer and colleagues' ultrastructural observation of efferent re-innervation of C57 IHCs during aging and demonstrate that these efferent contacts are indeed functional.

Along with the proportion of apical IHCs innervated at these two ages, the frequency of postsynaptic events also increased from 0.06 ±0.02 Hz at 8.5-9.5 months to 0.5 ± 0.14 Hz at 11-12 months (Figure 5.3 C). This increase in event frequency is due to an age-related increase in the number of efferent contacts per IHC, as demonstrated by Lauer and colleagues. Additional processes, such an increase in release probability of existing efferent contacts may be at play as well but were not tested. Such experiments would require electrical stimulation of efferent axons, optogenetic stimulation, or other methods that provide the experimenter with direct control of efferent release.

These recordings were from apical cochlear tissue, corresponding to ~4-10 kHz along the tonotopic axis. To assess cochlear function within this region, we characterized 8 kHz hearing thresholds by performing ABR recordings on P30, 8.5-9.5 month-old, and 11-12 month-old animals (Figure 5.4 A). Thresholds means and SEM db SPL were 38.15 (3.29), 53.72 (4.58), and 91.14 (3.78) respectively. Thus,

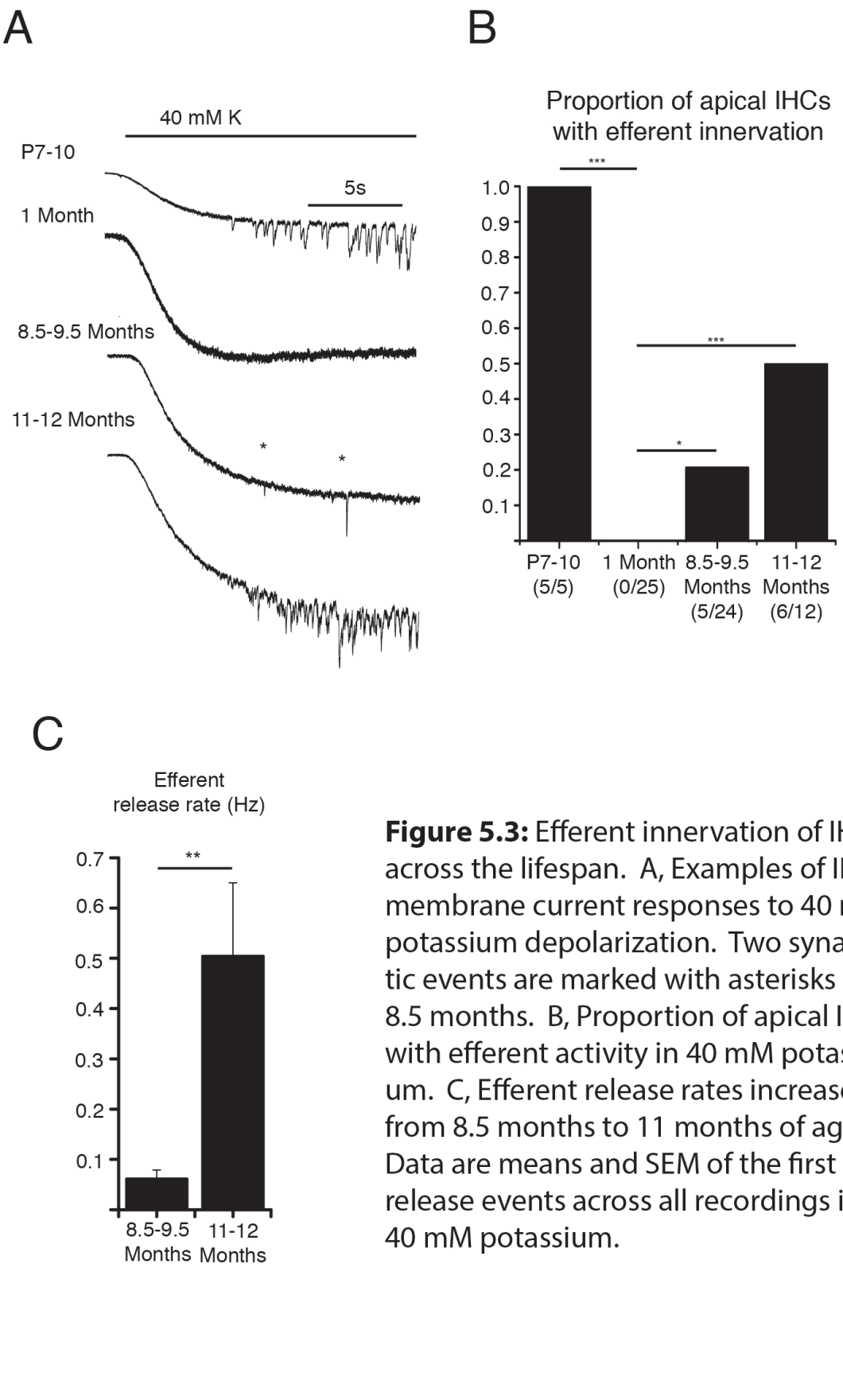

Figure 5.3: Efferent innervation of IHCs across the lifespan. A, Examples of IHC membrane current responses to 40 mM potassium depolarization. Two synaptic events are marked with asterisks at 8.5 months. B, Proportion of apical IHCs with efferent activity in 40 mM potassium. C, Efferent release rates increase from 8.5 months to 11 months of age. Data are means and SEM of the first 10 release events across all recordings in 40 mM potassium.

efferent re-innervation of apical IHCs occurs alongside low frequency threshold elevation.

Thresholds were also determined at 4 kHz, 16 kHz, and 32 kHz. Thresholds at 4 kHz increased by 36.1 dB SPL(52.7 to 88.8) from P30 to 11-12 months of age. At 16 kHz, 3 of the 5 animals tested at 11-12 months had no detectable thresholds; and the 2 animals with detectable thresholds displayed an average increase of 65 dB SPL from P30 to 11-12 months (30.9 to 95.9). At 32 kHz, no animals tested at 11-12 months had detectable thresholds. Average threshold at 32 kHz for P30 animals was 55.3 dB SPL. The P30 thresholds obtained are consistent with a "U-shaped" audiogram, with low and high frequencies showing higher thresholds than middle frequencies.

To assess anatomical changes at the same ages, OHCs and afferent contacts on IHCs were quantified. As described above, OHC death and afferent synaptopathy are important pathological features of age-related hearing loss. Such pathology may play a causative role in efferent re-innervation of IHCs, as OHCs and afferent dendrites are each contacted by efferent terminals.

Because there is a 1:1 relationship between presynaptic ribbons and afferent dendrites, ribbon quantification is a reliable assay of afferent innervation during the aging process (Sergeyenko et al., 2013). We quantified ribbon survival via CTBP2 immunoreactivity in whole-mounted apical turns and observed ~37% ribbon loss by 8.5-9.5 months and ~55% ribbon loss by 11-12 months (relative to that of 1-month-

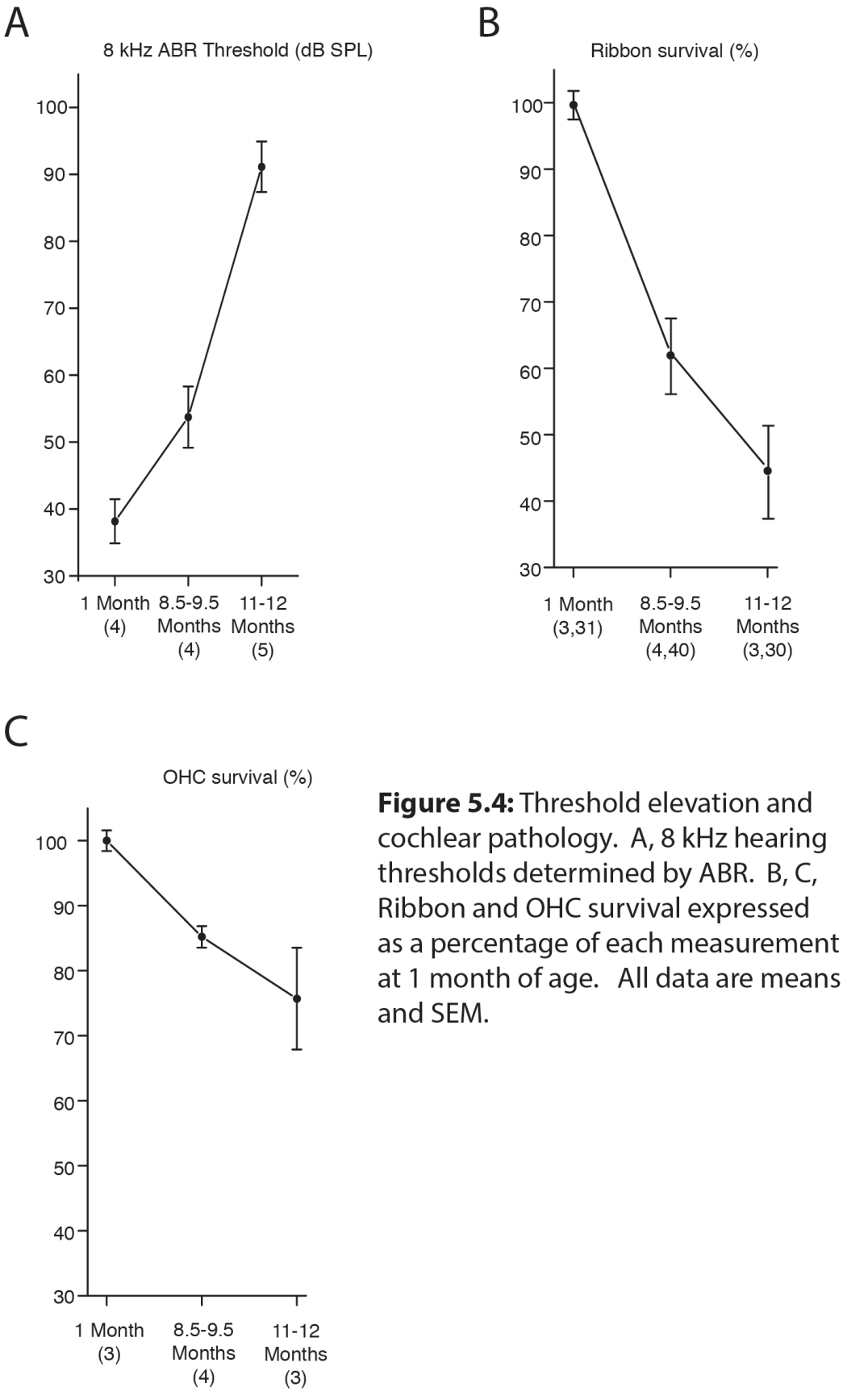

Figure 5.4: Threshold elevation and cochlear pathology. A, 8 kHz hearing thresholds determined by ABR. B, C, Ribbon and OHC survival expressed as a percentage of each measurement at 1 month of age. All data are means and SEM.

old animals, Figure 5.4 B). Mean (SEM) ribbon values per IHC were 10.1 (.22) at P30, 6.3 (.36) at 8.5-9.5 months, and 4.5 (.32) at 11-12 months.

Outer hair cell counts, via Myosin 7A immunoreactivity, in the same samples also showed a reduction with aging, though to a lesser extent than for ribbon loss (Figure 5.4 C). OHCs were quantified across a 200 μM distance in the same tonotopic region. OHC numbers (SEM) were 73.15 (1.15), 62.25 (1.03), and 55.33 (4.33) for P20, 8.5-9.5 months, and 11-12 months of age, respectively. The known pattern of degeneration in this mouse broadly follows a basal to apical trajectory, similar to that of human cochlear pathology; thus cytological changes would be still greater in basal regions.

Figure 5.5: Efferents contacting aged IHCs do not activate a chloride conductance. Inward currents indicate that efferent transmitter release does not activate chloride channels because those currents would be outward. E_{Cl} = -132 mV, cells voltage clamped at -80 mV.

5.2.3 Transmitter system and receptor characterization

Because α9/α10 nAChRs have overlapping antagonist pharmacology with glycine and GABA receptors (Rothlin et al., 1999), we performed an experiment to distinguish cationic and anionic postsynaptic currents based on their relative driving force. IHC recordings were made from animals at least 11 months old and efferent transmitter release was evoked with 80 mM external potassium. The pipette solution used set E_{Cl} at -132 mV; and since the hair cells were held at -80mV, chloride flux would produce an outward current under these conditions. However, only inward postsynaptic currents were observed, indicating that efferent transmitter release does not activate a chloride conductance (Figure 5.5).

The receptor mediating these synaptic currents was characterized using several diagnostic antagonists. 1 μM curare reversibly blocked postsynaptic activity, indicating that efferents contacting aged IHCs are cholinergic (n = 4 cells; Figure 5.6 A). Strychnine, a potent antagonist of α9/10 receptors (Rothlin et al., 1999), also blocked activity reversibly at 1μM, (n = 2 cells; Figure 5.6 B). In addition, the α9-specific toxin ACV1 (Vincler et al., 2006) reversibly blocked events at 500nM (n = 2 cells; Figure 5.6 C). These data indicate that, as for early postnatal IHCs, aged IHCs are contacted by cholinergic efferents that activate α9-containing nAChRs.

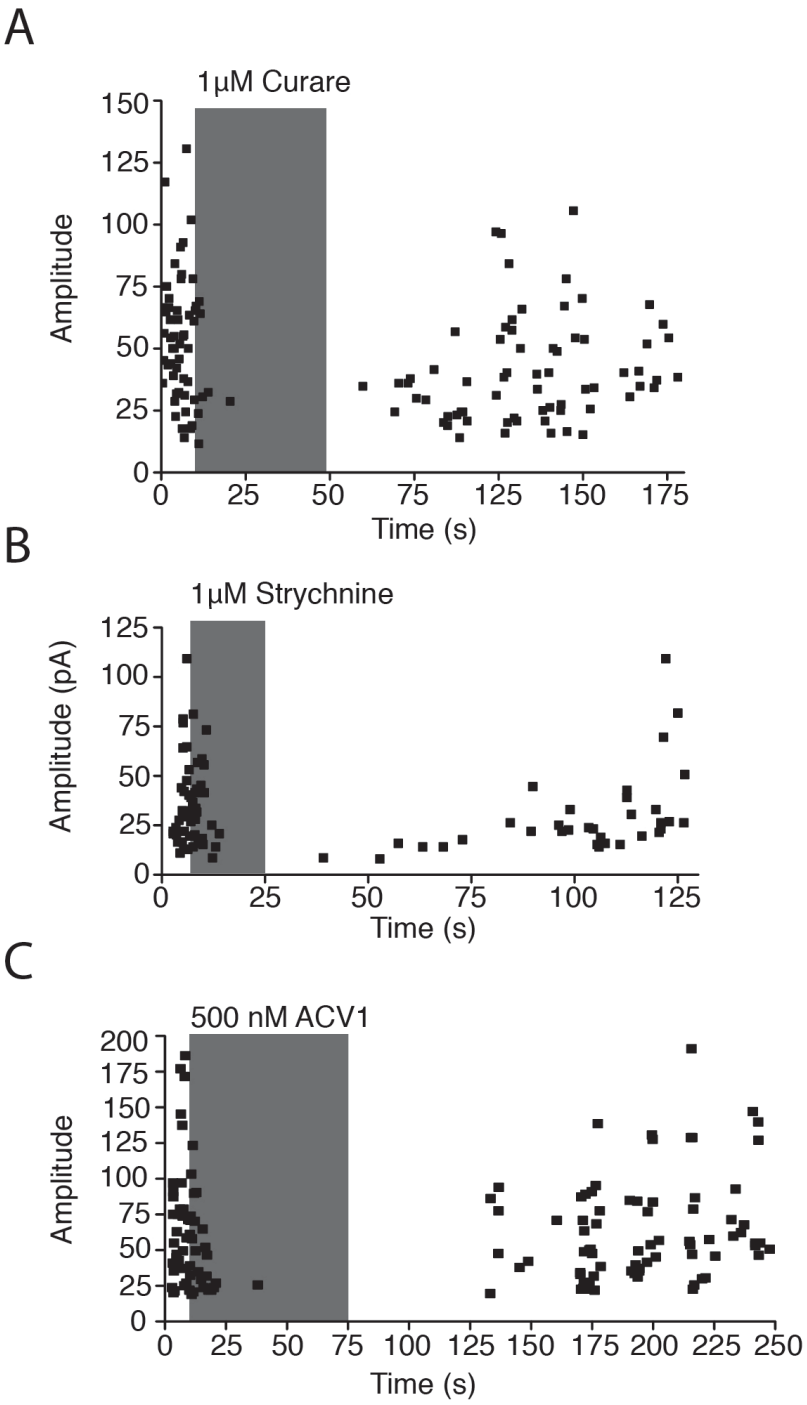

Figure 5.6: Efferents contacting IHCs are cholinergic and IHCs use α9-containing nAChRs. A-C, Exemplar diary plots of event amplitudes. A, 1µM curare blocked synaptic activity. B, 1 µM strychnine blocked synaptic activity. C, 500 nM ACV1 blocked synaptic activity.

5.2.4 Potassium channel coupling

Consistent with the pharmacology described above, local application of ACh to aged IHCs held at -80 mV (E_K) induced inward current, presumably through nAChRs. However, when ACh was applied to cells held at -40mV, the ACh-induced current was outward (Figure 5.7 A). Thus, nAChRs are functionally coupled to potassium channels in aged IHCs, making efferent transmission inhibitory as in immature IHCs. The mean reversal potential for the ACh-induced current, determined via a voltage ramp protocol, was -68.71 ± 0.4 mV, (n = 5 cells; Figure 5.7 B).

To determine the specific subtype of potassium channel that mediates the inhibitory component, we recorded inward synaptic currents in 80 mM external potassium and then applied 400 nM apamin, a specific antagonist for SK channels. As is the case for immature efferent postsynaptic currents (Oliver et al., 2000; Gómez-Casati et al., 2005; Rohmann et al., 2015), apamin reduced the time constant of decay of the synaptic currents (from 35.88 ms ± 2.01ms to 13.34 ms ±0.81ms; 2 cells), indicating that SK channels are involved in the synaptic response to ACh (Figure 5.8). Apamin also reduced the mean amplitude (from 70.62 ± 4.0 pA to 46.23 ± 2.0 pA), as expected from the large inward driving force on potassium in these conditions.

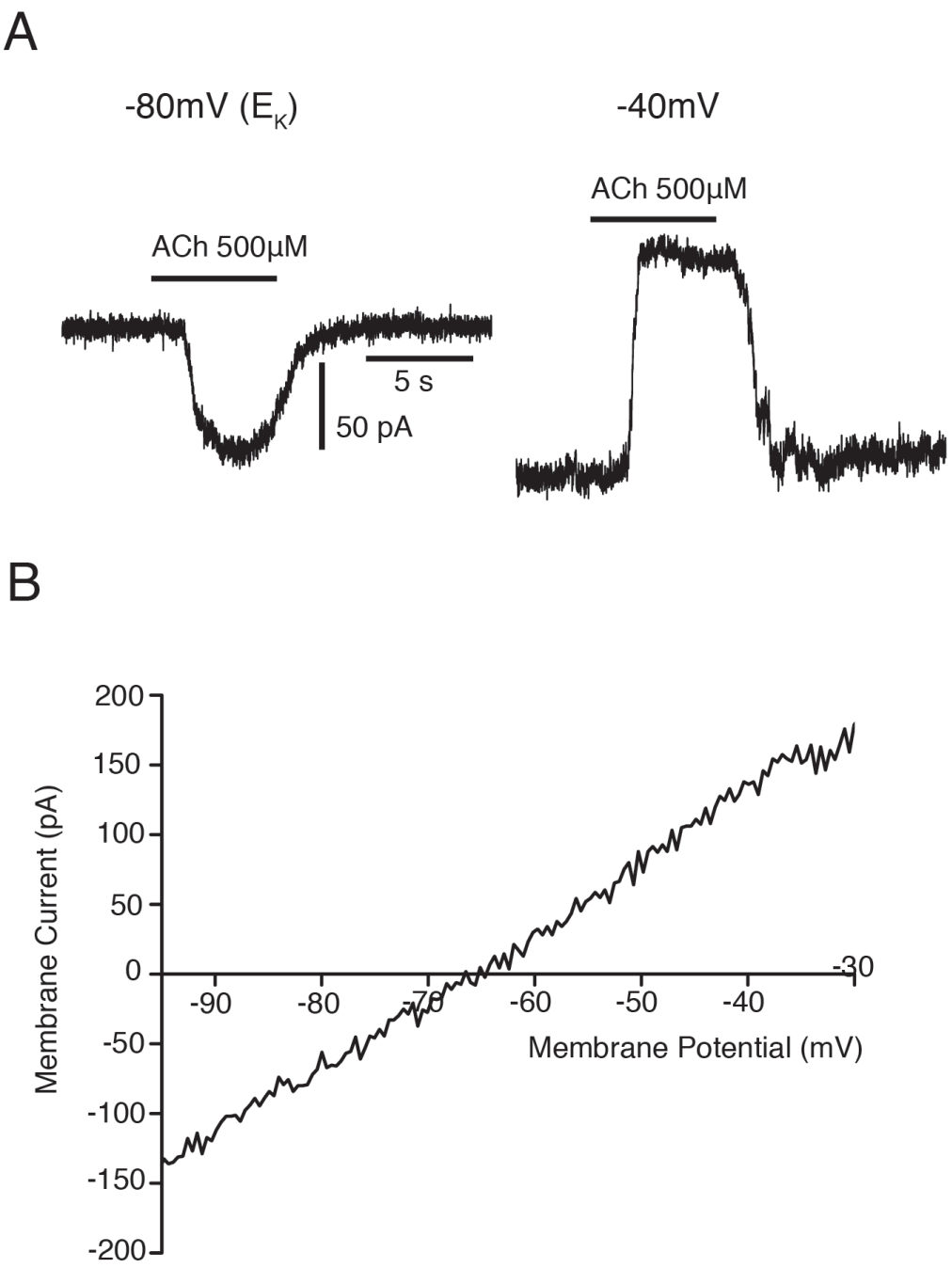

Figure 5.7: Potassium channels are coupled to nAChRs in aged IHCs. A, Exemplar membrane current responses to locally applied ACh while voltage clamped at -80 mV and -40 mV. B, The I-V relationship of the acetylcholine-induced current in aged IHCs.

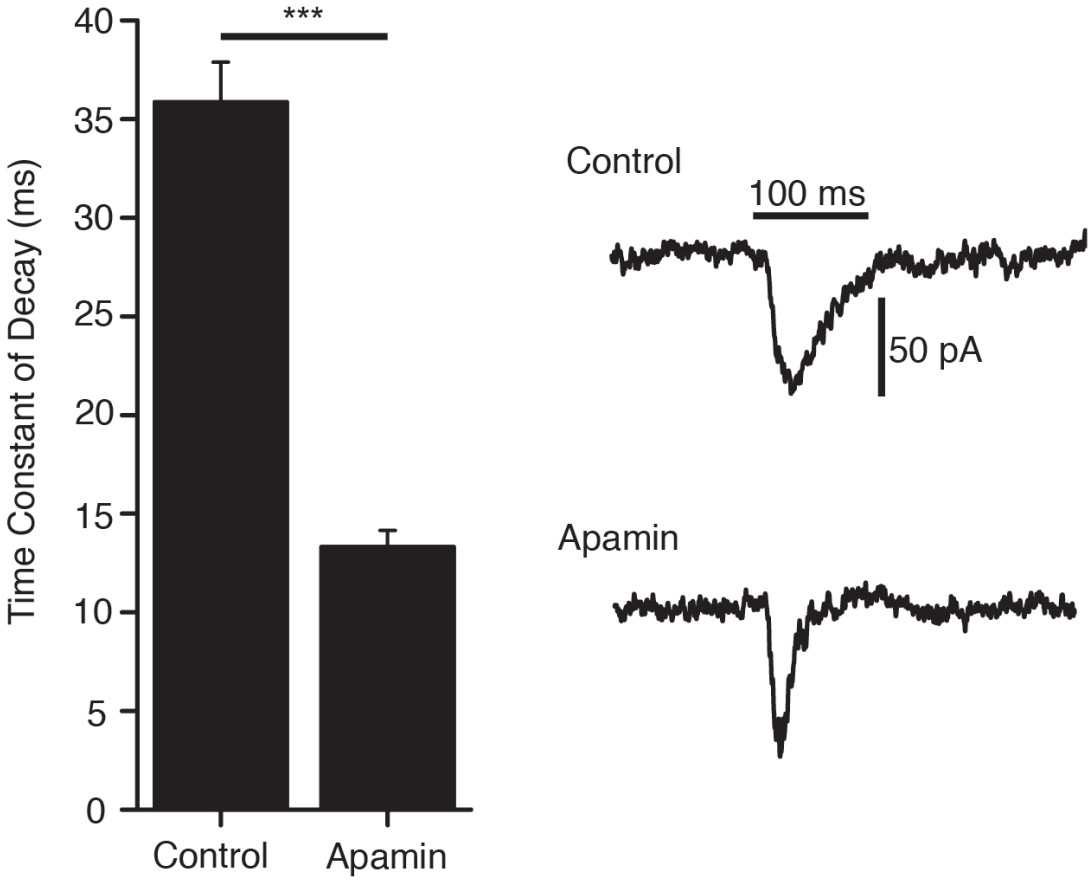

Figure 5.8: SK channels are involved in the synaptic response to ACh. Apamin reduced the time constant of decay of synaptic events evoked by 80 mM external potassium solution.

5.3 Discussion

The recordings presented here are the first from aged hair cells. Since elevated potassium stimulation produces large inward synaptic events, innervated IHCs were clearly identifiable based on the presence of synaptic activity. Cells that lacked efferent activity after 5 minutes of continuous exposure to elevated potassium were classified as lacking efferent innervation. Even after proficiency in recording from aged tissue was achieved, occasionally recordings were lost before this 5-minute cutoff point. Though the exclusion of these cells may represent a sample bias that increased the apparent proportion of innervated cells, some recordings revealed efferent activity that did not manifest until the IHC was exposed to high potassium for several minutes. The criteria for exclusion was established before the collection of the data and adhered to throughout the study. Waveforms of synaptic events recorded during pharmacological manipulation were analyzed manually in MiniAnalysis software, and the experimenter was not blinded. Therefore, bias may have been introduced in the analysis of those waveforms.

Efferent synapse formation is contemporaneous with hearing threshold elevation, IHC afferent loss, and OHC death. The recordings presented here were made in apical cochlear tissue, and the ultrastructural characterization of efferent innervation of aged IHCs (Lauer et al., 2012) was carried out in more basal regions. Therefore, efferent innervation of IHCs may arise across the tonotopic axis, and it is likely that the onset and progression of this innervation pattern follows a basal-to-apical trajectory similar to other features of hearing loss. While there are suggestions

in the literature that efferent re-innervation of IHCs is a common feature of the damaged cochlea, additional physiology across mouse lines and further histology across species is necessary. It will be of interest to know what efferent population gives rise to the synaptic arrangement detailed here as well as the specific cellular pathology that produces re-innervation. Most importantly, the function of efferent re-innervation of IHCs in hearing loss is unknown, and challenging experiments will be required to define the systems and behavioral outcomes of IHC re-innervation.

5.3.1 C57 mice

Many inbred laboratory mouse strains, including the C57, have age-related hearing loss phenotypes (Jones et al., 2006). The C57 is a commonly used model for hearing loss because it mimics many features of human hearing impairment: auditory function declines progressively, beginning at high frequencies, and is sensorineural in origin (Henry & Chole, 1980; Zheng et al., 1999).

Some researchers, however, utilize mouse lines with well-preserved hearing across the lifespan for aging studies (such as the CBA; Sergeyenko et al., 2013). Indeed, the progressive hearing loss characteristic of the C57 is due to a single nucleotide polymorphism in the coding sequence of cadherin 23, leading to in frame skipping of exon 7 (Noben-Trauth et al., 2003). Along with protocadherin 15, cadherin 23 forms the tip links responsible for coupling stereocilia and applying force to mechanotransduction channels (Siemens et al., 2004; Ahmed et al., 2006).

The possibility exists that efferent re-innervation of IHCs may be consequent to this mutation. Such a scenario seems remote, however, given that synaptic structures are normal in the C57 during development and in the healthy adult. Additionally, EM studies of the guinea pig cochlea after AMPA administration reveal re-emergent efferent contacts on IHCs, suggesting that efferent innervation of IHCs may be a common feature of the damaged cochlea (Ruel et al., 2007). Additional physiological studies across mouse lines and species are necessary to describe the extent to which this innervation pattern arises during hearing loss and pathology. Immunohistological and confocal analysis of human temporal bones has been demonstrated recently (Viana et al., 2015); and should reliable postsynaptic antibodies become available it will be of interest to investigate re-innervation in human samples.

5.3.2 Identity of re-innervating efferents

The re-emergent efferent synapses on aged IHCs could arise from medial (MOC) or lateral (LOC) olivocochlear efferents. The cholinergic efferents innervating IHCs during development are MOC in origin, and it is possible that MOC efferents recapitulate IHC innervation after cochlear damage. OHC death leaves MOC efferents without synaptic partners, which may lead to retraction of MOC terminals into the IHC area or reactive sprouting of MOC processes. Additionally, during aging, MOC terminals below OHCs can be lost even when OHCs themselves remain intact (Fu et al., 2010). This observation is interesting in the context of 11 –

12 month-old C57s, when ~50% of apical IHCs are re-innervated and OHC loss is only ~25% (Figures 5.3 & 5.4).

LOC efferents synapse with the dendrites of type I afferents just below the basal pole of IHCs. The apposition of the IHCs membrane, afferent dendrite, and LOC terminal is so close that EM level resolution is required to determine if an LOC is innervating an IHC or an afferent dendrite. Given this close proximity, LOCs are perhaps better positioned to move onto IHCs during re-innervation. The greater proportional loss of afferents (ribbons) than of OHCs may argue in favor of LOC efferents as the source of these IHC synapses (Figure 5.4).

Experiments utilizing differential flux of cations and anions failed to show Cl- mediated ion flux, suggesting that efferents re-innervating IHCs are not GABAergic or glycinergic (Figure 5.5). Additional pharmacological experiments indicate that synaptic currents are produced by ACh release (Figure 5.6). Therefore, if LOC efferents are producing IHC re-innervation, it seems as if this ability is restricted to the cholinergic population. The number of transmitter systems utilized by the LOC system is not fully understood, but there is wide agreement that a diversity of transmitters are at work. MOC efferents, on the other hand, are thought to be exclusively cholinergic.

Future experiments may determine the specific population of efferents involved in IHC re-innervation while also describing the cellular processes that give rise to efferent synapse formation. The cholinergic synapses found on aged IHCs utilize the same ionic mechanisms of efferents innervating IHCs during early postnatal development. During development, efferent innervation of IHCs disappears

as afferent functional maturation occurs (Roux et al., 2011; Wong et al., 2014; Wichmann & Moser, 2015). As described above, efferent innervation of aged IHCs occurs alongside deafferentation. Thus, in both of these epochs, an apparent reciprocity exists between efferent and afferent innervation of IHCs.

Cochlear administration of ouabain via round window injection has been shown to ablate type I afferents while leaving OHCs intact (Yuan et al., 2014). Ouabain administration could be paired with recordings from adult IHCs to test if deafferenation, in the absence of other cochlear pathology, produces re-innervation. Should immunostains in these tissues reveal normal numbers of efferent terminals per OHC, the LOC system would be strongly implicated.

Conversely, experiments producing the ablation of OHCs may be instructive. OHCs are more sensitive than IHCs to aminoglycoside drugs; and, depending on the dosage, aminoglycoside toxicity may be a strategy to selectively ablate OHCs. Genetic strategies are also available. For instance, one could produce the expression of diphtheria toxin fragment A selectively in OHCs (Prestin CreER + RosaDTA). Regardless of the strategy, IHC recordings after selective OHC ablation might reveal if OHC death is a causative factor in re-innervation and may implicate MOC efferents as the population at work.

Whatever their origin, efferent synapses on aged IHCs include the near-membrane postsynaptic cistern (Smith & Sjöstrand, 1961; Saito, 1980; Lauer et al., 2012). This cistern is thought to segregate and control synaptic calcium (Chapter 4; Sridhar et al., 1997; Liudyno et al., 2012). Postsynaptic cisterns are also a feature of cholinergic synaptic contacts on spinal motor neurons (Nagy et al., 1993), in which

they have been shown to enlarge with afferent denervation (Pullen & Sears, 1978) and in upper motor neuron disease (Pullen & Athanasiou, 2009). The present work provides another example of cisternal synaptic plasticity during deafferentation; and, due to the relatively simple organization of the IHC synaptic complex, the aged cochlea might serve as a general model for cisternal synaptic reorganization during disease.

5.3.3 Function of renascent efferent-IHC synapses

Expansion of cisternal synapses during motor neuron disease has been interpreted as a compensatory mechanism arising from a loss of excitatory drive. Although the present work provides parallels with such expansion, the re-emergent efferent synapses found on aged IHCs are clearly not for excitatory compensation. The two-channel mechanism at work, consisting of nAChRs coupled to potassium channels, produces IHC hyperpolarization. The role of this inhibition in the context of hearing and behavior, however, is unclear.

The most obvious hypothesis is that re-emergent IHC synapses contribute to hearing loss, via inhibition of IHC receptor potential and subsequent afferent signaling. Not only does this efferent innervation pattern arise alongside common forms of cochlear pathology, but it also occurs alongside auditory functional decline measured via ABR. Testing such a hypothesis, however, will be challenging. Though a constitutive α9 knockout mouse exists (Vetter et al., 1999), a conditional knockout is better suited for studying efferent re-innervation of IHCs. In the

constitutive knockout, all efferent synapses on hair cells are non-functional. Thus, not only is efferent function at aged IHC synapses absent, but also is efferent function at premature IHC and mature OHC synapses. This complete loss of efferent activity in the periphery confounds comparisons of α9 knockout and wild type mice. A conditional α9 knockout utilizing the Cre-ER system would allow for α9 deletion specifically in IHCs after their developmental efferent synapses have disappeared.

Even with such a mouse model, further challenges associated with testing the hypothesis that efferent re-innervation of IHCs contributes to hearing loss arise due to the high degree of individual variation mice exhibit in hearing loss onset and severity. This variability can be seen during age-related hearing loss and noise-induced hearing loss and occurs even in highly inbred strains. Such variability may obscure the effect of any experimental manipulation. Thus, large animal populations and numerous assays of hearing function will likely be necessary. Such assays could include ABRs, behavioral threshold testing, "gap discrimination," acoustic conditioning, and acoustic startle reflexes and their growth curves.

A competing, more tractable hypothesis is that efferent inhibition of IHCs protects SGNs. Excitotoxicity is a major contributor to SGN damage and death, so perhaps efferents reduce glutamate release in a neuroprotective fashion. The pathological correlates of hearing loss (i.e., afferent synaptic loss) are less variable than hearing loss assessments (i.e., ABRs). This is because far more data points exist per animal for synapse quantification than auditory thresholds. Using a conditional α9 deletion mouse (or perhaps even the constitutive knockout, given the proper controls) a comparison of afferent integrity in the absence of efferent re-innervation

of IHCs could be performed. Such experiments would tie in well with the growing interest in synaptopathy and so-called "hidden hearing loss."

More sophisticated hypotheses could also be proposed. For instance, it is known that MOC efferents help OHCs shape frequency selection via modulation of the cochlear amplifier. Given the widespread OHC death that occurs during hearing loss, perhaps this mechanism of discrimination is reconfigured at the level of IHCs via efferent inhibition. Testing such a hypothesis would require *in vivo* recordings of efferent neurons and histological reconstructions of their tonotopic projections, perhaps from animals performing a behavioral task such as frequency discrimination. Such experiments are all the more ambitious, as they would have to occur after aging, acoustic trauma, or some other manipulation to induce efferent re-innervation of IHCs.

5.3.4 Therapeutic implications

Well-controlled experiments will be required to determine the function or functions efferent re-innervation of IHCs serves. Should this innervation pattern be found in other models and human tissues, these synapses may become therapeutic targets via positive or negative modulation. While many molecular elements operate at efferent synapses, α9/ α10 nAChRs are the most appealing targets because (i) their gating initiates hair cell inhibition, (ii) they have a unique pharmacological profile (see Chapter 4 for discussion), and (iii) their expression is very limited in other tissues.

The blockade of α9/α10 nAChRs on IHCs during hearing loss would be beneficial if these synapses contribute to threshold elevation or other auditory impairments, such as difficulty hearing in noisy environments. Indeed, the efferent innervation of IHCs described here increases alongside threshold elevation (Figures 5.3 & 5.4). While the possibility clearly exists that these IHC efferent synapses play a pathological role, the cholinergic MOC efferent system is typically associated with cochlear protection (discussed in Section 5.1.4). Because those MOC efferent contacts activate α9/α10 nAChRs as well, the benefits of blocking efferent synapses on IHCs may be outweighed by the consequences of blocking MOC activity at OHCs. It is worth noting, however, that the majority of α9/α10 nAChRs found in the aged cochlea may be located on IHC membranes, as a large percentage of the OHC population may die during age-related hearing loss (the relatively slight OHC loss reported in Figure 5.4 is a feature of the apex; basal OHCs are lost earlier).

If re-emergent efferent synapses on IHCs protect type I afferents from further glutamate excitotoxicity, prolonging α9/α10 nAChR open time or increasing receptor calcium permeability might be therapeutic. This scenario is preferable to the one described above, as positive modulation of both IHC and OHC efferent synapses might function synergistically to protect the cochlea. The α9 gain-of-function mouse (Taranda et al., 2009), which harbors a point mutation that increases channel mean open time, may serve as a valuable model of nAChR potentiation in the context of hearing loss. Inhibition could also be potentiated via modulation of SK channel function directly or by increasing cisternal calcium release (Chapter 4), but systemic drug administration may not be appropriate for such approaches.

The synaptic organization of IHCs is dynamic during hearing loss, with progressive efferent re-innervation of IHCs accompanying type I afferent synaptic retraction. While a great deal of research focuses on increasing afferent drive during hearing loss, modulation of efferent function may be clinically relevant as well.

Chapter 6

Conclusion

Efferent synapses on IHCs undergo plasticity at the synaptic and organizational levels. During early postnatal development, efferents innervate IHCs, and the activity of those efferent neurons is modulated synergistically by presynaptic and postsynaptic mechanisms. These synapses are eliminated around the onset of hearing, but efferent innervation returns to IHCs during aging. As is the case during development, aged IHCs experience efferent inhibition via ionic mechanisms involving nAChRs and SK channels.

Recordings from young (P7-9) IHCs demonstrated that cisternal calcium release and voltage-gated calcium influx shape IPSC waveforms and that cholinergic responses are potentiated after IHC depolarization. While the present work focuses on postsynaptic mechanisms potentiating inhibition, raising IHC calcium levels has also been shown to increase presynaptic release probability. These findings support a model in which the IHC regulates the strength of efferent inhibition it undergoes via calcium handling and second messenger effects. Such interactions take place during an important period of afferent maturation and may play a role in the functional development of the auditory pathway.

Though IHCs lack efferent innervation in the healthy adult cochlea, recordings from aged animals revealed that efferents re-innervate IHCs late in life. This innervation pattern arises alongside highly elevated auditory thresholds, the loss of type I afferent contacts, and OHC cell death. The molecular components of these

aged efferent synapses appear to be identical to those of efferent synapses found on young IHCs, and ultrastructural studies reveal that these synapses also feature the postsynaptic cistern characteristic of all efferent synapses on hair cells. Thus, at least in terms of efferent synaptic organization, the damaged cochlea recapitulates features found during early postnatal development.

Efferent synapses on IHCs were studied at the extremes of the lifespan, and the experiments presented here reveal forms of plasticity that occur at individual synapses as well as in the broader organization of the auditory periphery. Future work may provide valuable insights into the regulation of efferent synaptic contacts and the functional role of efferent activity in auditory processing.

References

Ahmed ZM, Goodyear R, Riazuddin S, Lagziel A, Legan PK, Behra M, Burgess SM, Lilley KS, Wilcox ER, Riazuddin S, Griffith AJ, Frolenkov GI, Belyantseva IA, Richardson GP, Friedman TB (2006) The tip-link antigen, a protein associated with the transduction complex of sensory hair cells, is protocadherin-15. *J. Neurosci.* **26**(26): 7022-34.

Alam SA, Oshima T, Suzuki M, Kawase T, Takasaka T, Ikeda K (2001) The expression of apoptosis-related proteins in the aged cochlea of Mongolian gerbils. *Laryngoscope.* **111**(3):528-34.

Art JJ, Fettiplace R, Fuchs PA (1984) Synaptic hyperpolarization and inhibition of turtle cochlear hair cells. *J. Physiol.* **356**:525-50.

Ashmore JF, Russell IJ (1983) Sensory and effector functions of vertebrate hair cells. *J. Submicrosc. Cytol.* **15**(1):163-6.

Avan P, Giraudet F, Büki B (2015) Importance of binaural hearing. *Audiol. Neurootol.* **20**Suppl(1):3-6

Bahmad F, O'Malley J, Tranebjaerg L, Merchant SN (2008) Histopathology of nonsyndromic autosomal dominant midfrequency sensorineural hearing loss. *Otol. Neurotol.* **29**(5):7601-6.

Ballestero J, Zorrilla de San Martin J, Goutman J, Elgoyhen AM, Fuchs PA, Katz E (2011) Short-term synaptic plasticity regulates the level of olivocochlear inhibition to auditory hair cells. *J. Neurosci.* **31**(41):14763-74.

Benson TE, Brown MC (2004) Postsynaptic targets of type II auditory nerve fibers in the cochlear nucleus. *J. Assoc. Res. Otolaryngol.* **5**(2):111-25.

Beurg M, Fettiplace R, Nam JH, Ricci AJ (2009) Localization of inner hair cell mechanotransducer channels using high-speed calcium imaging. *Nat. Neurosci.* **12**(5):553-8.

Bizley JK, Cohen YE (2013) The what, where and how of auditory-object perception. *Nat. Rev. Neurosci.* **14**(10):693-707.

Bobbin RP (1979) Glutamate and aspartate mimic the afferent transmitter in the cochlea. *Exp. Brain Res.* **34**(2):389-93.

Bohne BA, Harding GW (2000) Degeneration in the cochlea after noise damage: primary versus secondary events. *Am. J. Otol.* **21**(4):505-9.

Brant LJ, Gordon-Salant S, Pearson JD, Klein LL, Morrell CH, Metter EJ, Fozard JL (1996) Risk factors related to age-associated hearing loss in the speech frequencies. *J. Am. Acad. Audiol.* **7**(3):152-60.

Brandt A, Striessnig J, Moser T (2003) CaV1.3 channels are essential for the development and presynaptic activity of cochlear inner hair cells. *J. Neurosci.* **23**(34):10832-40.

Brown MC (1994) Antidromic responses of single units from the spiral ganglion. *J. Neurophysiol.* **71**(5):1835-47.

Bulankina AV, Moser T (2012) Neural circuit development in the mammalian cochlea. *Physiology.* **27**(2):100-12.

Christopher Kirk E, Smith DW (2003) Protection from acoustic trauma is not the primary function of the medial olivocochlear efferent system. *J. Assoc. Res. Otolaryngol.* **4**(4):445-65.

Clause A, Kim G, Sonntag M, Weisz CJ, Vetter DE, Rubsamen R, Kandler K (2014) The precise temporal pattern of prehearing spontaneous activity is necessary for tonotopic map refinement. *Neuron* **82**(4):822-835.

Dallos P, He DZ, Lin X, Sziklai I, Mehta S, Evans BN (1997) Acetylcholine, outer hair cell electromotility, and the cochlear amplifier. *J. Neurosci.* **17**(6):2212-26.

Dallos P (2008) Cochlear amplification, outer hair cells and prestin. *Curr. Opin. Neurobiol.* **18**(4):370-6.

Davis A, McMahon CM, Pichora-Fuller KM, Russ S, Lin F, Olusanva BO, Chadha S, Tremblay KL (2016) Aging and hearing health: the life-course approach. *Gerontologist* **56**Suppl(2):S256-76.

Ding D, McFadden SL, Salvi RJ (2001) Cochlear cell densities and inner ear staining techniques. In: Handbook of mouse auditory research (Willott JF, ed), pp189-204. Boca Raton, FL: CRC Press.

Dong S, Mulders WH, Rodger J, Woo S, Robertson D (2010) Acoustic trauma evokes hyperactivity and changes in gene expression in guinea-pig auditory brainstem. *Eur J Neurosci* **31:**1616-1628.

Duthey B (2013) Background paper 6.21: Hearing loss. World Health Organization.

Effertz T, Scharr AL, Ricci AJ (2015) The how and why of identifying the hair cell mechano-electrical transduction channel. *Pflugers Arch.* **467**(1)73-84.

Elgoyhen AB, Katz E (2012) The efferent medial olivocochlear-hair cell synapse. *J. Physiol. Paris* **106**(1-2):47-56.

Elgoyhen AB, Johnson DS, Boulter J, Vetter DE, Heinemann S (1994) Alpha 9: an acetylcholine receptor with novel pharmacological properties expressed in rat cochlear hair cells. *Cell* **79**(4):705-715.

Elgoyhen AB, Vetter DE, Katz E, Rothlin CV, Heinemann SF, Boulter J (2001) Alpha10: a determinant of nicotinic cholinergic receptor function in mammalian vestibular and cochlear mechanosensory hair cells. *Proc. Natl. Acad. Sci. USA* **98**(6):3501-6.

Ernfors P, Van De Water T, Loring J, Jaenisch R (1995) Complementary roles of BDNF and NT-3 in vestibular and auditory development. *Neuron* **14**(6):11553-64.

Esterberg R, Hailey DW, Coffin AB, Raible DW, Rubel EW (2013) Disruption of intracellular calcium regulation is integral to aminoglycoside-induced hair cell death. *J. Neurosci.* **33**(17):7513-25.

Felix D, Ehrenberger K (1992) The efferent modulation of mammalian inner hair cell afferents. *Hear. Res.* **64**(1):1-5.

Fessenden JD, Coling DE, Schacht J (1994) Detection and characterization of nitric oxide synthase in the mammalian cochlea. *Brain Res.* **668**(1-2):9-15.

Fettiplace R, Kim KX (2014) The physiology of mechanoelectrical transduction channels in hearing. *Physiol. Rev.* **94**(3):951-86.

Frank T, Khimich D, Neef A, Moser T (2009) Mechanisms contributing to synaptic Ca2+ signals and their heterogeneity in hair cells. *Proc. Natl. Acad. Sci. USA* **106**(11):4483-8.

Fransen E, Bonneux S, Corneveaux JJ, Schrauwen I, Di Berardino F, White CH, Ohmen JD, Van de Heyning P, Abrosetti U, Huentelman MJ, Van Camp G, Friedman RA (2015) Genome-wide association analysis demonstrates the highly polygenic character of age-related hearing impairment. *Eur. J. Hum. Genet.* **23**(1):110-5.

Fritzsch B, Silos-Santiago I, Bianchi LM, Farinas I (1997) Effects of neurotrophin and neurotrophin receptor disruption on the afferent inner ear innervation. *Semin. Cell Dev. Biol.* **8**:227-84.

Fu B, Le Prell C, Simmons D, Lei D, Schrader A, Chen AB, Bao J (2010) Age-related synaptic loss of the medial olivocochlear efferent innervation. *Mol Neurodegener* **5:**53.

Fuchs PA (1996) Synaptic transmission at vertebrate hair cells. *Curr. Opin. Neurobiol.* **6**(4):514-9.

Fuchs PA, Murrow BW (1992a) Cholinergic inhibition of short (outer) hair cells of the chick. *J. Neurosci.* **12**(3):800-9.

Fuchs PA, Murrow BW (1992b) A novel cholinergic receptor mediates inhibition of chick cochlear hair cells. *Proc. Biol. Sci.* **248**(1321):35-40.

Fuchs PA, Lehar M, Hiel H (2014) Ultrastructure of cisternal synapses on outer hair cells of the mouse cochlea. *J. Comp. Neurol.* **522**(3):717-29.

Furman AC, Kujawa SG, Liberman MC (2013) Noise-induced cochlear neuropathy is selective for fibers with low spontaneous rates. *J. Neurophysiol.* **110**(3):577-86.

Furness DN (2015) Molecular basis of hair cell loss. *Cell Tissue Res.* **361**(1):387-99.

Gale JE, Piazza V, Ciubotaru CD, Mammano F (2004) A mechanism for sensing noise damage in the inner ear. *Curr. Biol.* **14**(6):526-9.

Glowatzki E, Fuchs PA (2000) Cholinergic synaptic inhibition of inner hair cells in the neonatal mammalian cochlea. *Science* **288:**2366-2368.

Glowatzki E, Fuchs PA (2002) Transmitter release at the hair cell ribbon synapse. *Nat. Neurosci.* **5**(2):147-54.

Gómez-Casati ME, Fuchs PA, Elgoyhen AB, Katz E (2005) Biophysical and pharmacological characterization of nicotinic cholinergic receptors in rat cochlear inner hair cells. *J Physiol* **566:**103-118.

Gopinath B, Schneider J, McMahon CM, Burlutsky G, Leeder SR, Mitchell P (2013) Dual sensory impairment in older adults increases the risk of mortality: a population-based study. *PLoS One* **8**(3).

Goutman JD, Glowatzki E (2007) Time course and calcium dependence of transmitter release at a single ribbon synapse. *Proc. Natl. Acad. Sci. USA* **104**(41):16341-6.

Goutman JD, Fuchs PA, Glowatzki E (2005) Facilitating efferent inhibition of inner hair cells in the cochlea of the neonatal rat. *J. Physiol.* **566**(1):49-59.

Grant L, Yi E, Glowatzki E (2010) Two modes of release shape the postsynaptic response at the inner hair cell ribbon synapse. *J. Neurosci.* **30**(12):4210-20.

Guinan JJ (1996) Physiology of olivocochlear efferents. In *The Cochlea*. Vol. 8. Dallos P, Popper AN, Far R editors. Springer, New York. 435-502.

Guinan JJ (2010) Cochlear efferent innervation and function. *Curr. Opin. Otolaryngol. Head Neck Surg.* **18**(5):447-53.
Henderson D, Bielefeld EC, Harris KC, Hu BH (2006) The role of oxidative stress in noise-induced hearing loss. *Ear Hear* **27**(1):1-19.

Henry KR, Chole RA (1980) Genotypic differences in behavioral, physiological and anatomical expressions of age-related hearing loss in the laboratory mouse. *Audiology* **19**(5):369-83.

Hinojosa R (1977) A note on the development of Corti's organ. *Acta Otolaryngol.* **84**(3-4):238-51.

Hirose K, Discolo CM, Kaesler JR, Ransohoff R (2005) Mononuclear phagocytes migrate into the murine cochlea after acoustic trauma. *J. Comp. Neurol.* **489**(2):180-94.

Hu BH, Henderson D, Nicotera TM (2006) Extremely rapid induction of outer hair cell apoptosis in the chinchilla cochlea following exposure to impulse noise. *Hear Res.* **211**(1-2):16-25.

Hudspeth AJ (1997) How hearing happens. *Neuron* **19**(5):947-50.

Humes, LE, Dubno, JR (2010) Factors affecting speech understanding in older adults. In *In The Aging Auditory System* (Gordon-Salant, S. et al., eds), pp 211-258.

Im GJ, Moskowitz HS, Lehar M, Hiel H, Fuchs PA (2014) Synaptic calcium regulation in hair cells of the chicken basilar papilla. *J Neurosci* **34:**16688-16697.

Jensen-Smith HC, Hallworth R, Nichols MG (2012) Gentamicin rapidly inhibits mitochondrial metabolism in high-frequency cochlear outer hair cells. *PLoS One* **7**(6).

Johnsson LG (1974) Sequence of degeneration of Corti's organ and its first-order neurons. *Ann. Otol. Rhinol. Laryngol.* **83**(3):294-303.

Johnson SL, Marcotti W, Kros CJ (2005) Increase in efficiency and reduction in Ca2+ dependence of exocytosis during development of mouse inner hair cells. *J. Physiol.* **563**(Pt 1):177-91
Johnson SL, Adelman JP, Marcotti W (2007) Genetic deletion of SK2 channels in mouse inner hair cells prevents the developmental linearization in the Ca2+ dependence of exocytosis. *J. Physiol.* **583**(Pt 2):631-46.

Johnson SL, Eckrich T, Kuhn S, Zampini V, Franz C, Ranatunga KM, Roberts TP, Masetto S, Knipper M, Kros CJ, Marcotti W (2011) Position-dependent patterning of spontaneous action potentials in immature cochlear inner hair cells. *Nat Neurosci* **14:**711-717.

Johnson SL, Wedemeyer C, Vetter DE, Adachi R, Holley MC, Elgoyhen AB, Marcotti W (2013) Cholinergic efferent synaptic transmission regulates the maturation of auditory hair cell ribbon synapses. *Open Biol.* **3**(11):130163.

Jones SM, Jones TA, Johnson KR, Yu H, Erway LC, Zheng QY (2006) A comparison of vestibular and auditory phenotypes in inbred mouse strains. *Brain Res.* **1091**(1):40-6.

Karlin A (2002) Emerging structure of the nicotinic acetylcholine receptors. *Nat. Rev. Neurosci.* **3**(2):102-14.

Katz E, Elgoyhen AB, Gómez-Casati ME, Knipper M, Vetter DE, Fuchs PA, Glowatzki E (2004) Developmental regulation of nicotinic synapses on cochlear inner hair cells. *J Neurosci* **24:**7814-7820.

Kong JH, Adelman JP, Fuchs PA (2008) Expression of the SK2 calcium-activated potassium channel is required for cholinergic function in mouse cochlear hair cells. *J. Physiol.* **586**(22):5471-85.

Kong JH, Zachary SP, Rohmann KN, Fuchs PA (2013) Retrograde facilitation of efferent synapses on cochlear hair cells. *J. Assoc. Res. Otolaryngol.* **14**(1):17-27.

Kujawa SG, Liberman MC (1997) Conditioning-related protection from acoustic injury: effects of chronic deefferentation and sham surgery. *J. Neurophysiol.* **78**(6):3095-106.

Kujawa SG, Liberman MC (2009) Adding insult to injury: cochlear nerve degeneration after "temporary" noise-induced hearing loss. *J. Neurosci.* **29**(45):14077-85.

Lauer AM, Fuchs PA, Ryugo DK, Francis HW (2012) Efferent synapses return to inner hair cells in the aging cochlea. *Neurobiol Aging* **33:**2892-2902.

Le Novère N (2002) The diversity of subunit composition in nAChRs: evolutionary origins, physiologic and pharmacological consequences. *J. Neurobiol.* **53**(4):447-56.

Le Novère N, Changeux JP (1995) Molecular evolution of the nicotinic acetylcholine receptor: an example of multigene family in excitable cells. *J. Mol. Evol.* **40**(2):155-72.

Liberman MC (1982) Single-neuron labeling the cat auditory nerve. *Science* **216**(4551):1239-41.

Liberman MC (2016) Noise-induced hearing loss: permanent versus temporary threshold shifts and the effects of hair cell versus neuronal degeneration. *Adv. Exp. Med. Biol.* **875**:1-7.

Liberman MC, Dodds LW (1987) Acute ultrastructural changes in acoustic trauma: serial-section reconstruction of streocilia and cuticular plates. *Hear Res.* **26**(1):45-64.

Liberman MC, Kaing NY (1978) Acoustic trauma in cats. Cochlear pathology and auditory-nerve activity. *Acta Otolaryngol. Suppl.* **358**:1-63.

Liberman MC, Kiang NY (1984) Single-neuron labeling and chronic cochlear pathology. IV. Stereocilia damage and alterations in rate- and phase-level functions. *Hear Res.* **16**(1):75-90.

Liberman MC, Liberman LD, Maison SF (2014) Efferent feedback slows cochlear aging. *J. Neurosci.* **34**(13):4599-607.

Lin FR, Ferrucc L (2012) Hearing loss and falls among older adults in the United States. *Arch Intern. Med.* **172**(4):369-71.

Lin FR, Yaffe K, Xia J, Xue QL, Harris TB, Purchase-Helzner E, Satterfield S, Avonayon HN, Ferrucci L, Simonsick EM, Health ABC Study Group (2013) Hearing loss and cognitive decline in older adults. *JAMA Intern. Med.* **173**(4):293-9.

Lioudyno M, Hiel H, Kong JK, Katz E, Waldman E, Parameshwaran-Iyer S, Glowatzki E, Fuchs PA (2004) A "synaptoplasmic cistern" mediates rapid inhibition of cochlear hair cells. *J Neurosci* **24:**11160-11164.

Liu C, Glowatzki E, Fuchs PA (2015) Unmyelinated type II afferent neurons report cochlear damage. *Proc. Natl. Acad. Sci. USA* **112**(47):14723-7.

Manley GA, Köppl C (1998) Phylogenetic development of the cochlea and its innervation. *Curr. Opin. Neurobiol.* **8**(4):468-74.

Marcotti W, Johnson SL, Rusch A, Kros CJ (2003a) Sodium and calcium currents shape action potentials in immature mouse inner hair cells. *J. Physiol.* **552**(Pt 3):743-61.

Marcotti W, Johnson SL, Holley MC, Kros CJ (2003b) Developmental changes in the expression of potassium currents of embryonic, neonatal and mature mouse inner hair cells. *J. Physiol.* **548**(Pt 2):383-400.

Marcotti W, Johnson SL, Kros CJ (2004) A transiently expressed SK current sustains and modulates action potential activity in immature mouse inner hair cells. *J. Physiol.* **560**(Pt 3):691-708.

Martin AR, Fuchs PA (1992) The dependence of calcium-activated potassium currents on membrane potential. *Proc. Biol. Sci.* **250**(1327):71-6.

Martinez-Monedero R, Liu C, Weisz C, Vyas P, Fuchs PA, Glowatzki E (2016) GluA2-containing AMPA receptors distinguish ribbon-associated from ribbonless afferent contacts on rat cochlear hair cells. *eNeuro* **3**(2).

McPherson PS, Kim YK, Valdivia H, Knudson CM, Takekura H, Franzini-Armstrong C, Coronado R, Campbell KP (1991) The brain ryanodine receptor: a caffeine-sensitive calcium release channel. *Neuron* **7**(1):17-25.

Meyer AC, Frank T, Khimich D, Hoch G, Riedel D, Chapochnikov NM, Yarin YM, Harke B, Hell SW, Egner A, Moser T (2009) Tuning of synapse number, structure and function in the cochlea. *Nat. Neurosci.* **12**(4):444-53.

Morley BJ, Simmons DD (2002) Developmental mRNA expression of the alpha10 nicotinic acetylcholine receptor subunit in the rat cochlea. *Brain Res Dev Brain Res* **139:**87-96.

Muñoz DJ, Kendrick IS, Rassam M, Thorne PR (2001) Vesicular storage of adenosine triphosphate in the guinea-pig cochlear lateral wall and concentrations of ATP in the endolymph during sound exposure and hypoxia. *Acta Otolaryngol.* **121**(1):10-5.

Murugasu E, Russell IJ (1996) The effect of efferent stimulation on basilar membrane displacement in the basal turn of the guinea pig cochlea. *J. Neurosci.* **16**(1):325-32.

Nagańska E, Matyia E (2001) Ultrastructural characteristics of necrotic and apoptotic mode of neuronal cell death in a model of anoxia in vitro. *Folia Neuropathol.* **39**(3):129-39.

Nagy JI, Yamamoto T, Jordan LM (1993) Evidence for the cholinergic nature of C-terminals associated with subsurface cisterns in alpha-motoneurons of rat. *Synapse* **15:**17-32.

Nevado J, Sanz R, Casqueiro JC, Ayala A, García-Berrocal JR, Ramírez-Camacho R (2006) Aging evokes an intrinsic pro-apoptotic signaling pathway in rat cochlea. *Acta Otolaryngol.* **126**(11):1134-9.

Noben-Trauth K, Zheng QY, Johnson KR (2003) Association of cadherin 23 with polygenic inheritance and genetic modification of sensorineural hearing loss. *Nat. Genet.* **35**(1):21-3.

Oliver D, Klöcker N, Schuck J, Baukrowitz T, Ruppersberg JP, Fakler B (2000) Gating of Ca2+-activated K+ channels controls fast inhibitory synaptic transmission at auditory outer hair cells. *Neuron* **26:**595-601.
Olson ES, Duifhuis H, Steele CR (2012) Von Békésy and cochlear mechanics. *Hear Res.* **293**(1-2):31-42.

Park JS, Kang SJ, Seo MK, Jou I, Woo HG, Park SM (2014) Role of cysteinyl leukotriene signaling in a mouse model of noise-induced cochlear injury. *Proc. Natl. Acad. Sci. USA* **111**(27):9911-6.

Patuzzi RB, Yates GK, Johnstone BM (1989) Outer hair cell receptor current and sensorineural hearing loss. *Hear Res.* **42**(1):47-72.

Peelle JE, Wingfield A (2016) The neural consequences of age-related hearing loss. *Trends Neurosci.* **39**(7):486-97.

Pettigrew AM, Liberman MC, Kiang NY (1984) Click-evoked gross potentials and single-unit thresholds in acoustically traumatized cats. *Ann. Otol. Rhinol. Laryngol. Suppl.* **112**:83-96.

Plazas PV, Katz E, Gomez-Casati ME, Bouzat C, Elgoyhen AB (2005) Stoichiometry of the alpha9alpha10 nicotinic cholinergic receptor. *J. Neurosci.* **25**(47):10905-12.

Puel JL (1995) Chemical synaptic transmission in the cochlea. *Prog. Neurobiol.* **47**(6):449-76.

Pujol R, Puel JL (1999) Excitotoxicity, synaptic repair, and functional recovery in the mammalian cochlea: a review of recent findings. *Ann NY Acad Sci* **28:**249-254.

Pullen AH, Athanasiou D (2009) Increase in presynaptic territory of C-terminals on lumbar motoneurons of G93A SOD1 mice during disease progression. *Eur J Neurosci* **29:**551-561.

Pullen AH, Sears TA (1978) Modification of "C" synapses following partial central deafferentation of thoracic motoneurones. *Brain Res* **145:**141-146.

Rajan R (1988) Effect of electrical stimulation of the crossed olivocochlear bundle on temporary threshold shifts in auditory sensitivity. *J. Neurophysiol.* **60**(2):569-79.

Reijntjes DO, Pyott SJ (2016) The afferent signaling complex: regulation of type I spiral ganglion neuron responses in the auditory periphery. *Hear Res.* **336**:1-16.

Retzius G (1884) *Das Gehörorgan der Wirbelthiere*. II. *Das Gehörorgan der Reptilien, der Vögel und Säugethiere*. Samson & Wallin, Stockholm.

Robertson D (1984) Horseradish peroxidase injection of physiologically characterized afferent and efferent neurones in the guinea pig spiral ganglion. *Hear Res.* **15**(2):113-21.
Robertson D, Gummer M (1985) Physiological and morphological characterization of efferent neurons in the guinea pig cochlea. *Hear Res.* **20**(1):63-77.

Robertson D, Johnstone BM, McGill TJ (1980) Effects of loud tones on the inner ear: a combined electrophysiological and ultrastructural study. *Hear Res.* **2**(1):39-43.

Robertson D, Sellick PM, Patuzzi R (1999) The continuing search for outer hair cell afferents in the guinea pig spiral ganglion. *Hear Res.* **136**(1-2):151-8.

Robles L, Ruggero MA (2001) Mechanics of the mammalian cochla. *Physiol. Rev.* **81**(3):1305-52.

Rohmann KN, Wersinger E, Braude JP, Pyott SJ, Fuchs PA (2015) Activation of BK and SK channels by efferent synapses on outer hair cells in high frequency regions of the rodent cochlea. *J Neurosci* **35:**1821-1830.

Rothlin CV, Katz E, Verbitsky M, Elgoyhen AB (1999) The alpha9 nicotinic acetylcholine receptor shares pharmacological properties with type A gamma-aminobutyric acid, glycine, and type 3 serotonin receptors. *Mol Pharmacol* **55:**248-254.

Roux I, Wersinger E, McIntosh JM, Fuchs PA, Glowatzki E (2011) Onset of cholinergic efferent synaptic function in sensory hair cells of the rat cochlea. *J Neurosci* **31:**15092-15101.

Ruel J, Wang J, Rebillard G, Eybalin M, Lloyd R, Pujol R, Puel JL (2007) Physiology, pharmacology and plasticity at the inner hair cell synaptic complex. *Hear Res* **227:**19-27.

Ryan AF, Woolf NK, Bone RC (1980) Ultrastructural correlates of selective outer hair cell destruction following kanamycin intoxication in the chinchilla. *Hear Res.* **3**(4):335-51.

Safieddine S, El-Amraoui A, Petit C (2012) The auditory hair cell ribbon synapse: from assembly to function. *Annu. Rev. Neurosci.* **35**:509-28.

Saito K (1980) Fine structure of the sensory epithelium of the guinea pig organ of Corti: afferent and efferent synapses of hair cells. *J Ultrastruct Res* **71:**222-232.

Schuknecht HF, Woellner RC (1955) An experimental and clinical study of deafness from lesions of the cochlear nerve. *J. Laryngol. Otol.* **69**(2):75-97.

Seal RP, Akil O, Yi E, Weber CM, Grant L, Yoo J, Clause A, Kandler K, Noebels JL, Glowatzki E, Lustig LR, Edwards RH (2008) Sensorineural deafness and seizures in mice lacking vesicular glutamate transporter 3. *Neuron* **57**(2):263-75.

Seimens J, Lillo C, Dumont RA, Reynolds A, Williams DS, Gillespie PG, Müller U (2004) Cadherin 23 is a component of the tip link in hair-cell stereocilia. *Nature* **428**(6986):950-5.

Sergeyenko Y, Lall K, Liberman MC, Kujawa SG (2013) Age-related cochlear synaptopathy: an early-onset contributor to auditory functional decline. *J Neurosci* **33**:13686-13694.

Sha SH, Taylor R, Forge A, Schacht J (2001) Differential vulnerability of basal and apical hair cells is based on intrinsic susceptibility to free radicals. *Hear Res.* **155**(1-2):1-8.

Shi X, Nuttall AL (2003) Upregulated iNOS and oxidative damage to cochlear stria vascularis due to noise stress. *Brain Res.* **976**(1-2):1-10.

Shigemoto T, Ohmori H (1991) Muscarinic receptor hyperpolarizes cochlear hair cells of chick by activating Ca(2+)-activated K+ channels. *J. Physiol.* **442**:669-90.

Shmigol A, Verkhratsky A, Isenberg G (1995) Calcium-induced calcium release in rat sensory neurons. *J. Physiol.* **489**(3):627-36.

Simmons DD (2002) Development of the inner ear efferent system across vertebrate species. *J Neurobiol* **53**:228-250.

Smith CA, Sjöstrand FS (1961) Structure of the nerve endings on the external hair cells of the guinea pig cochlea as studied by serial sections. *J Ultrastruct Res* **5**:523-556.

Spoendlin H (1971) Primary structural changes in the organ of Corti after acoustic overstimulation. *Acta Otolaryngol.* **71**(2):166-76.

Spoendlin H, Schrott A (1989) Analysis of the human auditory nerve. *Hear Res.* **43**(1):25-38.

Sridhar TS, Liberman MC, Brown MC, Sewell WF (1995) A novel cholinergic "slow effect" of efferent stimulation on cochear potentials in the guinea pig. *J Neurosci* **15**(5):3667-78.

Sridhar TS, Brown MC, Sewell WF (1997) Unique postsynaptic signaling at the hair cell efferent synapse permits calcium to evoke changes on two time scales. *J Neurosci* **17:**428-437.

Stamataki S, Francis HW, Lehar M, May BJ, Ryugo DH (2006) Synaptic alterations at inner hair cells precede spiral ganglion cell loss in aging C57BL/6J mice. *Hear Res.* **221**(1-2):104-8.
Takeno S, Wake M, Mount RJ, Harrison RV (1998) Degeneration of spiral ganglion cells in the chinchilla after inner hair cell loss induced by carboplatin. *Audiol. Neurootol.* **3**:281-290.

Taranda J, Maison SF, Ballestero JA, Katz E, Savino J, Vetter DE, Boulter J, Liberman MC, Fuchs PA, Elgoyhen AB (2009) A point mutation in the hair cell nicotinic cholinergic receptor prolongs cochlear inhibition and enhances noise protection. *PLoS Biol.* **7**(1):e18.

Tiede L, Steyger PS, Nichols MG, Hallworth R (2009) Metabolic imaging of the organ of Corti – a window on cochlea bioenergetics. *Brain Res.* **1277**:37-41.

Tritsch NX, Yi E, Gale JE Glowatzki E, Bergles DE (2007) The origin of spontaneous activity in the developing auditory system. *Nature* **450**(7166):50-5.

Tritsch NX, Rodriguez-Contreras A, Crins TT, Wang HC, Borst JG, Bergles DE (2010). Calcium action potentials in hair cells pattern auditory neuron activity before hearing onset. *Nat. Neurosci.* **13**(9):1050-2.

Valdés-Baizabal C, Soto E, Vega R (2015) Dopaminergic modulation of the voltage-gated sodium current in the cochlear afferent neurons of the rat. *PLoS One* **10**(3).

Verkhratsky A, Shmigol A (1996) Calcium-induced calcium release in neurons. *Cell Calcium* **19**(1):1-14.

Vetter DE, Liberman MC, Mann J, Barhanin J, Boulter J, Brown MC, Saffiote-Kolman J, Heinemann SF, Elgoyhen AB (1999) Role of alpha9 nicotinic ACh receptor subunits in the development and function of cochlear efferent innervation. *Neuron* **23**(1):93-103.

Vetter DE, Katz E, Maison SF, Taranda J, Turcan S, Ballestero J, Liberman MC, Elgoyhen AB, Boulter J (2007) The alpha10 nicotinic acetylcholine receptor subunit is required for normal synaptic function and integrity of the olivocochlear system. *Proc. Natl. Acad. Sci. USA* **104**(51):20594-9.

Viana LM, O'Malley JT, Burgess BJ, Jones DD, Oliveira CA, Santos F, Merchant SN, Liberman LD, Liberman MC (2015) Cochlear neuropathy in human presbycusis: confocal analysis of hidden hearing loss in post-mortem tissue. *Hear Res.* **327**:78-88.

Viberg A, Canlon B (2004) The guide to plotting a cochleogram. *Hear Res* **197:**1-10.

Vincler M, Wittenauer S, Parker R, Ellison M, Olivera BM, McIntosh JM (2006) Molecular mechanisms for analgesia involving specific antagonism of alpha9 alpha10 nicotinic acetylcholine receptors. *Proc Natl Acad Sci USA* **103:**17880-17884.

Von Békésy G (1960) Experiments in hearing. McGraw-Hill, New York.

Wada T (1923) Anatomical and physiological studies on the growth of the inner ear of the albino rat. *The American Anatomical Memoirs* **10**:1-174.

Wakabayashi K, Fujioka M, Kanzaki S, Okano HJ, Shibata S, Yamashita D, Masuda M, Mihara M, Ohsugi Y, Ogawa K, Okano H (2010) Blockade of interleukin-6 signaling suppressed cochlear inflammatory response and improved hearing impairment in noise damaged mouse cochlea. *Neurosci. Res.* **66**(4):345-52.

Wang JC, Raybould NP, Luo L, Ryan AF, Cannell MB, Thorne PR, Housley GD (2003) Noise induces up-regulation of P2X2 receptor subunit of ATP-gated ion channels in the rat cochlea. *Neuroreport* **14**(6):17-23.

Wang HC, Lin CC, Cheung R, Zhang-Hooks Y, Agarwal A, Ellis-Davies G, Rock J, Bergles DE (2015) Spontaneous activity of cochlear hair cells triggered by fluid secretion mechanisms in adjacent support cells. *Cell* **163**(6):1348-59.

Weisstaub N, Vetter DE, Elgoyhen AB, Katz E (2002) The alpha9/alpha10 nicotinic acetylcholine receptor is permeable to and is modulated by divalent cations. *Hear Res.* **167**(1-2):122-35.

Weisz CJ, Glowatzki E, Fuchs PA (2009) The postsynaptic function of type II cochlear afferents. *Nature* **461**(7267):1126-9.

Weisz CJ, Glowatzki E, Fuchs PA (2014) Excitability of type II cochlear afferents. *J. Neurosci.* **34**(6):2365-73.

Wichmann C, Moser T (2015) Relating structure and function of inner hair cell ribbon synapses. *Cell Tissue Res.* **361**(1):95-114.

Winslow RL, Sachs MB (1987) Effect of electrical stimulation of the crossed olivocochlear bundle on auditory nerve response to tones in noise. *J. Neurophysiol.* **57**(4):1002-21.

Wong AB, Rutherford MA, Gabrielaitis M, Pangrsic T, Gottfert F, Frank T, Michanski S, Hell S, Wolf F, Wichmann C, Moser T (2014) Developmental refinement of hair cell synapses tightens the coupling of Ca2+ influx to exocytosis. *EMBO* **33**(3):247-64.

Young ED (2008) Neural representation of spectral and temporal information in speech. *Philos. Trans. R. Soc. Lond. B Biol. Sci.* **363**(1493):923-45.

Yuan Y, Shi F, Yin Y, Tong M, Lang H, Polley DB, Liberman MC, Edge AS (2014) Ouabain-induced cochlear nerve degeneration: synaptic loss and plasticity in a mouse model of auditory neuropathy. *J. Assoc. Res. Otolaryngol.* **15**(1):31-43.

Zampini V, Johnson SL, Franz C, Lawrence ND, Münkner S, Engel J, Knipper M, Magistretti J, Masetto S, Marcotti W (2010) Elementary properties of CaV1.3 Ca(2+) channels expressed in mouse cochlear inner hair cells. *J. Physiol.* **559**(Pt 1):187-99.

Zheng QY, Johnson KR, Erway LC (1999) Assessment of hearing in 80 inbred strains of mice by ABR threshold analyses. *Hear Res.* **130**(1-2):94-107.

Zheng J, Shen W, He DZ, Long KB, Madison LD, Dallos P (2000) Prestin is the motor protein of cochlear outer hair cells. *Nature* **405**(6783):149-55.
Zilberstein Y, Liberman MC, Corfas G (2012) Inner hair cells are not required for survival of spiral ganglion neurons in the adult cochlea. *J. Neurosci.* **32**(2):405-10.

Zorrilla de San Martin J, Ballestero J, Katz E, Elgoyhen AB, Fuchs PA (2007) Ryanodine is a positive modulator of acetylcholine receptor gating in cochlear hair cells. *J. Assoc. Res. Otolaryngol.* **8**(4):474-83.

Zorrilla de San Martin J, Pyott S, Ballestero J, Katz E (2010) Ca(2+) and Ca(2+)-activated K(+) channels that support and modulate transmitter release at the olivocochlear efferent-inner hair cell synapse. *J. Neurosci.* **30**(36):12157-67.

Zwicker E (1979) A model describing nonlinearities in hearing by active processes with saturation at 40 dB. *Biol. Cybern.* **35**(4):243-50.

Appendix

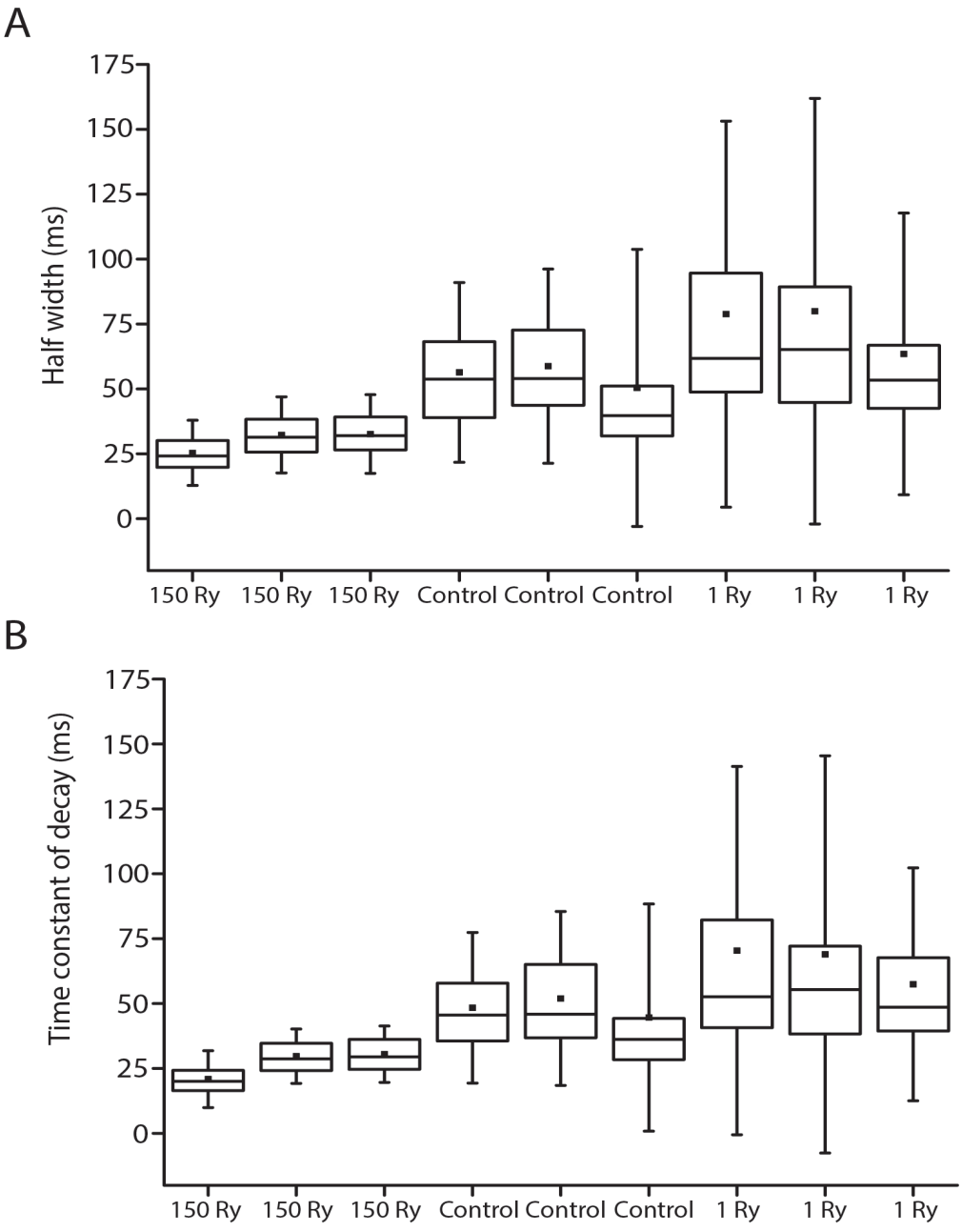

Figure A1: A, Box (upper and lower quartiles) and whisker (standard deviation) plots of event half width for individual cells recorded in 150 µM ryanodine, control conditions, and 1 µM ryanodine; center line: median; black box: mean. B, Box and whisker plots of time constants of decay for the same cells.

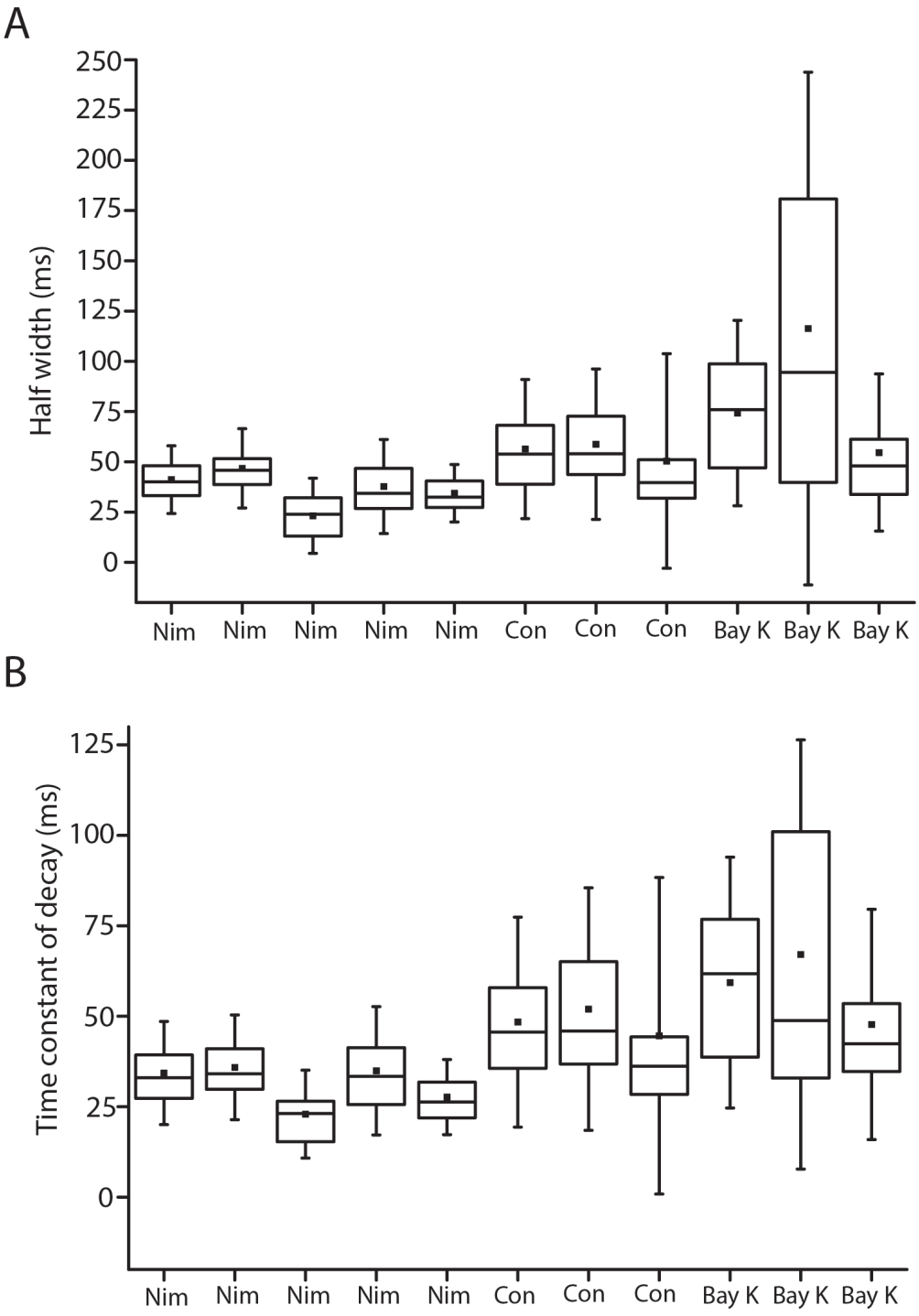

Figure A2: A, Box (upper and lower quartiles) and whisker (standard deviation) plots of event half width for individual cells recorded in 10 μM nimodipine, control conditions, and 10 μM Bay K; center line: median; black box: mean. B, Box and whisker plots of time constants of decay for the same cells.

Curriculum vitae

Stephen Paul Zachary November 2016

Educational History

Ph.D	2016	Program in Neuroscience	Johns Hopkins School of Medicine
BA	2004	Philosophy	Washington & Lee University

Other Research Experience

Neuroscience Graduate Program Rotations, Johns Hopkins School of Medicine

Sockanathan lab: September 2010-December 2010
Brown lab: January 2011-April 2011
Linden lab: May 2011-September 2012

Laboratory Technician, Connor lab, Johns Hopkins University
March 2008-September 2010

Fellowships and External Funding

National Institutes of Deafness and Other Communication Disorders: F31DC014184: Efferent innervation of inner hair cells in the damaged/aged cochlea. Includes stipend, tuition, and research support.

Travel award, 2014 Gordon Conference: The Auditory System.

Academic Honors

Invited participant, 2015 St. Jude National Graduate Student Symposium.

Teaching assistant, *Biology of the Inner Ear*, Marine Biological Laboratory in Woods Hole, MA, August 2013 & 2015.

Research Publications

Zachary SP & Fuchs PA (2015) Re-emergent inhibition of cochlear inner hair cells in a mouse model of hearing loss. *J. Neurosci.* 35(26):9701-06.

Kong JH, **Zachary SP**, Rohmann KN & Fuchs PA (2012) Retrograde facilitation of efferent synapses on cochlear inner hair cells. *J. Assoc. Res. Otolaryngol.* 14(1): 17-27.

Chapters

Fuchs PA, Wu JS, Vayas P & **Zachary SP** (in preparation) *Cochlear Microcircuits.* In: Handbook of Brain Microcircuits (Shepherd G & Grillner S, Eds.) Oxford University Press.

Podium Presentations

National Graduate Student Symposium, St. Jude Children's Research Hospital, Memphis TN. "Age-related hearing loss is accompanied by efferent synaptic inhibition of inner hair cells." April 2015.

Gordon Research Seminar: The Auditory System, Bates College, Lewiston ME. “Efferent synaptic rearrangement in the aged cochlea.” July 2014.

Association for Research in Otolaryngology Midwinter Meeting, San Diego CA. “Efferent synaptic formation during age-related hearing loss.” February 2014.